

**KONINKLIJK BELGISCH INSTITUUT
VOOR NATUURWETENSCHAPPEN**

**INSTITUT ROYAL DES SCIENCES
NATURELLES DE BELGIQUE**

ROYAL BELGIAN INSTITUTE OF NATURAL SCIENCES

MEMOIRS OF THE GEOLOGICAL SURVEY OF BELGIUM

N. 60 – 2014

The Boom Clay Geology
From sedimentation to present-day occurrence
A review

Noël VANDENBERGHE¹, Mieke DE CRAEN², Laurent WOUTERS³

¹ Geology KU Leuven, Belgium. E mail: noel.vandenbergh@ees.kuleuven.be

² SCK-CEN Nuclear Research Center, Mol, Belgium. E mail: mdcraen@sckcen.be

³ ONDRAF-NIRAS, Nuclear Agency, Brussels, Belgium. E mail: l.wouters@nirond.be

(76 pages, 70 figures)

Cover : XXXX

Contents

1. Introduction.....	3
2. The depositional area of the Boom Clay and its present day occurrence.....	4
2.1. Occurrence and nature of the Boom Clay.....	4
2.2. The palaeogeographical, palaeotectonical and palaeoclimatical setting of the Boom Clay	5
2.2.1. Palaeogeographical setting.....	7
2.2.2. Palaeotectonical setting.....	7
2.2.3. Palaeoclimatical setting.....	9
2.3. The physico-chemical nature of the Boom Clay in Belgium.....	9
3. The stratigraphic position and subdivisions of the Boom Clay	10
3.1. Unconformity bounded stratigraphy.....	10
3.2. The micro-lithostratigraphy of the Boom Clay.....	11
3.2.1. The outcrop area.....	11
3.2.2. The Antwerp Campine subsurface area.....	12
3.3. The formal lithostratigraphy and the extension to the south and the east.....	13
3.4. Biostratigraphy of the Boom and Eigenbilzen Formations.....	19
3.5. Magnetostratigraphic data.....	19
3.6. Radiometry and Sr-isotope dating.....	22
3.7. Oxygen isotope event stratigraphy.....	24
3.8. Cyclostratigraphy.....	25
3.9. Sequence stratigraphy.....	27
4. The geology of the Boom Clay	29
4.1. The sedimentological significance of the grain-size and the organic matter rhythms.....	29
4.1.1. Grain size.....	29
4.1.2. Organic matter.....	31
4.1.3. Detrital particle provenance	33
4.1.4. Sedimentary model for the silt-clay layering.....	33
4.2. Sedimentary model at larger scale.....	37
4.2.1. Lateral variations from basin to coast.....	37
4.2.2. Vertical low frequency variations.....	41
4.3. The carbonate-rich/marly horizons and the development of carbonate concretions in the Boom Clay.....	43
4.4. The oxygen conditions of the water in the Rupelian sedimentary basin.....	50
4.5. Climatic conditions during the Boom Clay deposition.....	52
4.6. Tectonic activity during the Rupelian	53
4.7. The post-Rupelian tectonic evolution of the area affecting Boom Clay	58
4.8. Natural discontinuities in the Boom Clay: the physical expression of the Boom Clay regional geological evolution	64
4.8.1. The discontinuity surfaces in the Boom Clay.....	64
4.8.2. Discussion on the origin of faulting, jointing and the slickensided surfaces.....	65
4.8.3. Permafrost induced deformation.....	67
4.8.4. Valley bulging.....	67
5. Conclusions	67
6. Acknowledgments.....	69
7. References.....	69

THE BOOM CLAY GEOLOGY

FROM SEDIMENTATION TO PRESENT-DAY OCCURRENCE

A REVIEW

Noël VANDENBERGHE¹, Mieke DE CRAEN², Laurent WOUTERS³

¹ Geology KU Leuven, Belgium. E mail: noel.vandenbergh@ees.kuleuven.be

² SCK-CEN Nuclear Research Center, Mol, Belgium. E mail: mdcraen@sckcen.be

³ ONDRAF-NIRAS, Nuclear Agency, Brussels, Belgium. E mail: l.wouters@nirond.be

ABSTRACT. In this Memoir, a review is presented of the present knowledge on the geology of the Rupelian Boom Clay, in particular its sedimentation history and diagenetic evolution. A synthesis of the following items is given: the present occurrence of the deposit, the paleogeographical context of its formation, the stratigraphical position and subdivisions with their correlation potential, the lithology and the sedimentation model, the characteristic occurrence of septaria, the paleoclimatic conditions, the tectonic influences on the sedimentation and the post-Rupelian evolution of the clay mass.

KEY-WORDS: Boom Clay, Rupelian, Belgium, sedimentology, diagenesis, septaria, paleoclimate, tectonics.

1. Introduction

The Boom Clay has a long history as a common study objective for geologists, soil engineers and industrial users.

During the nineteenth century, geologists have studied the fossils of the Boom Clay derived from the deposits in the outcrop area along the Rupel river as reference for the Middle Oligocene. More than a century later modern sedimentological studies started, making use of continuously improved analytical techniques. A boost in the study of the geology of the Boom Clay was initiated when it was investigated as a potential host rock for the long-term geological disposal of high level and long-lived nuclear waste since a first reconnaissance borehole was drilled in Mol in 1975. This interest also brought the study of the Boom Clay from the outcrop area south of Antwerp to the Campine subsurface where subsequently many new boreholes were drilled.

The present synthesis on the Boom Clay deals with its geology. It describes the history of the Boom Clay since its deposition until today. All sedimentological and sediment-petrological properties of the Boom Clay are described. The geometry and the stratigraphy of the clay deposit are discussed and the correlation with the geology in neighboring countries is described. All data are interpreted in terms of the original sedimentation conditions and in terms of the early diagenetic, physical, chemical and mineralogical phenomena that have occurred during its shallow burial and even uplift until today.

The geology of the Boom Clay is the basis for understanding its geochemical, mechanical hydrogeological or other engineering properties. It also forms the base for understanding how to extrapolate properties measured at one location to other localities.

In the Antwerp harbour area, soil engineers had to understand the geomechanical behavior of the clay as many constructions had their foundations in the Boom Clay. Also the excavations for the modern large docks reach the Boom Clay underneath Neogene sands. Engineers had to make underground connections in the clay between both banks of the Scheldt river for traffic and pipes for different uses. Subterranean rooms were excavated in the clay for gas storage.

Industrially, the Boom Clay is certainly best known for the production of bricks, and also roof and floor tiles, an industry that dominated the economic activity in the outcrop area since the Middle Ages until the energy crises in the previous century completely transformed this industry. These days the Boom Clay still is a resource for the brick industry in a few modern production units. Remarkably, already in the nineteenth century the Boom Clay has been a resource for other local industrial activities (Van den Broeck, 1887). Sulphuric acid was produced from the pyrites in the clay. Cement was firstly produced from septaria and later by mixing clay and chalk; today the rotary kiln used for the production of expanded clay grains near Antwerp is the only technological reminiscence of the former cement production.

2. The depositional area of the Boom Clay and its present day occurrence

2.1. Occurrence and nature of the Boom Clay

Boom Clay is the name given to a thick plastic clay unit outcropping along the rivers Rupel and Scheldt in Northern Belgium (Figure 1). It has been known in that area since several centuries as it was used for brick making ever since brick and roof tile making was reintroduced by monks after returning from the crusades, and its production is continuing till today. Also to the east of Leuven and in southern Limburg less continuous outcrops of the Boom Clay are known (Figure 1).

The name Boom Clay was introduced in the geological literature already in the first half of the 19th century and stems from the town of Boom situated along the Rupel river (Glibert & de Heinzelin, 1954; Dumont, 1849).

This river has also given its name to the Early Oligocene age and stage, the Rupelian. Ever since the early days of stratigraphy, it became common practice to have a three-fold subdivision of the Oligocene with the Rupelian as

the middle Oligocene stage. However, by the end of the 20th century the International Stratigraphic Commission has decided to use only a twofold division in the Oligocene, the lower one being the Rupelian thereby extending de facto its meaning to include the slightly older sediments that were named Tongrian, Sannoisian and Lattorfian before (Van Simaey & Vandenberghe, 2006).

The macro- and microfossils preserved in the clay, as well as the common occurrence of the mineral glauconite in the clay, indicate a marine depositional environment (Gulinck, 1954; Vandenberghe, 1978). Both fossils and sedimentological features point to depositional depths generally varying between 50 and 150 m.

Marine clays deposited at such depths can be expected to occur over a wider area and hence also deeper in the subsurface. Boreholes in which Boom Clay has been demonstrated and correlated in the subsurface of the Belgian Campine, the southeastern Netherlands and the Achterhoek and the Lower Rhine area, are indicated on Figure 2 (Vandenberghe et al., 2001). Even further towards the northeast and northwest, in the subsurface of northern Germany and under the North Sea, these lower Oligocene clays have been observed.

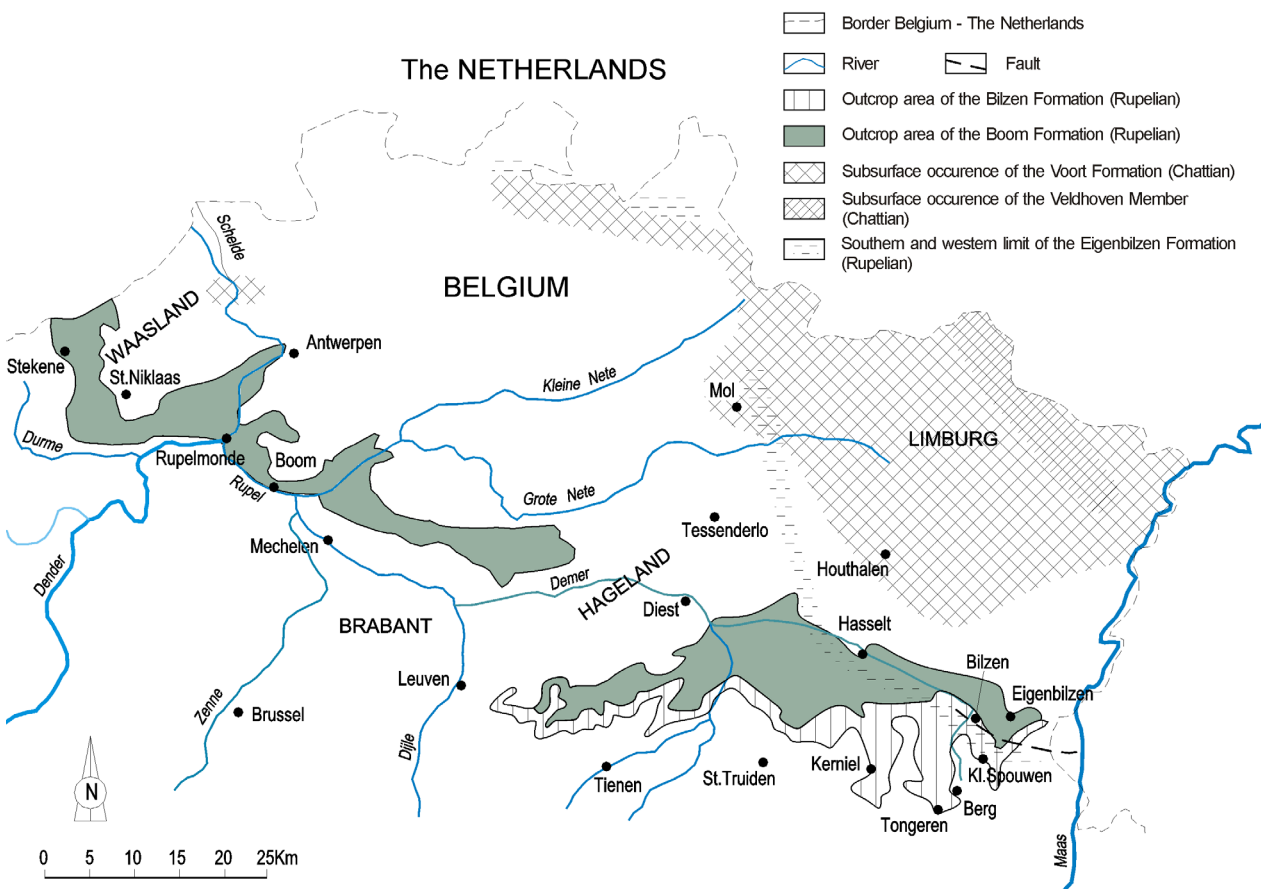


Figure 1. Outcrop area of the Boom Formation in northern Belgium. North of the outcrop area, the Boom Clay occurs in the subsurface. The other lithostratigraphic units on the map are part of the Oligocene Rupel Group (see Vandenberghe & Wouters, 2011).

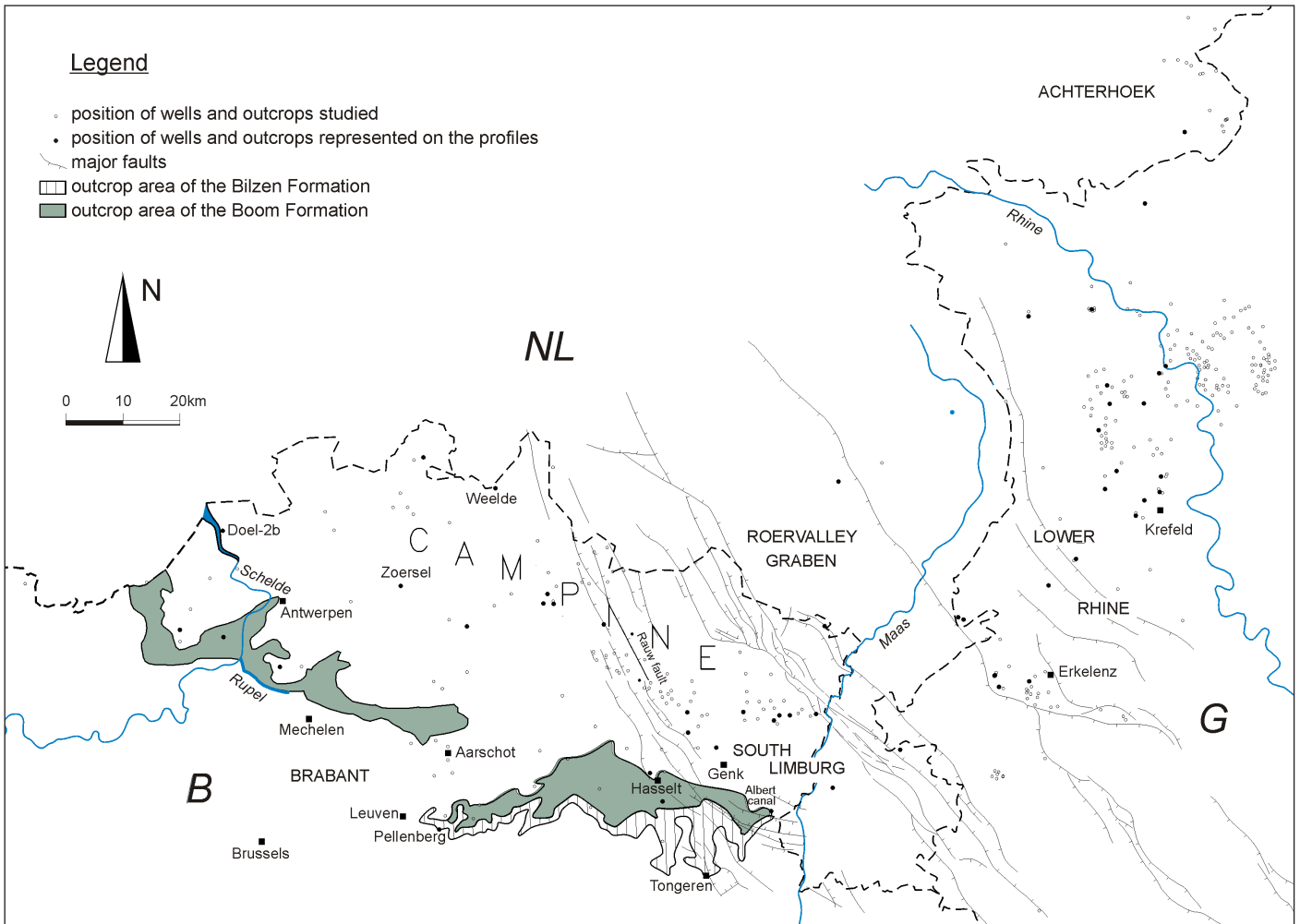


Figure 2. Outcrop area of the Boom and Bilzen Formations, and the selection of boreholes in the Belgian Campine, southeastern Netherlands and the Achterhoek, and the Lower Rhine area, where Boom Clay has been demonstrated in boreholes with suitable geophysical well-log data for the correlations established in Vandenberghe et al. (2001).

2.2. The palaeogeographical, palaeotectonical and palaeoclimatical setting of the Boom Clay

A map showing the general distribution of land and sea during the Early Oligocene (Figure 3) in Europe and the Tethys realm explains why clays as described by Merklin (1962) and Nosovsky (1962) in the area of the Black Sea-Caspian Sea and Aral Lake have similar lithology and macrofossil content as the Boom Clay in the North Sea area. A reference stratigraphic table is given in Figure 4.

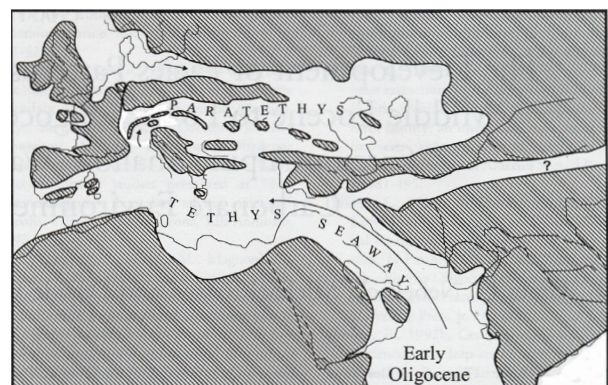


Figure 3. Palaeogeography of Europe and the Tethys area during the Lower Oligocene. The marine realm is white and land areas are striped (after Rögl, 1998 & 1999).

<u>Waasland-Boom and area Campine area</u>	<u>Brabant area</u>	<u>East Campine and Tongeren</u>
<u>RUPEL GROUP</u>		
		<u>Voort Formation</u> Veldhoven Member
<u>Eigenbilzen Formation</u>		<u>Eigenbilzen Formation</u>
<u>Boom Formation</u>	<u>Boom Formation</u>	<u>Boom Formation</u>
Boeretang Member Putte Member Terhagen Member Belsele-Waas Member	Putte Member Terhagen Member	Boeretang Member Putte Member Terhagen Member
		<u>Bilzen Formation</u> Kerniel Member Kleine-Spouwen Member Berg Member
<u>TONGEREN GROUP</u>		
<u>Zelzate Formation</u>		<u>Borgloon Formation</u>
	Heide Horizon Henis Member Boutersem Member Kerkom Member Hoogbutsel Horizon	Oude Biezen Member Henis Member
Ruisbroek Member (s4)		
		<u>Sint-Huibrechts-Hern Formation</u>
Watervliet Member (a4) Bassevelde Member (s3) (Ba1,Ba2,Ba3 sequences)	Kesselberg Member Neerrepen Member Grimmertingen Member	Neerrepen Member Grimmertingen Member

Figuur 4. General lithostratigraphic table of the Tongeren and Rupel Groups in northwest (Waasland, Boom, West Campine), central (Brabant) and northeast (East Campine and Tongeren) Belgium. The Sint-Huibrechts-Hern Formation corresponds to the former Tongrian 1 (marine) and the Borgloon Formation to the former Tongrian 2 (continental). The codes a and s are the abbreviations for ‘argile’ (clay) and ‘sable’ (sand) introduced by Gulinck (1965) as subdivisions of the now obsolete Kallo Complex (replaced by the Maldegem and Zelzate Formations). The Bilzen Formation corresponds, except the upper part of the Kerniel Member, to the R1 Rupelian cycle and the Boom and Eigenbilzen Formations to the R2 Rupelian cycle of Vandenbroeck & Rutot (1883). The Boeretang Member has been introduced (Vandenberghe & Wouters, 2011) to describe the more silty upper part in the Campine subsurface. Formal descriptions of the units and corresponding former nomenclature can be found at the National Stratigraphic Commission of Belgium website: <http://natstratcommbelgium.drupalgardens.com>

2.2.1. Palaeogeographical setting

The Boom Clay belongs to a series of Paleogene deposits in the North Sea Basin. The structural situation of the North Sea allows it to be qualified as an epicontinental sea.

The Boom Clay, as known in Belgium, does occur in other countries around the North Sea area (Figure 5). The clay is indicated as Rupel Clay Member in the Netherlands (Wong et al., 2007) and as Septarienton or Rupelton in Germany. The clay also occurs in the Rhine and Hessen grabens, the Mainz Basin in Germany and the Molasse basin in northern Switzerland. Underneath the North Sea, Rupelian muds are known as the Lark Formation (Neal et al., 1998). In the central and northern North Sea these muds were deposited in several hundred meters of water depth while the thickness may reach up to 1000m (fig 12.6c in Knox et al., 2010).

In the shallow waters around the main depositional area, sandy deposits occur as for example the Sables de Fontainebleau in the Paris Basin (see Lozouet, 2013). Early Oligocene sandy deposits also exist in the United Kingdom and south of Norway. In the south-east of Germany, lignites and sands occur, while shallow marine sand occurs to the east of Poland and the

northwest of Russia. The lithological similarity between the Boom Clay and the Rupelian clays and their macrofossil content around the Black, Caspian and Aral Seas is so striking that marine connections with the North Sea area must have existed (Figure 5).

2.2.2. Palaeotectonical setting

Tectonically, the Rupelian is a time interval of intense Alpine deformation. The geographical extension of the Boom Clay transgression and other Rupelian clays deposited in relatively deep water, in what can be considered as a north European branch of the Paratethys (Figure 5), required an important subsidence of that area. Indeed, for climatic reasons discussed in the next section, the global sea level should have been rather decreasing, and therefore the major Rupelian transgression in northern Europe is attributed to a regional subsidence that can be linked to the evolution of the Alpine chain in southern Europe. During the Late Eocene and Early Oligocene, the several hundred meter deep foreland basin started to form between the converging European plate and the now rapidly rising Alpine chain. The latter was later filled up with Molasse type sediments, which were derived from the erosion of the advancing thrust sheets (Sissingh, 2003,2006) (Figure 6).

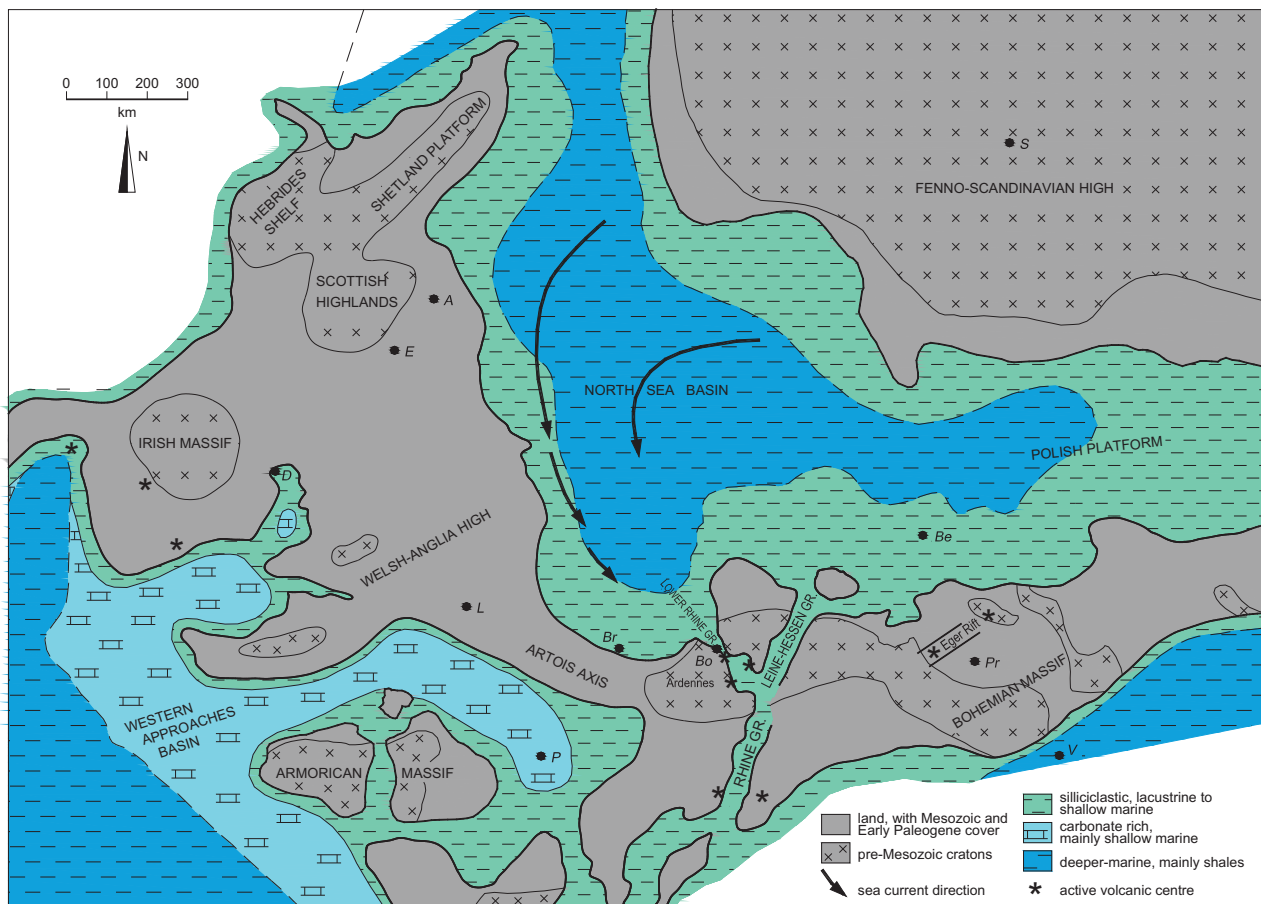


Figure 5. Palaeogeographic reconstruction of the Oligocene North Sea Basin showing the potential source areas of the Boom Clay sediment (after Laenen, 1998, from Vandenberghe & Mertens, 2013).

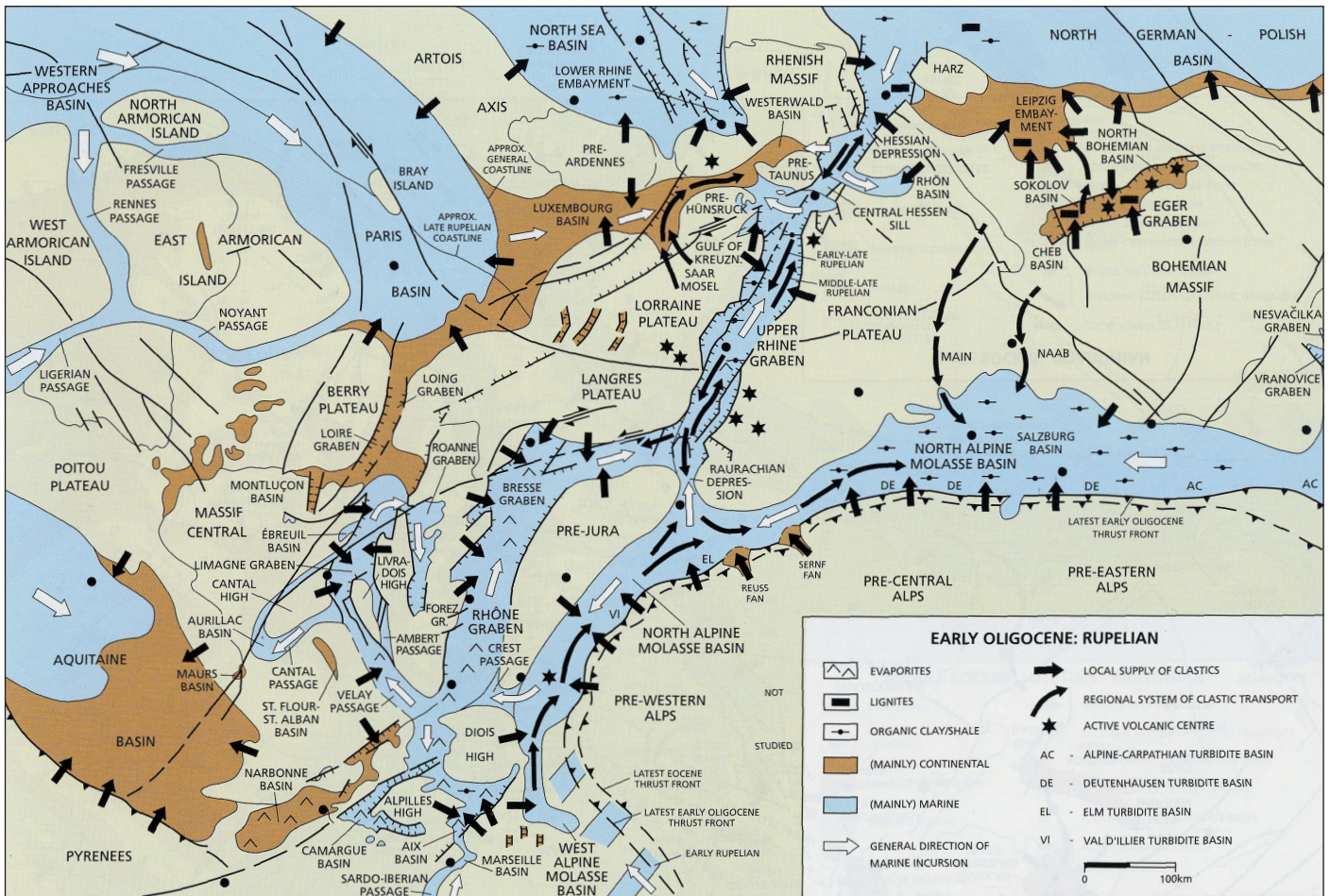


Figure 6. Rupelian palaeogeography of the area between the southern North Sea and the Alpine region connected by the Hessen and Upper Rhine grabens according to Sissingh (2006). Note also the existence of a large North German Polish Basin and the separation of the Paris Basin from the North Sea Basin by the Artois axis (appendix 6 of Sissingh, 2006).

A major unconformity in the sedimentary record of European basins is recorded at the Bartonian-Priabonian transition and known as the Pyrenean unconformity. It ends a regime dominantly controlled by North-Atlantic seafloor spreading during the Early and Middle Eocene and marks the start of a dominantly compressional tectonic regime. This is also the time of the start of inversions, such as Broad Fourteens and West Netherlands Basins, and uplift of large areas in western Europe leading to the presence of a major hiatus in the Oligocene. Some grabens started to subside and collect thick series of Oligocene sediments, such as the Upper Rhine Graben in the beginning of the Oligocene, others had a maximal subsidence at the beginning of the Late Oligocene (Chattian) such as the Bresse Graben. The Roer Valley Graben and the entire Lower Rhine embayment had a renewed important subsidence at the beginning of the Chattian, resulting in the reactivation of the NW-SE trending western bounding faults of the Roer Valley Graben occurring in the northeastern Campine area. The end of the Oligocene was marked by another widespread unconformity, the Savian tectonic pulse. In the Campine area this uplift explains also the absence

of sediments from the Aquitanian and the installation of rather shallow sandy glauconite rich sediments from the Burdigalian onwards.

The late Eocene to early Oligocene was also the time of Scandinavian uplift, either by tectonics or by increased isostatic uplift after dissection of a high-elevation peneplain by river erosion steered by climatic deterioration and sea-level drop. Therefore, the supply of coarse clastic sediments from southern Norway to the North Sea Basin increased notably at that time, resulting in an almost 1 km thick deltaic deposit of silty clays and sandy clays in the Norwegian-Danish Basins (Doré et al., 2002). This Scandinavian tectonic evolution will be at the origin of a major part of the sediment supply for the Boom Clay (see Figure 5 and 4.1.3).

Volcanic centers have been active during the Oligocene mainly in the neighbourhood of the active grabens such as the Rhine graben, the Hessen graben and the Eger rift in the northwestern part of the Bohemian Massif, as well as in the southern part of the Irish Massif (Figure 5 & 6).

identified consists dominantly of inversely correlated quartz (20 to 60 %) and 2:1 clay minerals (22 to 56 %), plagioclase, potassium-feldspar and kaolinite each reaching between 10 and 15 %. Chlorite varies between 1 and 4 %. Calcite varies between zero and maximum 4 %. Small amounts of siderite and dolomite are detected. Pyrite is a common mineral present in the clay and can reach up to 3 %. Also anatase is commonly present in quantities below 1 %. The 2:1 clay minerals are a mixture of illite (5-18 % of bulk), smectite (montmorillonite, 7-24 % of bulk) and randomly interstratified illite-smectite mixed clay minerals (7-23 % of bulk). The kaolinite consists of discrete kaolinite together with random mixed-layer kaolinite-smectite. The chlorite identified in the bulk samples is further specified as a mixture of chlorite, defective chlorite and random mixed-layer chlorite-expandable mineral (Zeelmaekers et al., in prep.)

Organic matter of marine origin is present in small quantities (about 0.5 %) but organic particles from terrestrial origin can reach a few percentages (3-5 %) in some horizons giving the grey clay an intense black colour (Vandenberghe, 1978). The evolution of the organic particles shows an early diagenetic stage still deep in the lignite zone (Figure 8). Carbonates as finely dispersed particles are present only in the lower part of the Boom Clay but layers containing septarian carbonate concretions, unmixed during the diagenetic history of the clay, can occur over the entire clay section.

3. The stratigraphic position and subdivisions of the Boom Clay

3.1. Unconformity bounded stratigraphy

Unconformities are expressions of tectonic activity. Even slight tectonic influences may tilt strata and induce erosion. Although not commonly practiced in the Belgian Cenozoic stratigraphy, it is useful to situate the Boom Clay with respect to such unconformities as this allows time correlation over the entire area where the tectonic activity took place and the unconformities can be recognised. The conformable package of layers between two successive unconformities is called a sythem.

The Boom Clay, with some other sedimentary units below and above, is comprised between the Pyrenean and Savian unconformities, respectively at the Bartonian-Priabonian and the Oligocene-Miocene boundaries (Figure 9). Within this sythem another more subtle tectonically linked unconformable boundary exists between the Boom Clay and the overlying Chatian Voort Sand. The base of the Ruisbroek Sand, underlying the Boom Clay, is also erosive; it represents the response to a low relative sea-level effect (see 3.9) but the influx of reworked microfossils in the Ruisbroek Sand (Vandenberghe et al., 2003) suggests also a slight tectonic effect between the earliest Oligocene sequence (Bassevelde 3-Watervliet-Sint Huibrechts-Hern units, Figures 9, 23) and the Ruisbroek Sand.

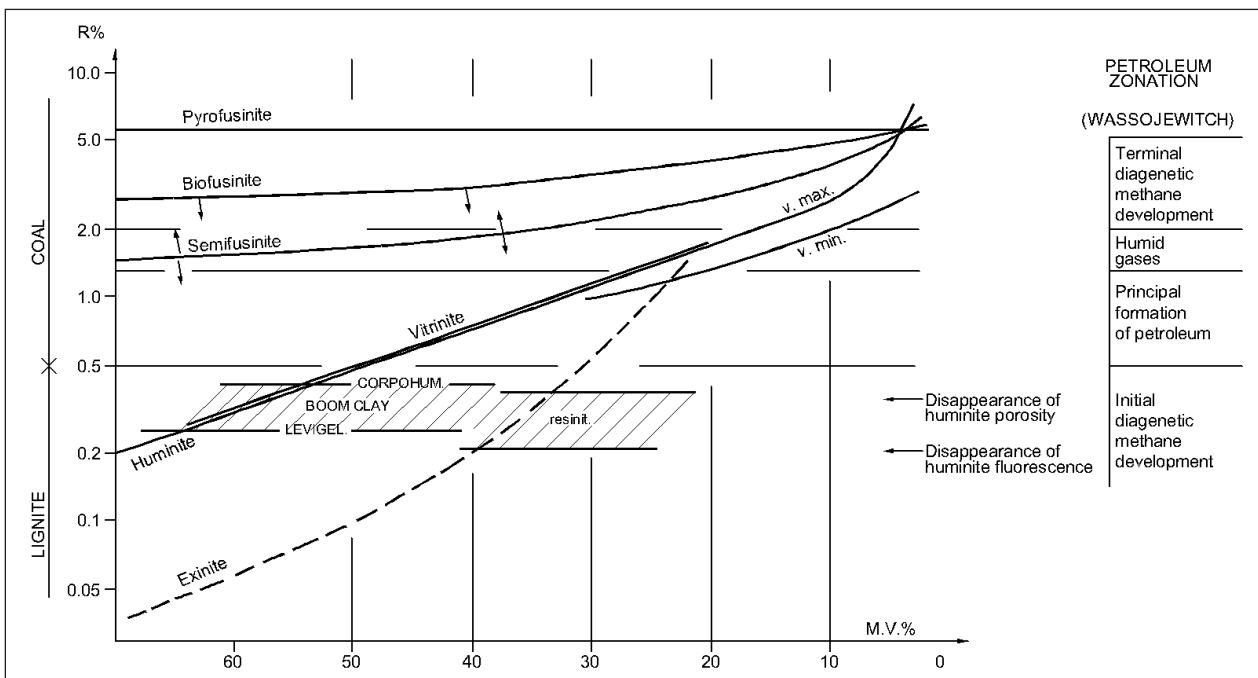
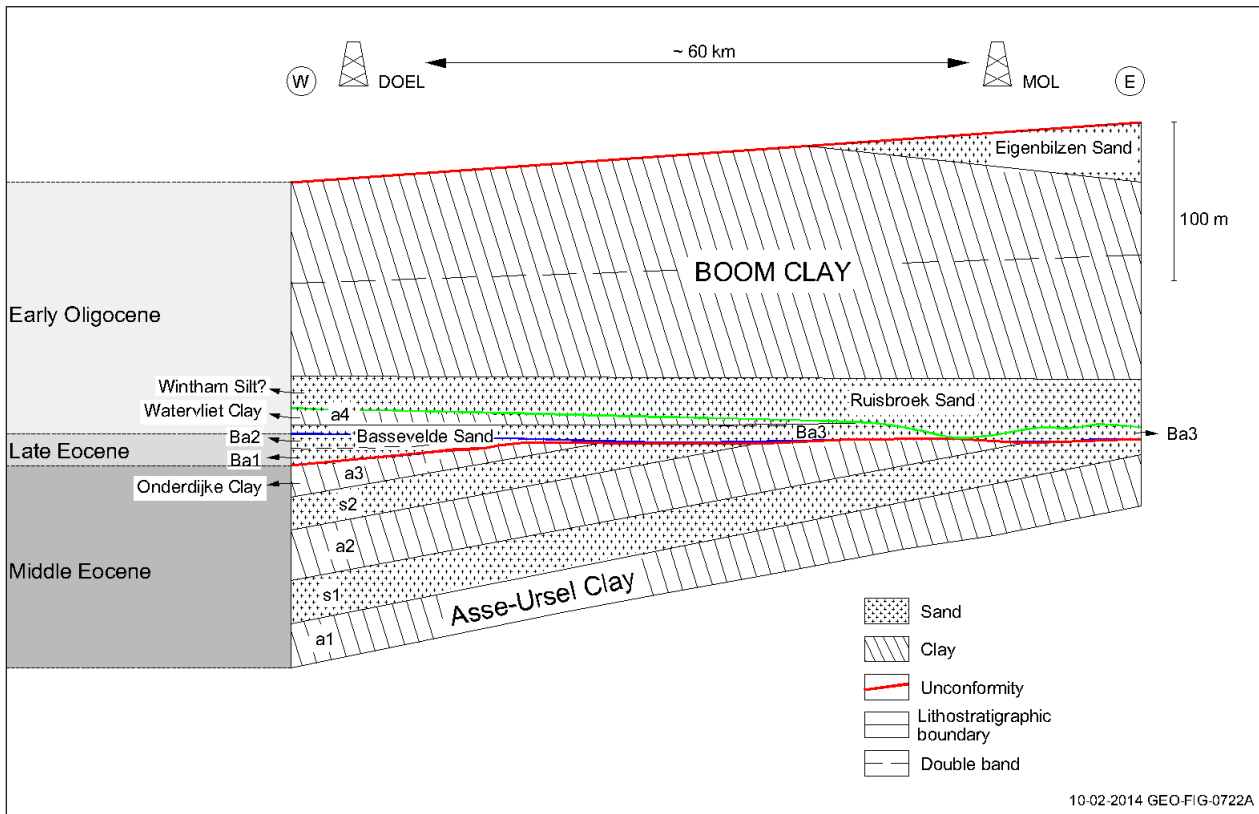


Figure 8. Organic diagenetic zonation and the position of the Boom Clay. M.V. (Matière Volatile) % is the volatile matter content and R% is the reflectivity of light measured under de microscope on polished sections of phytoclasts extracted from the clay. Different types of organic particles exist in sediments; the Boom Clay data are measured on huminite and resinite phytoclasts (from Vandenberghe, 1978).



Figuur 9. Schematic cross-section through the Upper Eocene to Lower Oligocene of northern Belgium (location of Doel see Figure 2 and of Mol see Figure 1). The vertical scale can be estimated from the Boom Clay thickness of about 100 m at Mol. The upper unconformity is Savian (see discussion in text). Note the erosive character of the base of the Ruisbroek Sand (green line) and the major unconformity underlying the Bassevelde Sands (Pyrenean unconformity). The precise extension of the Bassevelde 1, 2 (Ba1, Ba2) is not well known (see Saeys et al., 2004) but these two earliest Bassevelde sequences have a limited geographical extension compared to the Bassevelde 3 sands (Ba3); the Ba3 sands and Watervliet Clay can be correlated with the Sint-Huibrecht-Hern Formation more to the south and the east and together these deposits form the earliest Rupelian sequence (see Figure 23). In earlier stratigraphic literature the Onderdijke Clay and Watervliet Clay are indicated as respectively a3 and a4 and the Bassevelde Sand and Ruisbroek Sand as respectively s3 and s4 (see Figure 4) (from Vandenberghe et al., 2003).

3.2. The micro-lithostratigraphy of the Boom Clay

The key in understanding the detailed stratigraphy of the Boom Clay is the observation that the very characteristic layering of the clay, in bands of several dm thickness and with varying shades of grey, is continuous over the entire outcrop area and also in the subsurface of the Campine and even in part in the Netherlands and in the Lower Rhine area. This detailed correlation is first discussed below and followed in section 3.3 by the grouping of the layers with similar properties into formal lithostratigraphic units.

3.2.1. The outcrop area

The microstratigraphy of the Boom Clay was developed in the outcrop area (Vandenberghe, 1974, 1978; Gullentops & Vandenberghe, 1985; Vandenberghe & Van Echelpoel, 1987).

The main characteristic of the Boom Clay in the outcrop area is its layering (Figure 10); the layering originates from a periodic clay/silt sorting process in the basin resulting in clay layers rich in silt alternating with clay layers poor in silt content. These two types of grain-size layers in the Boom Clay have been described using varying nomenclature in the diverse publications cited in the reference section: ‘clays enriched in silt’ are also described as silt-rich clay, silty clay to clayey silt, silt and ‘clays poor in silt’ are also described as silt-poor clay, clay, pure clay, heavy clay. The nomenclature of sand-silt-clay mixtures is further discussed in 4.1.1. with reference to Figure 27.

Black horizons are rich in silt-sized particulate land-derived organic matter, and systematically occur in the upper part of the clay exposed in the outcrop area, staining this part of the clay black. In the grey clay below, a few black horizons occur as well. Each black horizon systematically starts in the top of a silt-rich clay band and ends in the basal part of the silt-poor clay band.



Figuur 10. Boom Clay outcrop in Terhagen-Rumst. The layered nature of the clay, i.e. the alternation of clay and silty clay layers, is clearly visible. The black horizons contain land-derived organic matter. Whitish-grey marly bands (as observed at the bottom of the picture) contain carbonate concretions. The pronounced two pale grey and closely spaced layers of silty clay in the middle of the picture correspond to the coarse double band (DB).

Whitish-grey marly bands can also be observed in the Boom Clay: the original horizons enriched in carbonate later developed into horizons with septarian carbonate concretions ('septaria' for short). The characteristics of the concretions are similar within a single horizon but differ between various horizons. These characteristics are mainly related to their size, their composition (calcium or ferroan carbonate) and to the nature of the mineral precipitates in the septae.

In practice, similar sections in different outcrops can be correlated using bands that have particular and easily recognisable properties; these layers have the official stratigraphic-bed status in the lithostratigraphic nomenclature (Vandenberghe & Wouters, 2011). These key horizons to the field geologist are (Figure 11): the sideritic septaria horizon S60, two successive coarse silt bands known as the double layer (DB), a pinkish to brownish horizon (R red), a sharp contact between grey and black clay due to the start of the systematic and pronounced occurrence of organic rich layers, two thick silt units at the base of the clay and finally several septaria horizons (indicated as S in Figure 11). In particular S20 and S50 have characteristic properties: S20 has the largest septaria - at least in the outcrop zone - and

concretions with a diameter up to a few meters has even been observed in Steendorp by one of the authors (MDC), S50 consists of flat septaria with multicoloured pyrite crystals covering the septae fracture walls. Using these key horizons for correlation, it appears that all other bands in between the key horizons also remain constant over the entire outcrop area, and therefore a composite stratigraphic section could be established for the outcrop area. On such a composite section, the stratigraphic section of the clay exposed in a particular clay pit, or at another observation point such as a borehole, can be indicated as shown for some clay pits in Figure 11.

3.2.2. The Antwerp Campine subsurface area

The Antwerp Campine is the western part of the Campine area; its eastern limit approximately corresponds to the location of the Mol Rauw fault (Figure 2). The numerous investigation boreholes drilled in the subsurface of the Antwerp Campine area allowed to extend the microstratigraphic knowledge of the Boom Clay, mainly by the use of geophysical well logging. Examples of such natural gamma ray and resistivity logs and their use for subdividing the Boom Clay are shown in Figures 13, 21, 24.

The relationship between mainly resistivity signals on the logs and the known micro-lithological succession of the clay, as described in Figure 11, was established in some cored holes in the outcrop area; this relationship was then used to interpret the Campine subsurface geophysical borehole logs, mainly resistivity and natural gamma-ray, using all available calibration possibilities from cores and a variety of analyses (Vandenberghe et al., 2001). In the upper part of the Boom Clay section, which is not exposed in the outcrop area, the microlithostratigraphy is elaborated using the geophysical resistivity imaging tool (Figure 12).

As a result it was demonstrated that the micro-lithostratigraphy established in the outcrop area and depicted in Figure 11 could be followed layer by layer into the Antwerp Campine area. In addition, it was shown that the additional thickness in the Campine subsurface compared to the outcrop area was due to an additional stratigraphic section on top of the clay in the outcrop area, rather than to a stratigraphic thickening of the existing outcrop section. Therefore, it was possible to complete the outcrop section upwards. This more complete section of the Rupelian in the Campine subsurface is represented in Figure 12. As the layers are continuous, a numbering system for the different layers has been introduced. The numbering system was introduced in the outcrop area and afterwards applied to the subsurface part. Different numbering systems exist because the very silty base of the clay can be numbered in different ways, because in some schemes also septaria horizons are numbered and because a specific numbering was also introduced for mathematical periodicity analyses. All used micro-lithostratigraphic numbering systems have been plotted in Figure 12.

3.3. The formal lithostratigraphy and the extension to the south and the east

In the outcrop area along the Rupel and Scheldt rivers, and in the Antwerp Campine area, the clayey section between the underlying and overlying sandy deposits, respectively the Ruisbroek Sand and either Voort Sand of Chattian age or the sand deposits of the Miocene Berchem Formation, can be subdivided into formal formations and members all belonging to the Rupel Group. These subdivisions have a regional significance based on the established lateral continuity as discussed in 3.2.

Formally, the Chattian Voort Formation was also part of the Rupel Group. Although its larger grain size and macro-fossil fragment content could allow an easy distinction from the underlying Rupel Group units, identifying its base on geophysical well logs alone can be confusing and biostratigraphical data in cored boreholes may be needed (Van Simaey, 2004a,b; De Man, 2006; De Man et al., 2010). A proper biostratigraphically calibrated geophysical log boundary signature is shown for the Mol, Dessel and Weelde wells in Figure 13.

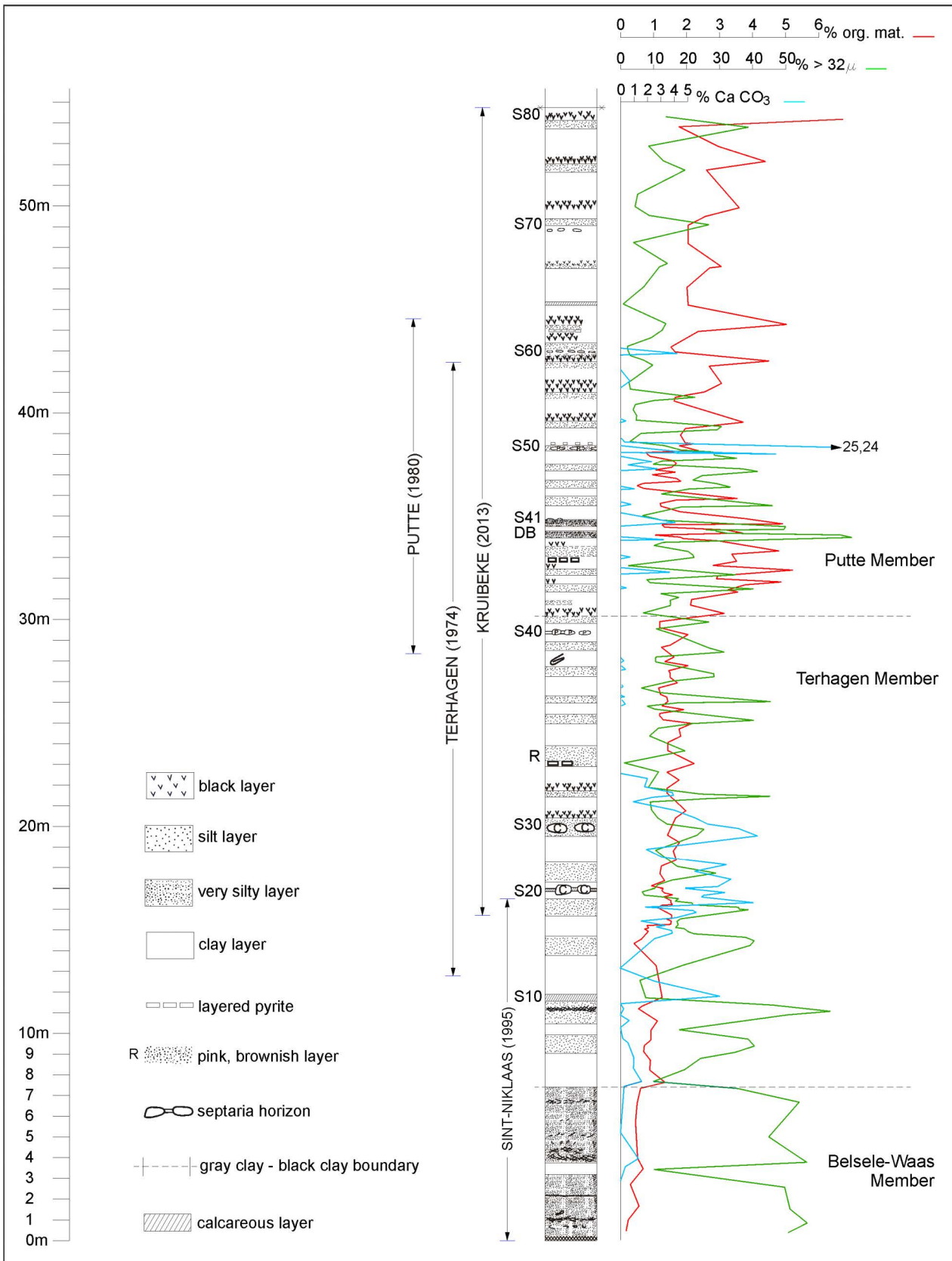
The lowest unit of the Rupel Group is the Belsele-Waas Member of the Boom Formation (Figure 11). This member is characterized by two unusually thick silt layers compared to the other layers commonly present in the Boom Formation. Initially, the Belsele-Waas Member was defined between the base of the Boom Clay and the base of the clay unit containing S10 at its base. However, based on geophysical well logs, the top of the Belsele-Waas Member has been redefined as the top of the upper thick silty layer because this top can very easily be identified on resistivity and natural gamma-ray well logs (Vandenberghe & Wouters, 2011).

The Terhagen Member overlies the Belsele-Waas Member. It is a grey clay with only a minor number of black stained layers. This clay unit contains dispersed carbonate in its lower part and contains three septaria horizons, all having the walls of the septae voids covered with a yellowish-brown iron bearing calcite. It also contains the pink, or reddish to brown band, its precise colour depending on humidity conditions of the clay surface. The top of the member is defined by the sudden systematic occurrence of black bands in the overlying clay, causing a distinct boundary between grey and black clay (Figures 10,36). This boundary is also easy to recognise on natural gamma-ray logs (P/T boundary on Figure 13).

The overlying clays, characterized by the systematic occurrence of black bands rich in vegetal organic matter, belong to the Putte Member. In this clay unit, the coarse grained silty 'double band' occurs, also easily recognised on resistivity and natural gamma-ray logs (Figure 13).

A characteristic large amount of pyrite is associated with the organic matter. Septaria horizon S50 has its septae walls even covered with pyrite crystals. Furthermore, the sideritic level S60 also occurs in the Putte Member. The upper boundary of this member has been placed where the clay starts to become more silty as expressed by the increasing resistivity values and decreasing gamma-ray response in the geophysical well logs (Figure 13).

The overlying silty clay unit is named the Boeretang Member of the Boom Formation. Note that this member was previously considered as the upper part of the Putte Member, also denoted as the 'Transition Zone', but recently redefined as the Boeretang Member (Vandenberghe & Wouters, 2011). This member gradually contains more silty clay than silt-poor clay bands as shown by cores and by the geophysical well logs, on the basis of which this package can easily be identified. Its top contains a well developed series of silt and clay layers, which can individually be numbered and identified on the logs (Neerdael et al., 1981; Dethy and Neerdael, 1983; Vandenberghe et al. 2001; Mertens, 2005b). The top of the Boeretang Member is placed where this distinct alternation stops and above which level increasing resistivity and decreasing gamma-ray values can be identified in well logs (Figure 13).



Figuur 11. Microstratigraphic lithology of the Boom Clay in its type outcrop area, with indication of some key horizons. S: Septaria layers, R: Red layer, DB: Double Band. The sections exposed in some classical clay pits are indicated to the left of the stratigraphic column; the exposed section in a clay pit changes over time and in the figure the maximal exposed section ever observed is selected, marked by one of the years during which this maximal exposure could be observed (after Vandenberghe & Van Echelpoel, 1987).

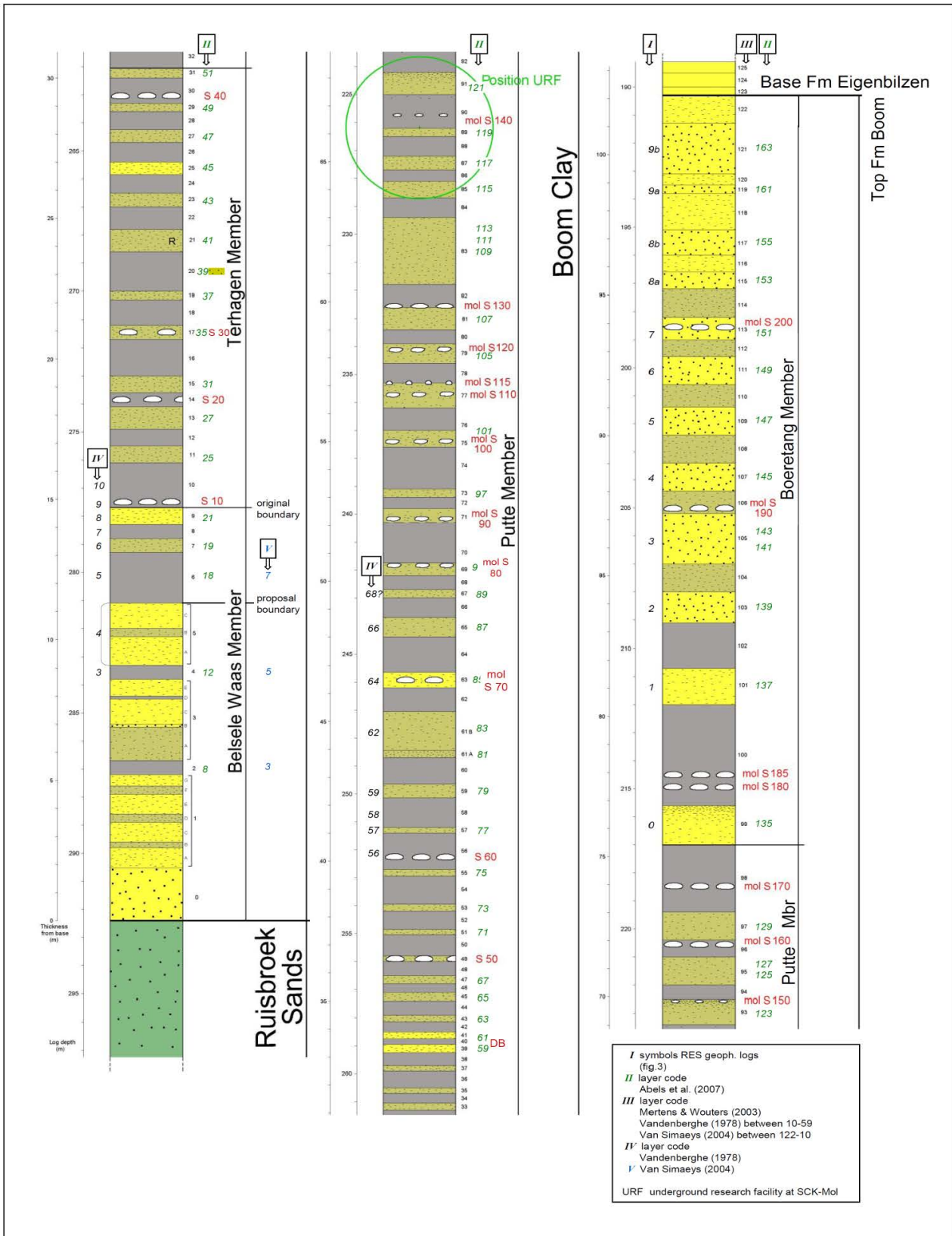
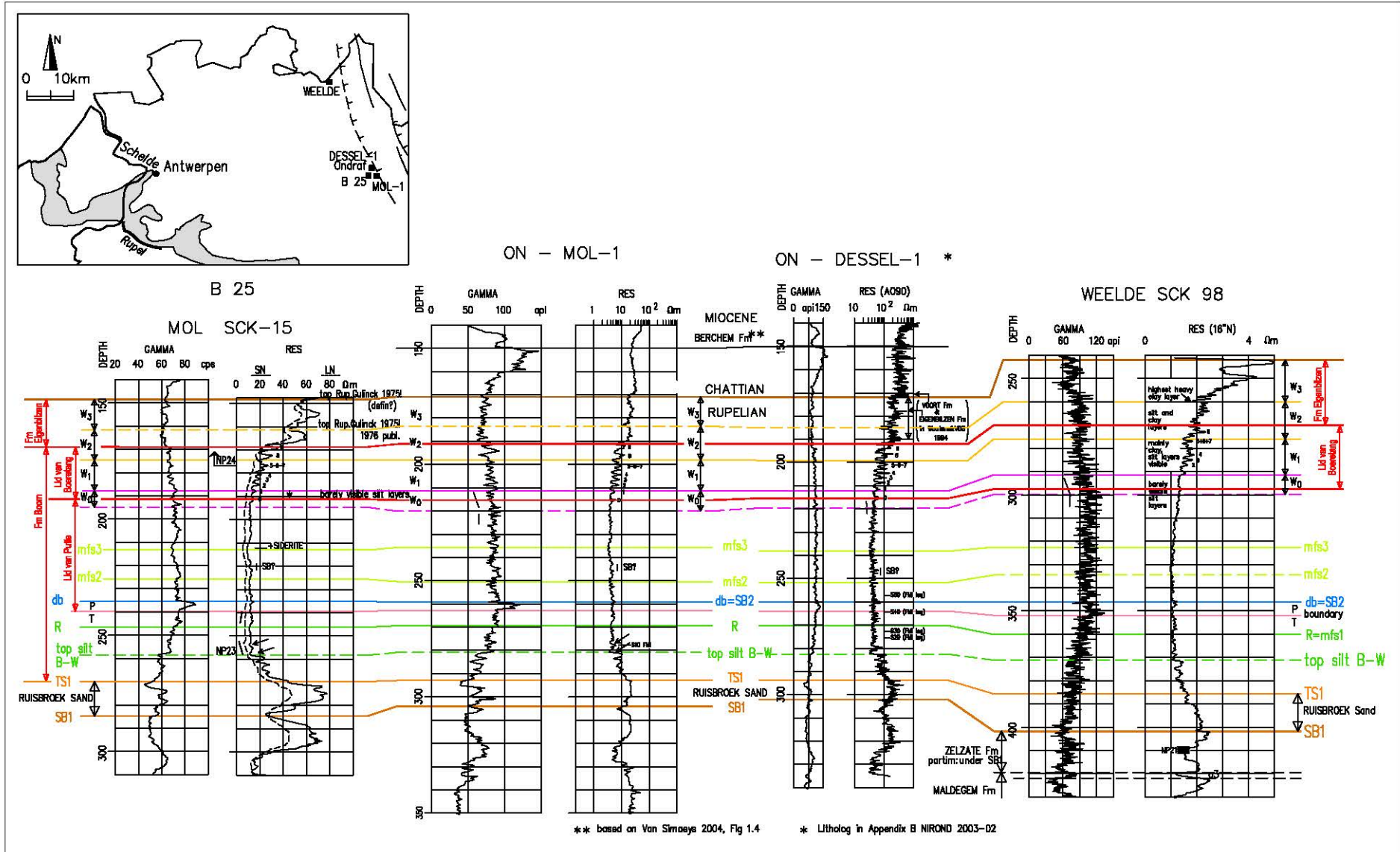
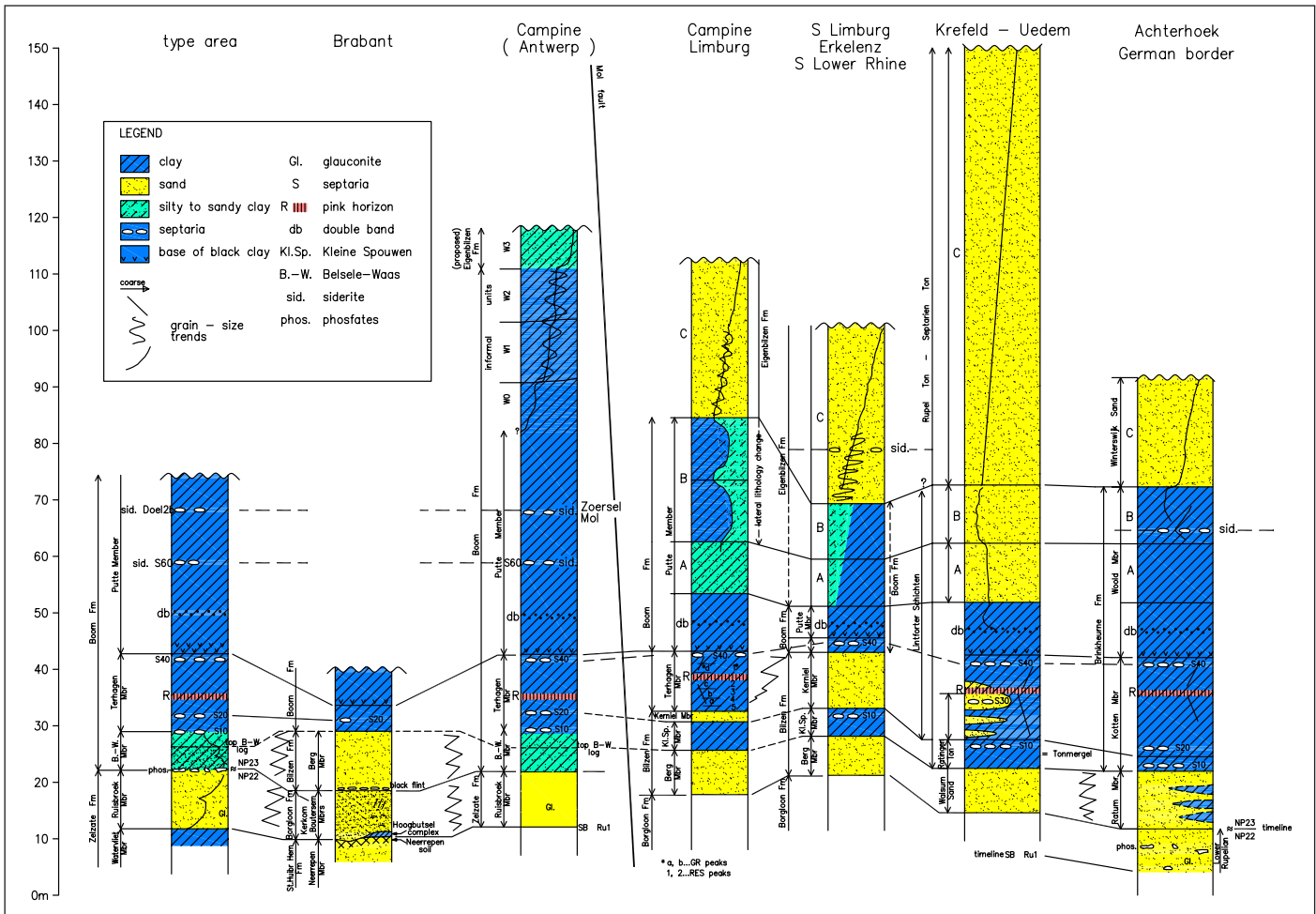


Figure 12. Microstratigraphic lithology of the Boom Formation based on the FMI (Formation Micro Imager, Schlumberger) of the ON-Mol-1 (log depth (m)) and ON-Dessel-1 boreholes (see Figure 13) (Mertens & Wouters, 2003). The existing numbering systems of the layers (Abels et al., 2007; Vandenberghe, 1978; Van Simaey, 2004a) are plotted in several columns in parallel to the layer codes introduced by Mertens & Wouters (2003); this microstratigraphic scheme can be found and is explained at the ncs website (reference in Figure 4) (Vandenberghe & Wouters, 2011). The green circle indicates the position of the HADES underground Research facility (URF) in Mol.



Figuur 13. Stratigraphic re-interpretation of the Rupelian-Chatthian boundary in boreholes drilled in the Mol-Dessel region. ‘P/T’ indicates the boundary between the Terhagen and Putte Members, and ‘top silt B-W’ the boundary between the Belsele-Waas and Terhagen Members (from Vandenberghe & Wouters, 2011). SB and mfs are respectively a Sequence Boundary and a main flooding surface in terms of sequence stratigraphy.



Figuur 14. Stratigraphic correlation of Boom Clay in the type area in northern Belgium, the Antwerp Campine, the Limburg Campine, southern Limburg, Krefeld in Germany, and the Achterhoek in the Netherlands (from Vandenberghe et al., 2001). Note the more sandy nature of the Rupel Group to the east of the Mol Rauw Fault. There, the units A,B,C make up the Eigenbilzen Formation as formally defined by the National Stratigraphic Commission (Vandenberghe & Wouters, 2011). However, in many situations a precise lithological boundary between the Eigenbilzen Formation and the underlying Boom Clay is difficult to assess; this is expressed also in the former identification of both formations on the figure which dates from 2001.

In the deposits overlying the Boeretang Member, and hence overlying the Boom Clay Formation, the amount of fine sand increases significantly while silty and clayey intervals are still present. Clay layers typically occur at the base and are absent higher up in the unit. As this unit is clearly more sandy than the underlying Boom Formation, this upper unit is called the Eigenbilzen Formation, analogous to the fine sandy deposits above the Boom Clay that are well developed in the Limburg Campine area (Matthijs, 1999; Vandenberghe et al., 2001). The geometrical outline of the Eigenbilzen Formation east of Mol is well described by the profiles on the 1:50 000 Hasselt geological map sheet. East of the Mol-Rauw fault zone, the sandy nature of this formation increases and it can be further subdivided based on the geophysical log response (Figure 14). Based on well logs, Vandenberghe et al. (2001) have distinguished three

units (A, B, C) in the sandy deposits between the Boom Clay and the Voort Sands (Figure 14). These three sandy units A, B, C have been defined as the Eigenbilzen Formation by Vandenberghe & Wouters (2011). However in Limburg the units A and B clearly represent a lithological transition from clay below to sand above as shown in Figure 14, suggesting that further stratigraphic studies are needed in the area to the east of the Mol Rauw Fault.

Also towards the east it can be noted on Figure 14 that the silty Belsele-Waas Member develops laterally into a sandy unit, the Berg Sand Member. In addition, a sandy intercalation develops laterally in the Terhagen Member, named the Kerniel Sand Member. In the middle of the Kerniel Sands in eastern Belgium, a gravelly horizon has been reported, together with a fauna representing very shallow water

conditions (Baut and Génault, 1999; Vervoenen, 1995). Where the Kerniel Sands occur, they split off a lower part of the Boom Clay in the top of which the lowest observed septaria horizon S10 occurs (Figure 14); this part of the clay is known as the Kleine-Spouwen Clay Member. The Berg Member, the Kleine-Spouwen Member and the Kerniel Member are grouped in the Bilzen Formation, underlying the Boom Formation (Figure 4). This subdivision in east Limburg was already recognised since the early mapping results by Van den Broeck (1883, 1884, 1893) and Van den Broeck & Rutot (1883).

Towards the former shoreline in the south the silty Belsele-Waas Member is also replaced by the Berg Sand Member of the Bilzen Formation. In the same direction as far south as the deposits are preserved today, namely the Leuven-Tienen area in Brabant, no Kerniel Sands have been observed intercalated in the clay. In the Terhagen and Putte Clay Members only a stratigraphic thinning towards the south is noticed, which had already started in the north (Figure 15).

The stratigraphic relationships between the different lithostratigraphic units underlying the Bilzen and Boom Formations and their interpretation as an early Rupelian sequence shown in Figure 23, is discussed in Vandenberghe et al. (1998, 2002, 2004)

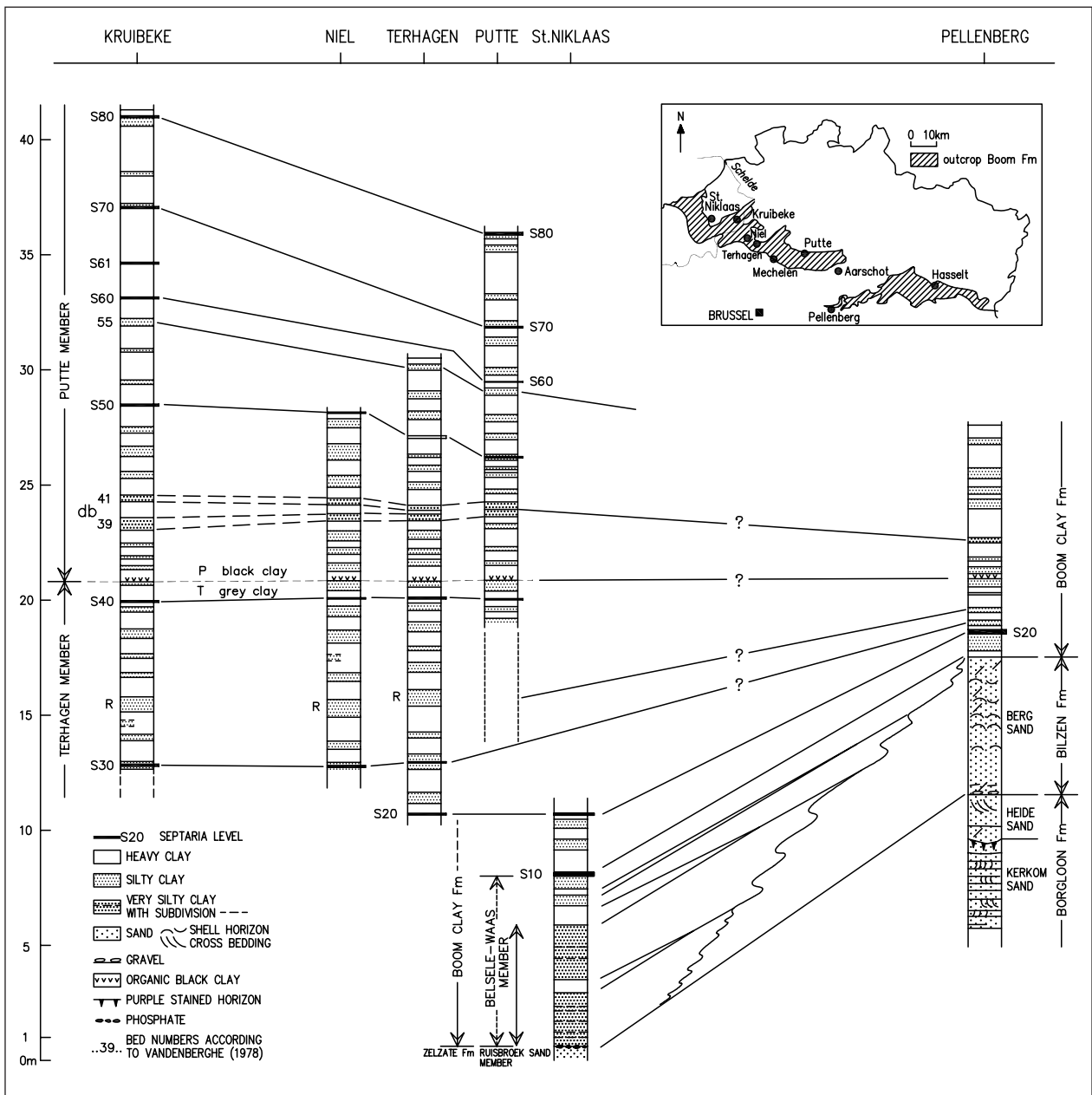


Figure 15. Stratigraphic correlation of the Boom Formation in the clay pits along a N-S profile. Key horizons are the septaria layers S, the red layer R, the double band DB, and the boundary between the grey and the black clay (from Vandenberghe et al., 2001, modified after Van Echelpoel, 1991).

When comparing the Boom and Bilzen Formation subdivisions in Belgium with the time equivalent clayey deposits in the neighbouring countries, using geophysical borehole logs and a few cored wells for calibration, some remarkable similarities and correspondences are observed (Vandenberghe et al., 2001). The Bilzen Formations in Limburg and in the Lower Rhine area are comparable, and also septaria-horizons S10 and S20 can be correlated as far as into the Achterhoek area in the Netherlands (Figure 14). The boundary between the Terhagen and Putte Clay Members is also a marked event that can be correlated into the Lower Rhine and the Achterhoek areas, including the septaria horizon S40 just below the boundary and the coarse double band (DB) a few meter above the boundary (Figure 14). Foraminiferal biofacies analysis in Belgium and in the Mainz Basin in Germany (Grimm & Steurbaut, 2001) has demonstrated that the boundary between the Foraminiferenmergel and the overlying Fischschiefer in the Mainz Basin, and probably also in the Upper Rhine Graben in general, corresponds exactly to the Terhagen/Putte boundary. Also the bio-events used to subdivide the Foraminiferenmergel B and the Fischschiefer in the Mainz basin, correspond to respectively the R horizon and the coarse double band of the Boom Formation (Grimm & Steurbaut, 2001).

3.4. *Biostratigraphy of the Boom and Eigenbilzen Formations*

Macrofossil studies have focused on bivalves (De Koninck, 1837; Ortlieb & Dollfus, 1873; Vincent, 1889; Glibert, 1955, 1957; Janssens, 1981), decapods (Van Beneden, 1872; Stainier, 1887; Verheyden, 2002; van Bakel et al., 2009) and fish remains (Leriche, 1910; Herman, 1984; Steurbaut & Herman, 1978). These fossil groups essentially indicate the paleoenvironment rather than the bio-chronostratigraphic position. To a large degree, this also holds for some of the studied microfossil groups, namely foraminifera (Batjes, 1958; Hooyberghs, 1983; Hooyberghs et al., 1992), calcareous nannoplankton (Steurbaut, 1992), ostracoda (Key, 1957), pollen and spores (Roche, 1978; Roche & Schuler, 1979) and dinoflagellate cysts (Stover & Hardenbol, 1994; Van Simaey, 2004a; Van Simaey et al., 2004c, 2005a). However, several microfossil groups also provide bio-chronostratigraphic information. Regarding the Oligocene Boom and Eigenbilzen Formations, calcareous nannoplankton, planktonic foraminifera, benthic foraminifera and dinoflagellate cysts contents provided valuable information concerning the stratigraphic position of these units in the international chronostratigraphic time scale (Vandenberghe et al., 2004; De Man, 2006). This is not an obvious challenge. The shape of the North Sea sedimentary basin had only few connections to the ocean that can be closed easily by either tectonics or global sea-level changes. The evolution of organisms in the North Sea basin happened somewhat differently than in the oceans and the correlation to oceanic organisms is not obvious and in several cases impossible.

International biostratigraphic schemes are preferably based on widely occurring oceanic organisms and therefore the correlation of the Boom Clay biozonations to such international schemes remains difficult.

Planktonic foraminiferal zones P17 to P21 of Blow (Blow, 1969) have been recognised but zonal boundaries could not be identified. The calcareous nannoplankton zone NP22/NP23 boundary can be placed at the transition of the Ruisbroek Sand to the Boom Clay (Figure 16) and the boundary NP23/NP24* is situated between S190 and S200 (Figure 16). The label * of a biozone means that the index marker of the zone is not present but a substitute marker species has been used to define the biozone.

A North Sea Basin benthic foraminiferal biozonation with intervals and facies subdivisions has been established that can be applied to the Boom and Eigenbilzen Formations: intervals OI to OVIII and facies 1 to 15 in Figure 16 (De Man, 2006). The dinoflagellate cyst content allowed to distinguish 4 dinocyst zones that can be used for international correlation: NSO3 to NSO5a (Figure 16). In the international biozonation schemes, time calibration of several bio-events is rather well established and these calibrated event for calcareous nannoplankton, dinoflagellate cysts and benthic foraminifera are reported in Figure 16. Based on this calibrated biostratigraphic information the Rupelian Boom and Eigenbilzen Formations are comprised between 32 (NP22/NP23 boundary) and 28,1 Ma (Rupelian/ Chattian boundary) (Vandenberghe et al., 2012).

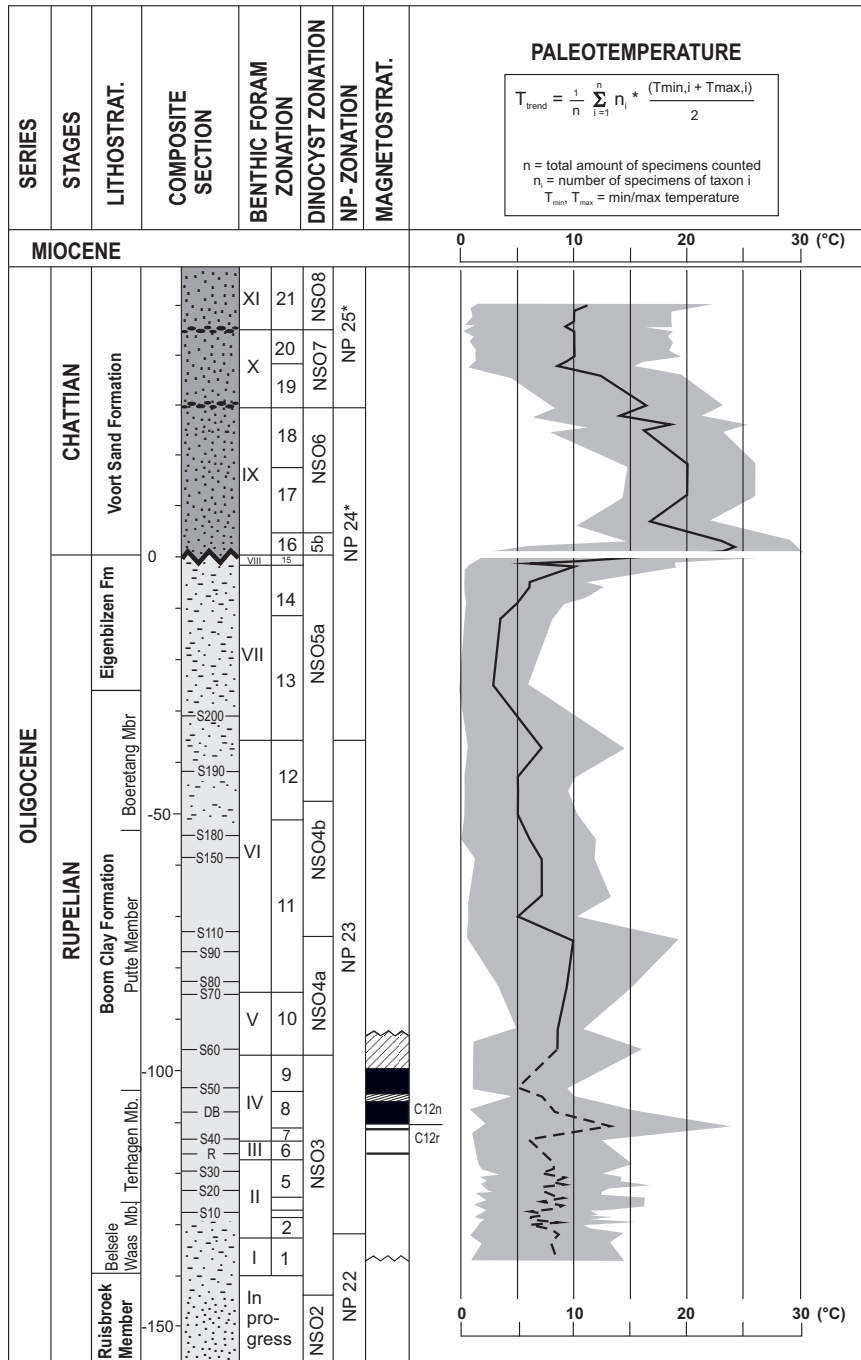
The presence of only some reworked *Svalbardella* dinoflagellate cysts at the top of the Boom Clay in the Campine area point to a short erosive interval, estimated at 500 ka, between the Rupelian and the Chattian, as this *Svalbardella* interval occurs in the Oligocene sections both in the more central North Sea and in the southern Italian Tethys realm (Van Simaey et al., 2005a).

3.5. *Magnetostratigraphic data*

Magnetostratigraphy uses time-calibrated pole reversals which are of very short duration and which can be identified if associated with detailed biostratigraphic data. The rock magnetism of the Rupelian Boom and Eigenbilzen Formations were studied in detail in the outcrop section and in the complete sections of the ON-Mol-1 and Zoersel boreholes (Lagrou, 2001; Lagrou et al., 1996, 2004). The results from the boreholes could not be interpreted in a reasonable way probably because the magnetic orientation of the cores could not be established due to the weak signal. In the outcrop section, a magnetic polarity zonation could be established, notwithstanding the relatively low intensity of the natural remanent magnetisation (on average 0,4 mA/m), and the often unstable behaviour during demagnetisation. Demagnetisation showed trend directions but a stable end point was never reached. Therefore, the interpreted Normal or Reversed magnetic polarity was based on the appreciated

reliability of the demagnetisation trend (Figure 17). A reverse normal boundary was observed at the base of the silt layer occurring just below the Terhagen/Putte Members boundary. Although the available biostratigraphic control (3.4) (dinoflagellate markers on Figure 18) and the cyclostratigraphy (3.8.) seem to point to the reversal C12r/C12n at 31.034 Ma (Figure 18), the reliability of the interpretation of this observed reversal in the Boom Clay for stratigraphic purposes remains debatable. The reason is the very close relationship with the

base of the organic-rich and pyrite-rich Putte Member. Indeed, the magnetomineralogy points to magnetic iron sulphides, pyrrhotite or greigite, and magnetite as the carriers of remanence, although classical mineral extraction techniques could not separate these minerals from the samples. Greigite, as a low temperature mineral much more probable than the high temperature pyrrhotite, could be associated with pyrite as a primary remnant or a secondary alteration, because pyrite itself is associated with the organic matter in the Putte Member.



Figuur 16. Benthic foraminiferal biozonation, dinoflagellate and nannoplankton biozonation, and palaeotemperature curve for the Oligocene North Sea Basin successions. The label * of biozones NP24 and NP25 means that the index marker of the zone is not present but a substitute marker species has been used to define the biozone. Grey zone indicates the confidence interval, as calculated from minimum and maximum values for the temperature range of taxa (from De Man, 2006).

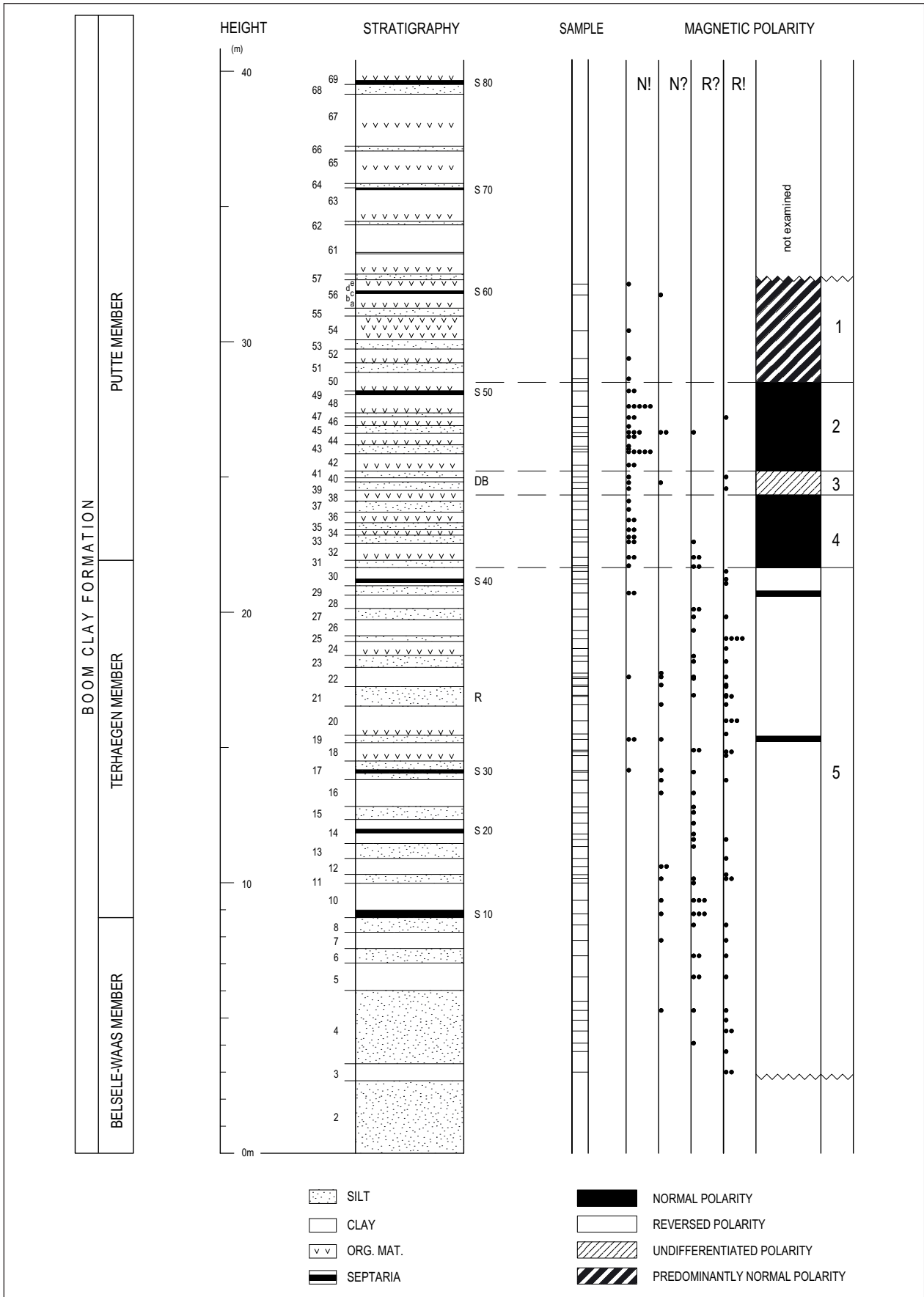


Figure 17. Magnetic Polarity classification of the polarity measurements plotted against the composite lithologic log of the type section of the Boom Clay. Five polarity intervals are distinguished (from Lagrou et al., 2004).

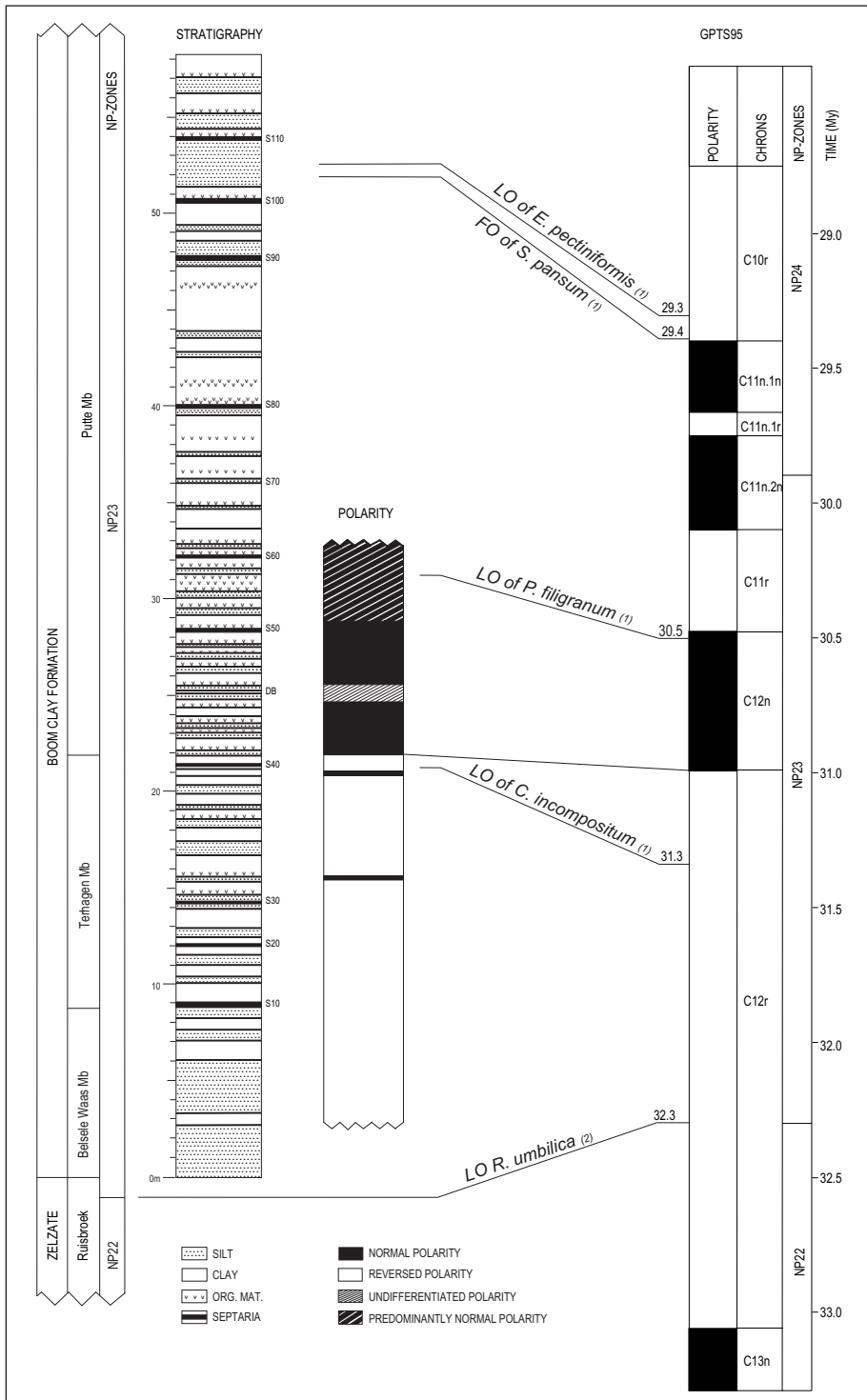


Figure 18. Correlation between the outcrop section of the Boom Formation and the magnetobiochronologic time scale (from Lagrou et al., 2004; time scale after Berggren et al., 1995). Absolute age of dinocyst events (1) after Hardenbol et al., 1998 and Williams et al., 2004; absolute age of nannoplankton events (2) after Hardenbol et al., 1998. Dinocyst events after Stover & Hardenbol, 1994 and Van Simaey et al., 2004. The R/N reversal in the outcrop area correlates with the C12r/C12n reversal. The combined-age-model ages in the GTS 2012 are for base C12r 33.16 Ma, base C12n 31.03 Ma, for base C11r 30.59 Ma, for base C11n.2n 29.97 Ma, for base C11n.1r 29.53 Ma, for base C11n.1n 29.48 Ma, and for base C10r 29.18 Ma (Vandenberghe et al., 2012).

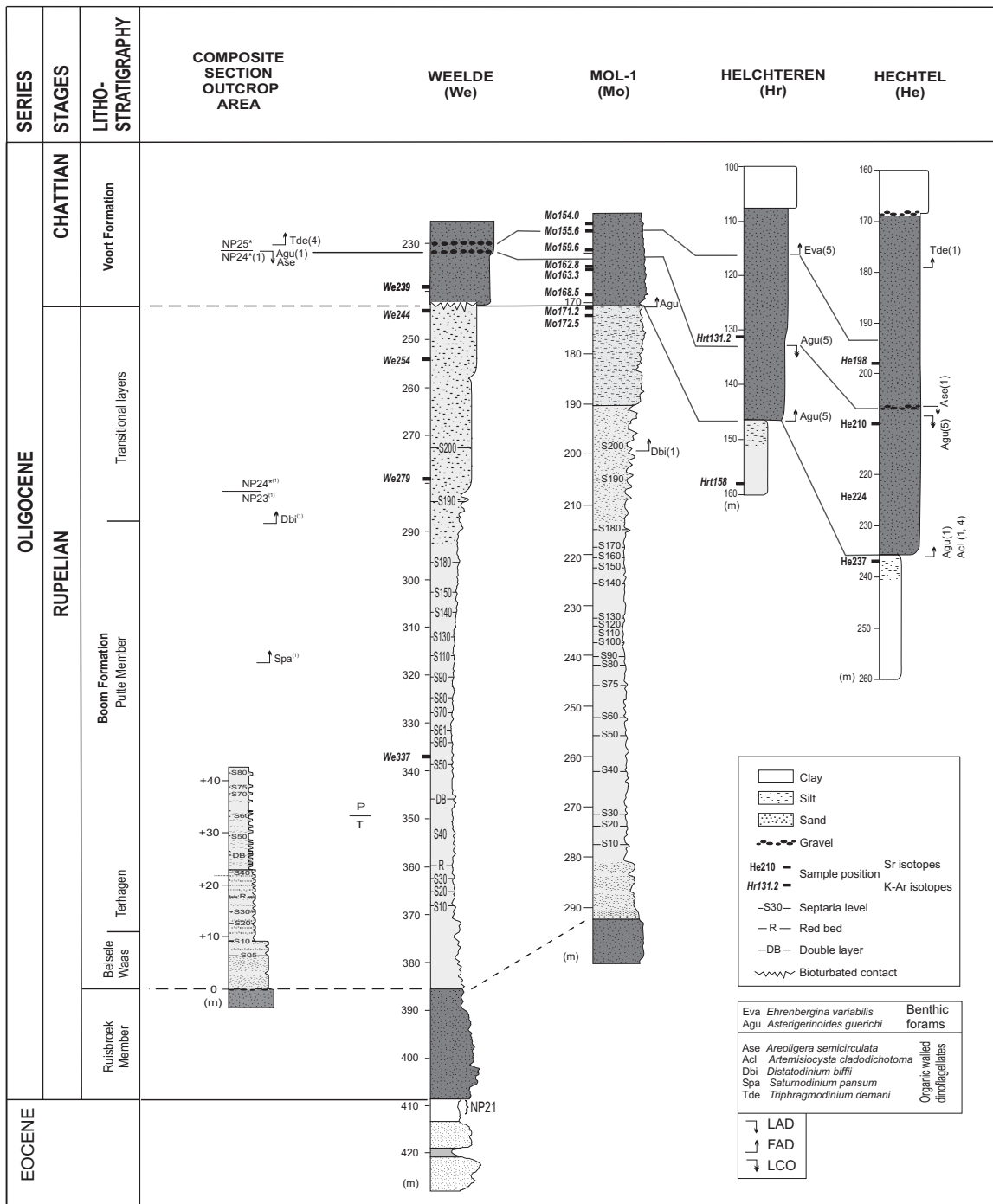
3.6. Radiometry and Sr-isotope dating

The stratigraphic time scale depends to a large extent on radiometric data, either directly or for calibration. In sedimentary rocks, it is difficult to obtain such data as the sediment particles are in almost all cases detrital. The current way to tackle this problem is the use of glauconite, which is the rare exception of a commonly occurring quasi-synsedimentary mineral, the use of isotope trends which has been formerly calibrated against time, and finally the radiometric calibration of the detailed

biozonation schemes in locations where datable volcanogenic minerals occur almost together with microfossils. The radiometric age data given with the fossil events in Figure 18 are obtained in the latter way. The age of the magnetostratigraphic reversal in Figure 18 is also a radiometric and cyclostratigraphic calibrated value of an initial age which was obtained from measured distances of the magnetic reversal boundary from spreading centers in different parts of the oceans, assuming a spreading rate model (see Vandenberghe et al., 2012).

The nature and the chronostratigraphic position of the Rupelian-Chattian boundary (Early-Late Oligocene) in the historical type areas in the southern North Sea Basin is examined using biostratigraphy, strontium isotope dating of benthic foraminifera, and K-Ar dating of glauconites (Figure 19, De Man et al., 2010). Especially the strontium isotope dating is a well-established technique that utilizes variations in the ratio of ^{87}Sr to ^{86}Sr in seawater to date the time of sedimentation (McArthur et al., 2001; Veizer et al., 1997). Authigenic carbonate,

such as foraminiferal tests, record fluctuations in seawater $^{87}\text{Sr}/^{86}\text{Sr}$ through time, and in combination with other techniques, such as biostratigraphy, $^{87}\text{Sr}/^{86}\text{Sr}$ can provide a numeric date (Elderfield, 1986; McArthur, 1994; McArthur et al., 2001). Most K-Ar measurements on glauconites are consistent with the strontium isotope data of the study of De Man et al. (2010). However, some discrepancies exist between glauconite dating and the stratigraphic position of the samples, showing the limitations of the age dating.



3.7. Oxygen isotope event stratigraphy

The stable oxygen isotope composition, namely the proportion of ^{18}O , in carbonate minerals such as shells or otoliths, also varies with time. In fact the oxygen isotope composition reflects the paleoclimatological condition as the composition is influenced by temperature and by ice volumes. Long-term climatic evolution trends can be recognised, also shorter cycles of climatic change are documented and even very short extreme climate aberrations can be detected.

For the Oligocene, the epoch of the Rupel Group sediments, such curves have been established in different parts of the oceans, in the North Sea and both for planktonic and benthic organisms.

In an isotope study using several organisms from the southern North Sea basin from middle Lutetian till the end of the Chattian, including the Rupel and the Campine areas, several world wide known isotopic marker events could be identified (Figure 20). These markers are enriched in the heavy isotope ^{18}O and point to cooling of the climate. The most remarkable cooling step (Oi 1 event) occurs at the base of the Ruisbroek Sands, underlying the Boom Clay. Other deep-sea benthic foraminiferal based known cooling events are less outspoken but still recognisable in the Boom Clay: near the double layer, near the base of the Boeretang Member, and at the Rupelian-Chattian boundary.

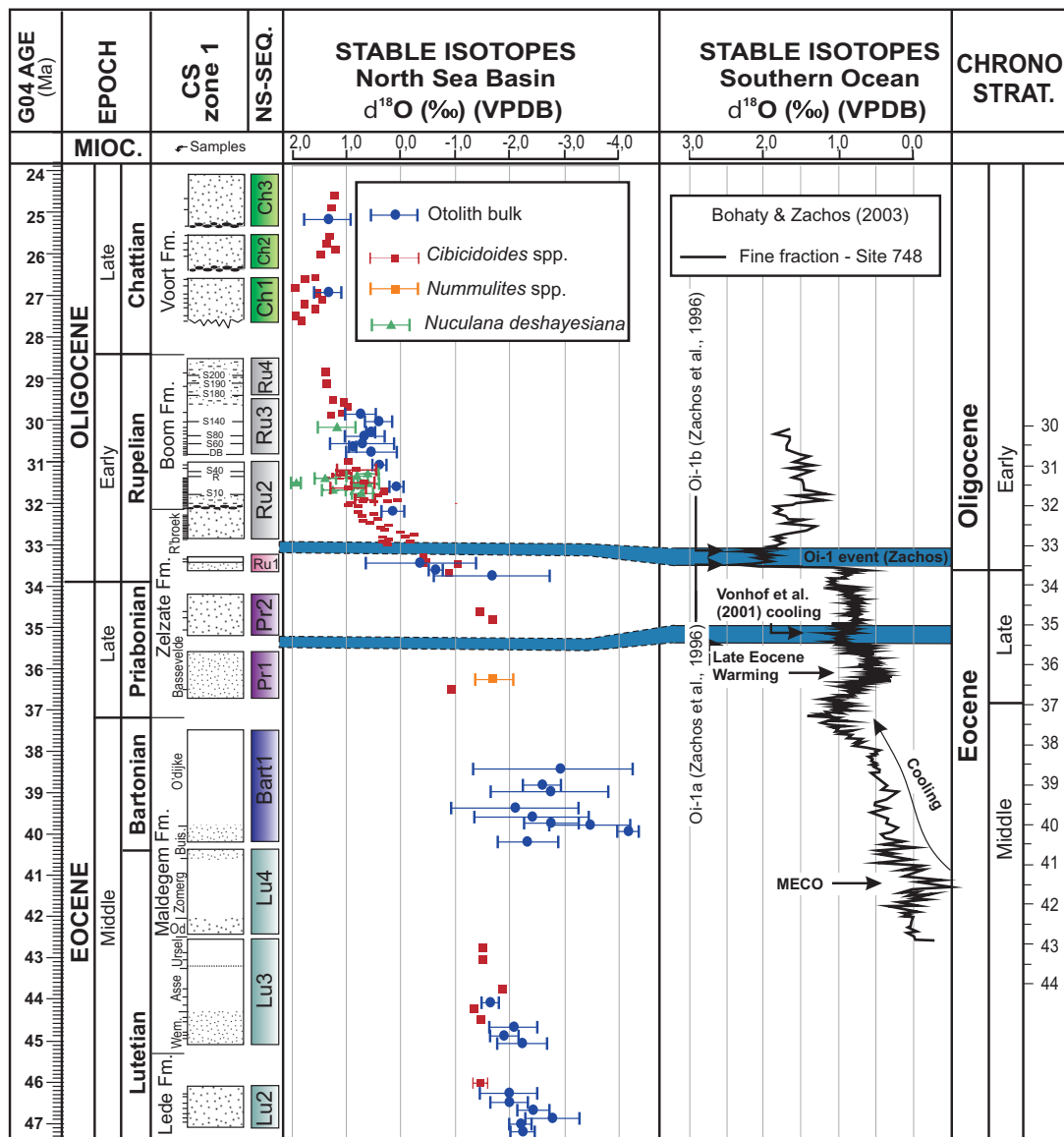


Figure 20. Oxygen isotope data obtained from different Eocene and Oligocene fossil types in the Belgian part of the southern North Sea Basin, reflecting the paleotemperature evolution and events. The data are plotted along a composite stratigraphic section subdivided in North-Sea sequences (NS-SEQ) (see 3.9 and also Vandenberghe et al., 2004). The positioning in the composite section of the global Rupelian Oi-1a,b isotope events of Zachos et al. (1996) and of other known temperature trends and events is done by calibration with the Bohaty & Zachos (2003) oxygen isotope curve (from De Man, 2006).

3.8. Cyclostratigraphy

Cyclostratigraphy has regained an important position in the stratigraphic methodology. It has been recognised that many of the sedimentary cycles long recognised in the sedimentary record are in fact astronomically

driven, so called Milankovitch cycles (Schwarzacher, 1993). Therefore such cycles can be used to accurately determine time durations of sedimentary intervals and even accurately date events if properly anchored at events with well known independent age control.

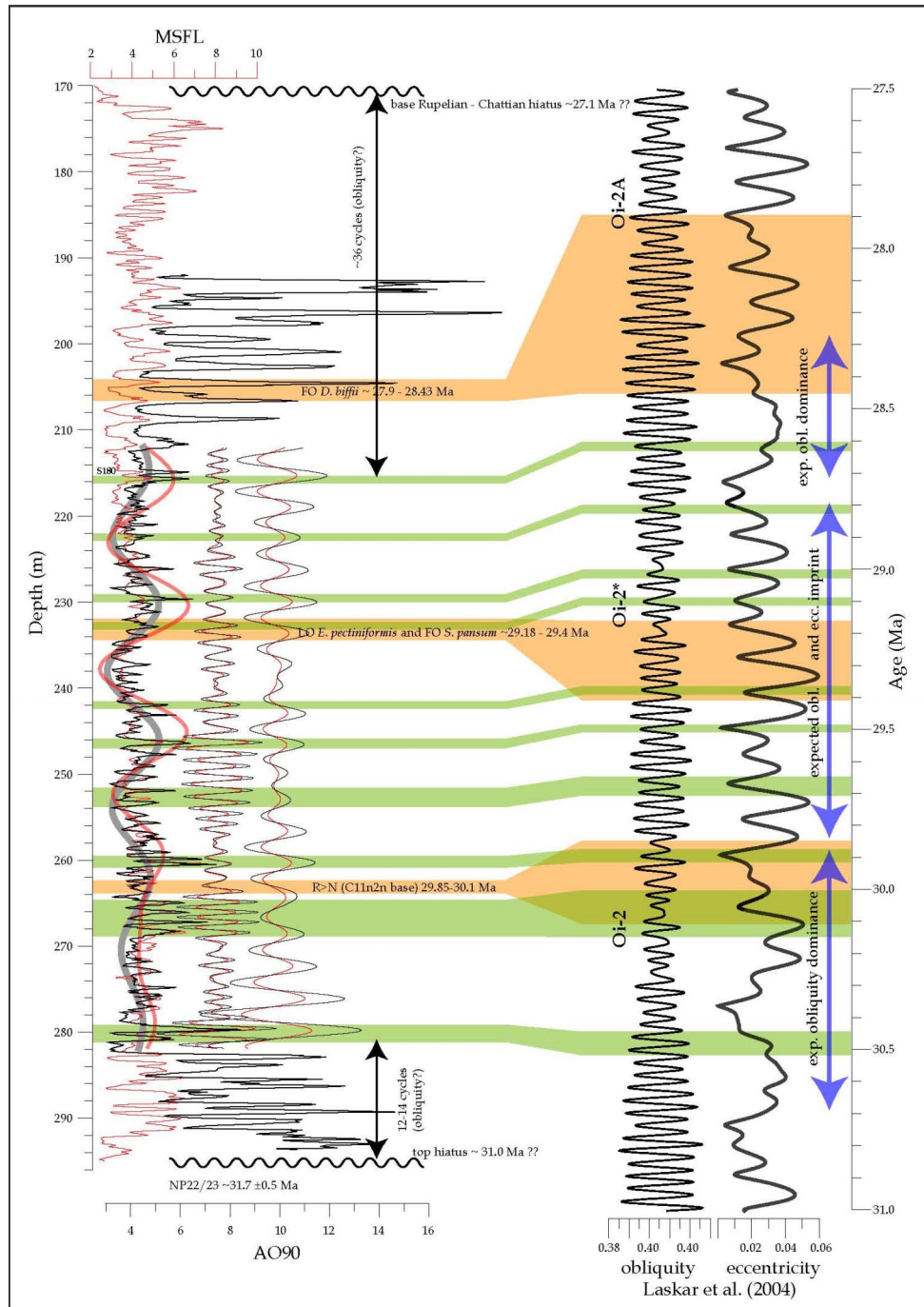


Figure 21. Tuning of the AO90 and MSFL resistivity records of the Dessel borehole to the Laskar et al. (2004) obliquity target curve using available ages. The frequency signals extracted from the resistivity curves are shown in the left part of the figure together with the original resistivity logs: the obliquity signals (center), the low eccentricity signals (right) and the long eccentricity signals (left). Dashed vertical arrows to the right show intervals where the astronomical target curves suggest periods of forcing dominance of obliquity or of obliquity and eccentricity. Ages of the top of the lower hiatus and the base of the upper hiatus were calculated by counting small-scale cycles that however may not continue to be obliquity cycles in those intervals. For the top interval, the cycle pattern for nearby well-logs is also used. Asterisks indicate used age tie-points for the time-series analysis. Indicated Oi-events are from Wade & Pälike (2004) (from Abels et al., 2006).

As the banding cyclicity in the Boom Clay is one of the most striking characteristics of the deposit, several attempts have been undertaken to prove its relationship with Milankovitch cycles and to determine which orbital parameters controlled the formation of the banding (Gullentops & Vandenberghe, 1985; Van Echelpoel & Weedon, 1990; Van Echelpoel, 1991, 1994; Vandenberghe et al., 1997).

Initially, Walsh step functions have been applied to band thickness series in the outcrop area (Van Echelpoel & Weedon, 1990; Van Echelpoel, 1991, 1994). Later on, a power spectral analysis was performed on continuous resistivity data of the ON-Dessel-1 borehole over the stratigraphically more complete Boom Clay section in that area, using also a better stratigraphic age control in the section than was possible in the earlier attempts (Abels et al.,

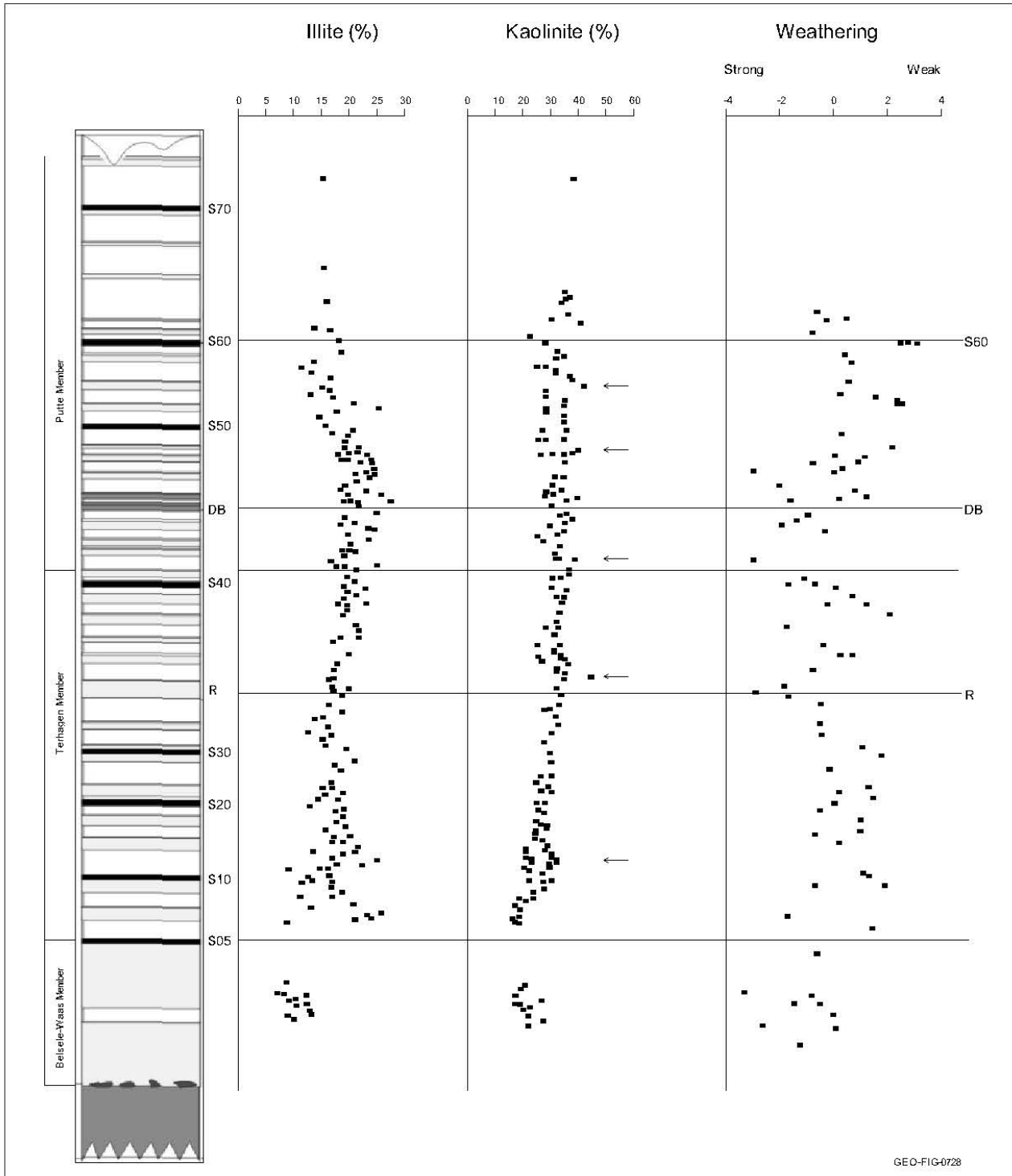


Figure 22. Variations in illite, kaolinite and weathering parameters through the Boom Clay in its outcrop area. The arrows mark higher kaolinite contents occurring at the maximal flooding position of the intermediate duration cycles (4.2) (after Laenen, 1997, 1998, and Vandenberghe et al., 1998).

2007). The result is that the grain-size and organic matter banding is primarily driven by the 41 ka obliquity cycle. In addition, a secondary imprint of about 100 and 405 ka eccentricity can be demonstrated, and even some precession related variations have been established (Figure 21). Tuning the results to the calculated astronomical target curves for the Rupelian time can only be tentative as no highly reliable age calibration point is available till now. The proposed correlation of the section with the calculated obliquity curve (Figure 16), displaying the 41 ka and the 1,2 Ma cyclicity, is based on linking the highest resistivity or coarse intervals, thought to represent the shallowest sea-level positions, to combined obliquity and eccentricity minima, as experiences in other Oligocene sections have learned (Wade and Pälke, 2004; Abels et al., 2005).

Detailed geochemical analyses in the outcropping Boom Clay have suggested the presence of cycles reflecting changes in water depth with durations between about one million and half a million year (Laenen, 1997, 1998). These geochemical variations could reflect sea-level variations. Weaker weathering can reflect increased erosion rates at low sea-level when climate was also colder; more preserved detrital illite can be explained in the same way. A higher kaolinite content occurs at high sea-level and reflects a northern provenance. Variations in illite, kaolinite and weathering parameters are presented in Figure 22.

3.9. Sequence stratigraphy

Sequence stratigraphy has become a standard tool in stratigraphy. The methodology has its origin in the reflection seismic exploration of sedimentary basins for oil and gas, where it was observed that sediments are arranged in individual packages corresponding to changes in sea-level. Initially, it was hoped that many of the observed sea-level changes were global and that this would lead to a global sequence chart (Haq et al., 1987,1988). It has turned out that the global sea-level variations expressed by the individual sequences, are disturbed and overprinted by local tectonic sequences and by the multiple scales on which the packages occur. Still, the identification of sequences remains a standard procedure as it integrates all data available on the sediments and as the succession of sequences does indeed reflect the evolution of relative sea-level, or more generally speaking of base-level, although the causes of this evolution are not always global and more often local. In any case, the identification of the sequences in a particular area is a good base for comparing the stratigraphy with the stratigraphic succession in neighbouring and more remote areas. The lateral variation in facies within a single sequence might then reflect the regional bathymetrical variability of the basin at that time.

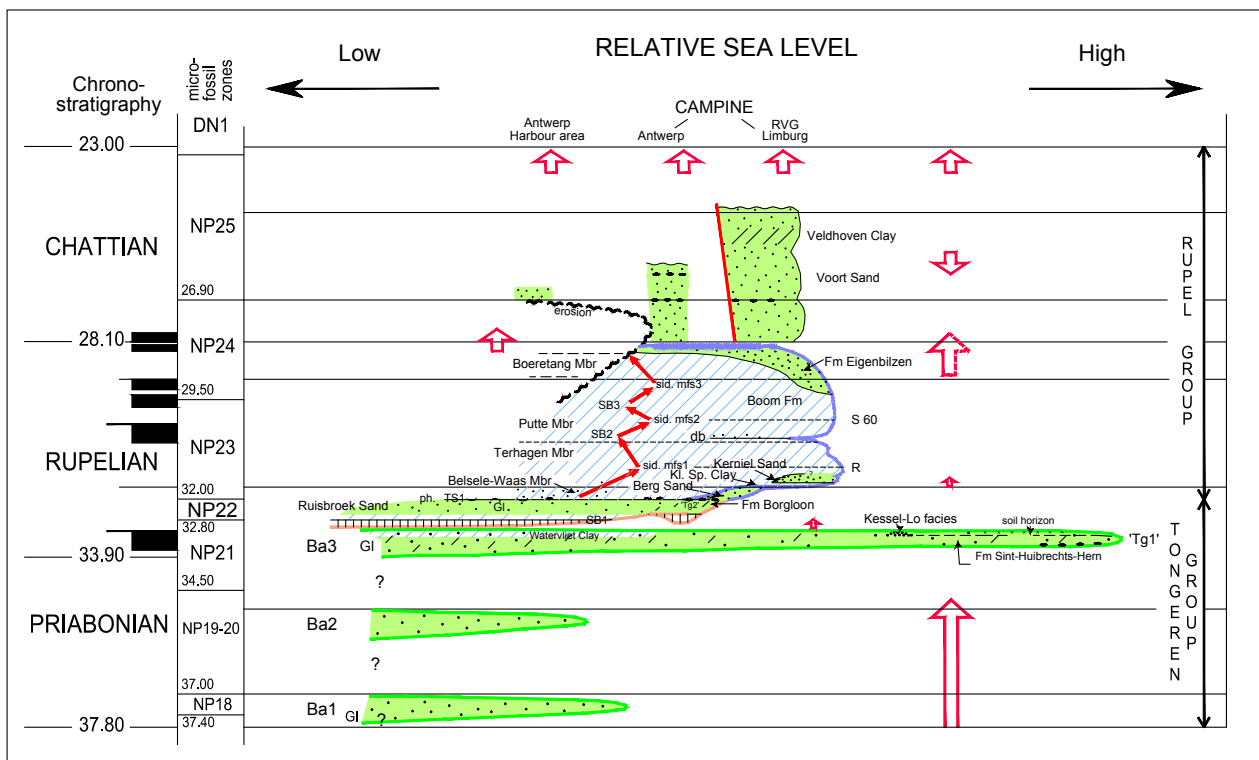
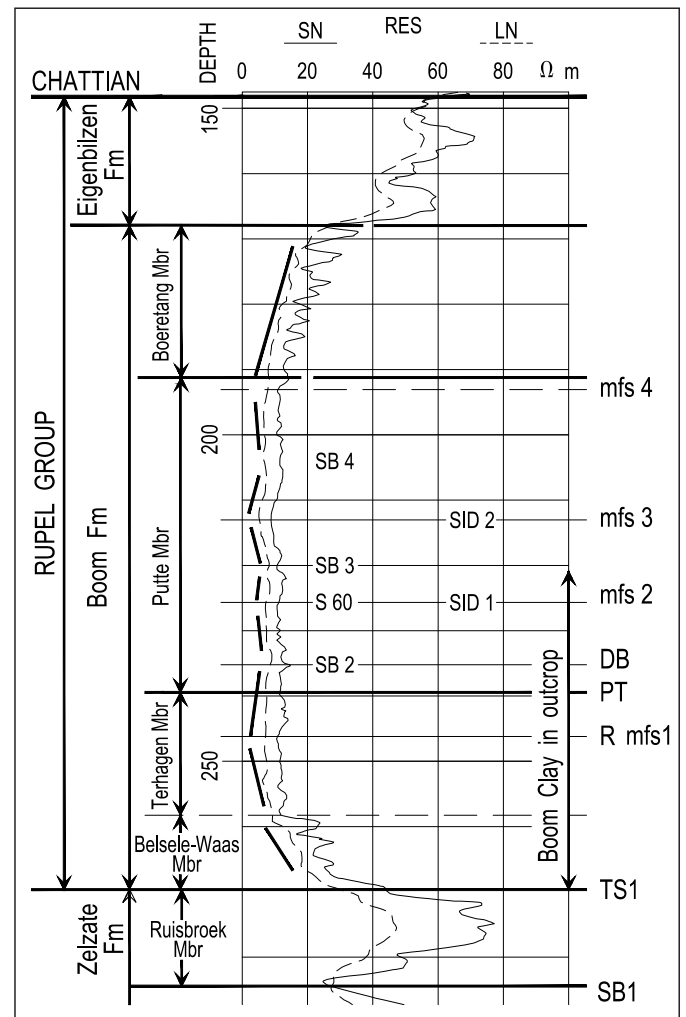


Figure 23. Sequence stratigraphic data and interpretation for the Rupelian (modified from Vandenberghe et al., 2004). In green are deep marine or coastal deposits, in blue are deeper marine clays. SB 1, 2, 3 are sequence boundaries and mfs 1, 2, 3 are main flooding surfaces as discussed in the text; SB 1.2, 1.3... are suggested additional sequence boundaries based on geochemistry by Laenen (1997). Siderite levels are indicated by Sid. Vertical hatching estimates the eroded interval. The full and dashed red line arrows to the right of the Rupelian-Chattian transition indicate uplift and subsidence tectonics at that time discussed in 4.6.

Identifying a sequence is based on the vertical evolution of the facies expressed by changes in lithology, fossils, grain-size trends, chemistry and mineralogy. In the shallow parts of epicontinental seas, such as the southern part of the North Sea, erosive levels may form the basis of a sequence. Continental deposits may fill the space created by the erosion, followed by a full transgression of the sea over the area till a maximum flooding is attained, after which the basin gradually fills up again till a new low sea-level starts eroding the earlier deposited sediments again, and a next sequence may start to form. In this way, the succession of sequences reflects the succession of local or global sea-level fluctuations (Vandenberghe et al., 1998, 2004).

In the Oligocene sediments of North Belgium, an earliest Oligocene sequence is developed during the NP21 biochron comprising facies of the Sint-Huibrechts-Herne Formation, upper Bassevelde Sand and Watervliet Clay (Figure 23). The next sequence has an erosive base (sequence boundary 1, SB1) filled with marine sands, the Ruisbroek Sand, in the deeper part of the basin and with lagoonal to estuarine deposits of the Borgloon Formation in the coastal area (Vandenberghe et al., 2002). These early deposits in the sequence have developed during the NP22 biochron. At the start of the NP23 biochron, the sea invades the entire area and the transgression causes the Boom Clay to deposit, while in the more coastal areas, Berg Sand and Kerniel Sand develop as time-equivalent lateral facies. The transgressive surface (TS1) associated with this flooding is expressed by a phosphatic horizon underlying the Belsele-Waas Member and a black flat flint pebble horizon underlying the Berg Sand (Figure 35 ,37). The R pink horizon corresponds to the very fine grain-size (Figure 11, 35) in the lower part of the clay and is interpreted as the deepest water deposit of this sequence (mfs 1). The sequence above the R horizon becomes coarser and ends at the coarse double layer above which a next sequence starts (SB2) as indicated by the fining of the grain size (Figure 11, 35). The main flooding surface (mfs 2) of this next sequence in the clay is again indicated by the change from fining to coarsening in the grain size evolution (Figure 11, 35) and remarkably corresponds to the sideritic septaria level S60. Another siderite level S90 has been observed in the Mol-SCK-15 borehole which could be the main flooding surface (mfs 3) of the next sequence (Figure 24). In between mfs 2 and mfs 3, SB3 should occur situated close to the top of the outcrop section in the Kruikebe clay pit where a maximum in silt content exists (Figures 23 and 24). The Boeretang Member, at the top of the Boom Formation, is characterized by a distinct coarsening upward and therefore must be the upper basin filling part of a sequence. This interpretation in terms of sedimentary sequences, taking the evolution of the measured borehole log resistivity

trends as a proxy for grain size and hence for water depth, is illustrated for two boreholes, Mol-SCK-15 (Figure 24) and Herentals (Figure 24).



Figuur 24. Resistivity well logs from the Rupelian interval in the Herentals well and the interpretation of the resistivity trends in terms of evolving water depths and therefore defining sequences (from Vandenberghe and Mertens, 2013). Full straight line fragments evolving to higher resistivity indicate shallowing water conditions, and evolving to lower values indicate deepening water. Lithostratigraphic units are indicated at the left side. PT is the boundary between Terhagen and Putte Members, the R horizon equals mfs1, DB horizon corresponds to SB2 level. The same approach was used to position the mfs and SB levels in Figure 13.

In the overlying Chattian Voort Sands of the Campine three sequences have been identified based on gravel in the glauconite sands and on dinocyst analysis (Van Simaey, 2004a).

4. The geology of the Boom Clay

4.1. The sedimentological significance of the grain-size and the organic matter rhythms

The key for understanding the sedimentological processes that formed the Boom Clay deposit lies in understanding the meaning of the coupled variations in grain size and organic matter content; they are expressed in the characteristic banding of the Boom Clay (Figure 11), the prominent appearance of the clay deposit in outcrop and on geophysical logs. As the septaria layers, also a prominent feature of the Boom Clay, do not seem to be related to neither grain-size nor organic matter, they will be discussed separately (4.3).

4.1.1. Grain size

Individual samples of Boom Clay are made up of mixtures of a population consisting of coarse silt and very fine sand, and a population consisting of clay and some fine silt (Figure 25). The proportion of the two populations gradually varies between the mid-points of the silty clay bands and the clay bands (Figure 276). Several sediment-nomenclature systems for fine-grained sediment exists in the literature. For this study, the classification of Shepard (1954) is used (Figure 27). From

continuous analyses (Figure 11, Figure 28) and resistivity logs (e.g. Figure 21, 24) it is clear that the variations are rather sinusoidal than graded, pointing to gradually varying sedimentological conditions.

A remarkable feature is that the coarsest grains in both silt-rich and silt-poor clay bands have the same size and that the size-proportion differences are expressed by a change in skewness of the coarse population accompanying the varying clay-sized particle proportions (Figure 26). The grain-size variation vertically across the banding therefore is expressed as a gradual change in skewness of the coarse population from the center of one silty band to opposite skewness in the center of the next clay band (Figure 28).

This type of vertical variation, coupled to the lateral continuity of the bands as was shown by the microstratigraphy (3.2) suggests a periodical winnowing of the sediment at the bottom or before it reaches the bottom. Waves are a good mechanism to do that and a few levels in the most silty layers of the Belsele-Waas Member showing flat gully type structures in which the sediment is sorted, and that also can be correlated between clay pits, support this wave sorting mechanism (Vandenberghe, 1978). The linking of the layering to an astronomically controlled mechanism (3.8) suggests that the wave controlled sorting mechanism must also be related to a fluctuating climate.

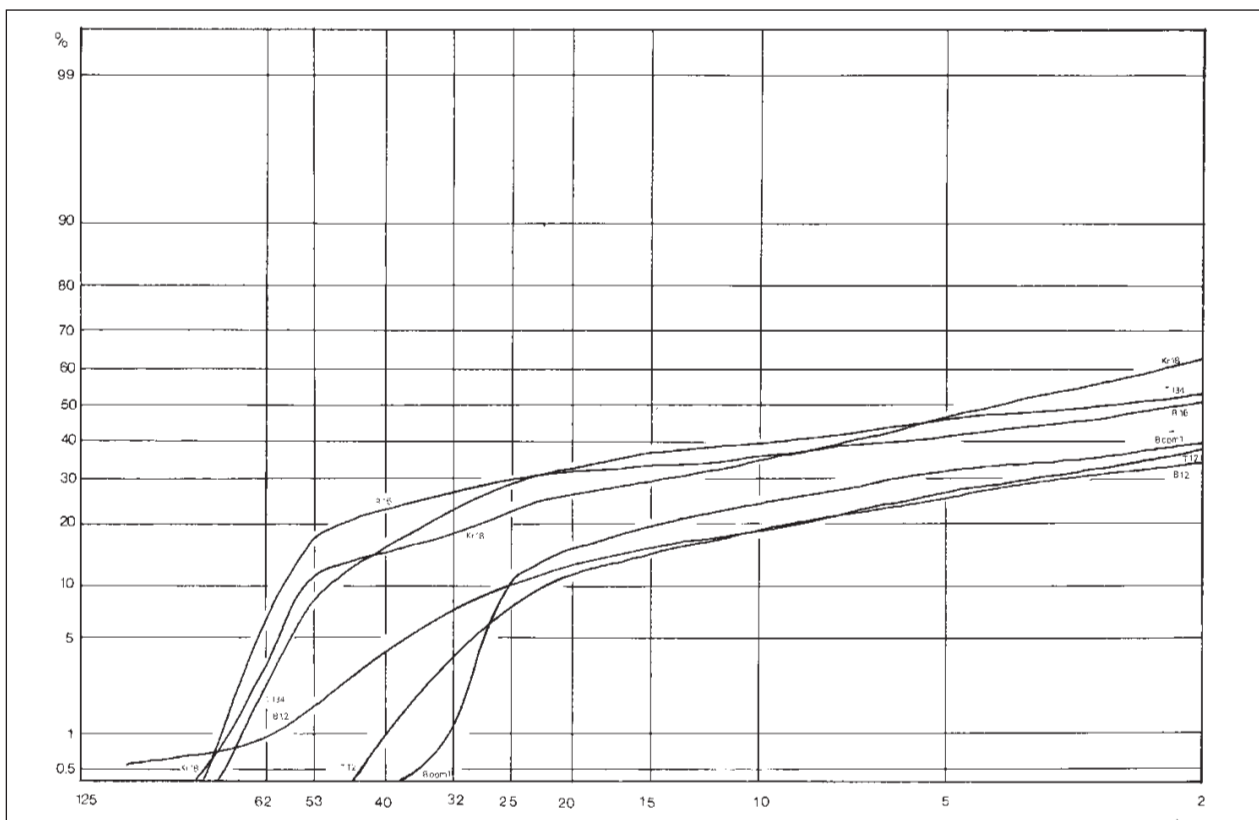
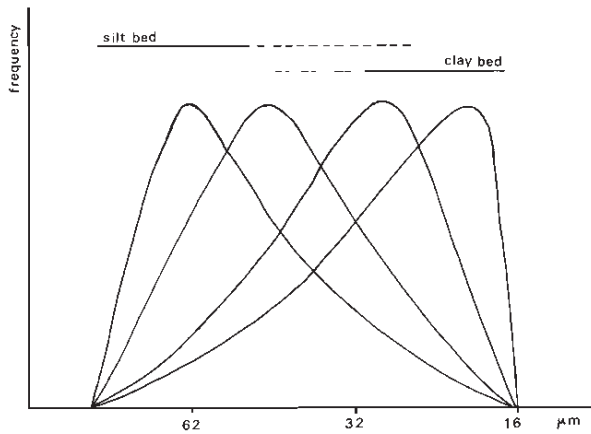


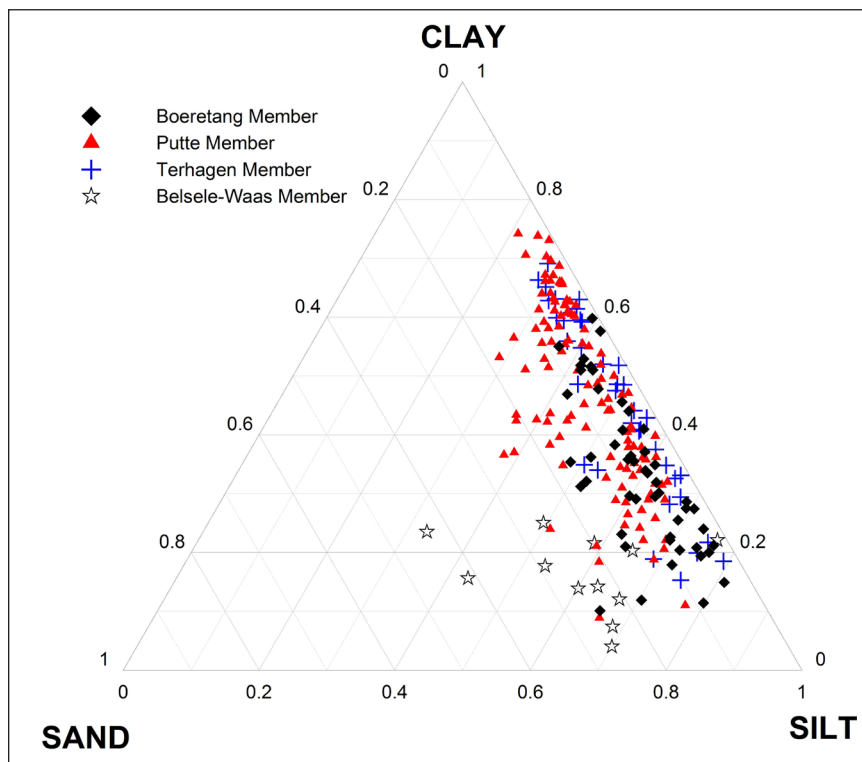
Figure 25. A selection of cumulative grain-size curves of the Boom Clay (from Vandenberghe, 1978). Note that the traditional subdivision between sand and silt at 62 μm does not have a sedimentological significance in this case of clay sediments. The 32 μm boundary often used in earlier work, for practical analytical reasons, to characterize the proportion of coarse and fine size populations appears a reasonable approach.



Figuur 26. Concept of the frequency distribution of grain sizes in the coarser subpopulation ($> 16 \mu\text{m}$) based on numerous grain-size analyses of the Boom Clay (from Vandenberghe, 1978). The gradual shift from a coarse-skewed distribution to a fine-skewed distribution and inversely, describes the grain-size shifts from the centre of a silty-clay layer to the centre of a silt-poor clay layer and inversely.

Wave controlled sorting with a sea bottom periodically in and out of the wave turbulence base also suggests a water depth between 50 to 150 m depending on the maximal wavelength in the sedimentary basin averaged over the duration that a freshly deposited sediment layer was

within the reach of the wave activity. The effective wave lengths in the epicontinental North Sea Basin during the Rupelian are estimated from present day measured wave characteristics in the southern North Sea; wavelength is derived from wave height and period and the longest yearly wavelength is 112 m but occasionally also 156 m wavelength occur (International Marine and Dredging Consultants, 2005). The time interval to be considered over which the upper Boom Clay deposited sediment is homogeneously sorted by frequently occurring waves can be estimated from the sedimentation rates obtained by the Milankovitch analysis (see 3.8). Supposing a 30 cm thick silt layer formed in 20 ka with most sorting occurring just above the sea bottom, because almost no wave sedimentary structures can be observed in the clay, and assuming that only the top 3 cm of the sediment is wave-influenced, then this slice of 3 cm remains for 2000 years under the influence of the waves. Therefore instead of 156 m an effective 200 m wavelength is considered. Turbulence depth is about half the wavelength and therefore 100 m is a reasonable water depth estimate, deeper during the deposition of the pure clay layers and shallower during the deposition of the silty clay layers. Water depth estimates from foraminiferal assemblages are around 100 m (De Man and Van Simaey, 2004) and from fish remains at least 50 m or deeper (Steurbaut and Herman, 1978). The most silty clays at the base of the clay are deposited at shallower depth considering the lower clay content and the presence of rare gutter channels (Vandenberghe et al. 2002).



Figuur 27. (top) Commonly used end-member triangle for classifying unconsolidated sediments on the basis of grain size taken from Shepard, 1954; (bottom) Similarly to the Shepard diagram constructed clay-silt-sand ternary diagram of the Boom Clay samples taken from various boreholes in Mol (from Honty, unpublished data).

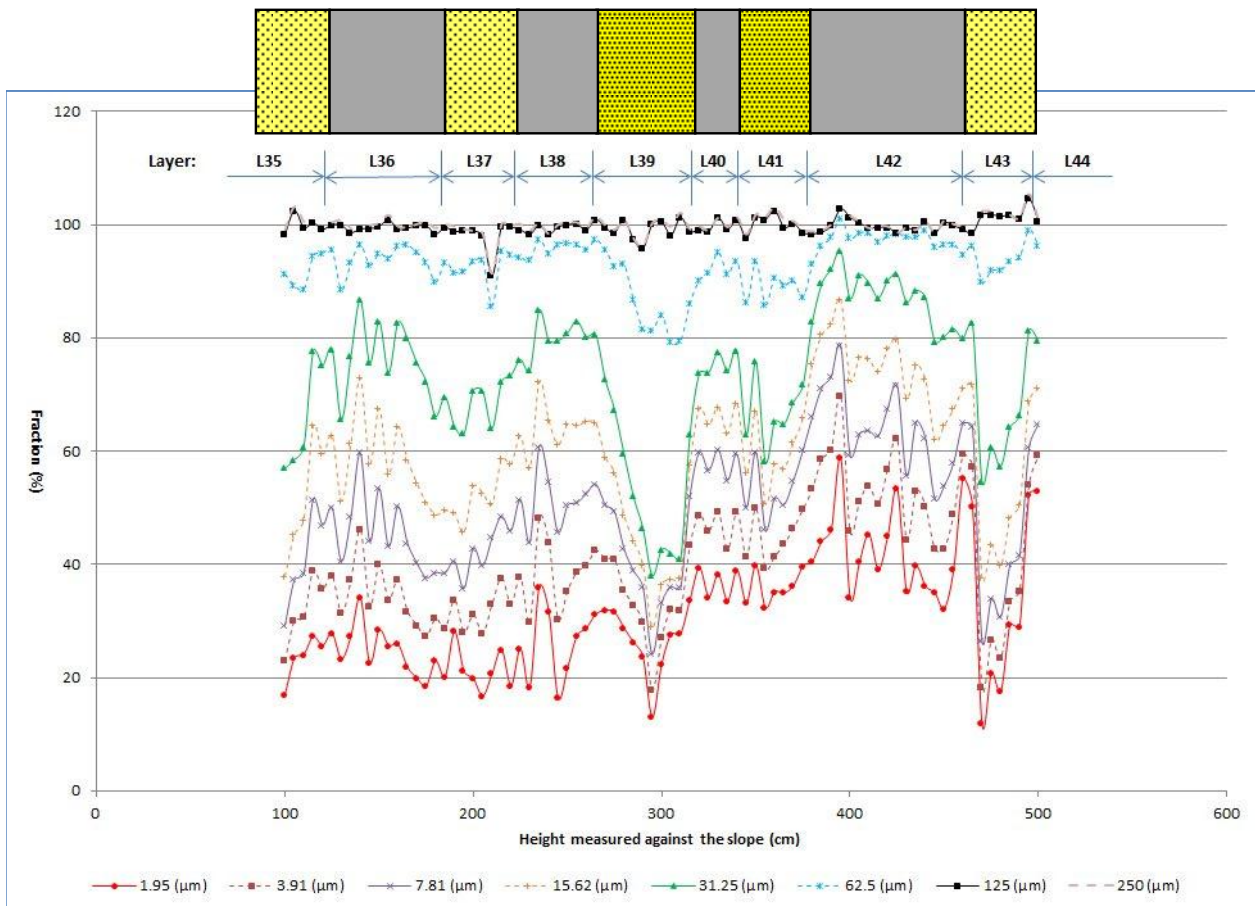


Figure 28. Detailed grain size variations (fraction in %) across several silt and clay layers (layers 35 to 43), sampled in the quarry at Rumst (from Labat, 2012). Note that layers 39 and 41 correspond to the two silty layers of the double band. This figure also demonstrates the usefulness of the $>32\mu\text{m}$ parameter to characterise the grain-size of the Boom Clay.

4.1.2. Organic matter

The organic matter from the Boom Clay was already subject of detailed petrographic (Vandenberghe, 1976, 1978) and geochemical (Laenen, 1997, 1998) studies, focussing on samples from the outcrop region. More recent studies (e.g., Deniau et al. (2001), Van Geet et al. (2003), and Blanchart (2011)) analysed Boom Clay samples from the Campine subcrop, specifically from the Mol site. The latter studies mainly focussed on the organic geochemistry, addressing questions related to the bulk geochemical and molecular organic geochemistry of the organic matter. The results obtained in the above mentioned studies have been compiled in a state-of-the-art report on the natural organic matter of Boom Clay (Bruggeman & De Craen, 2012).

The Boom Clay contains substantial amounts of total organic matter of low immaturity (total organic carbon content of 1-5 wt.%). The organic matter found in Boom Clay reflects its nearshore depositional environment: marine organic matter with detrital terrestrial organic matter input (Vandenberghe, 1978; Laenen, 1997; Wouters and Vandenberghe, 1994).

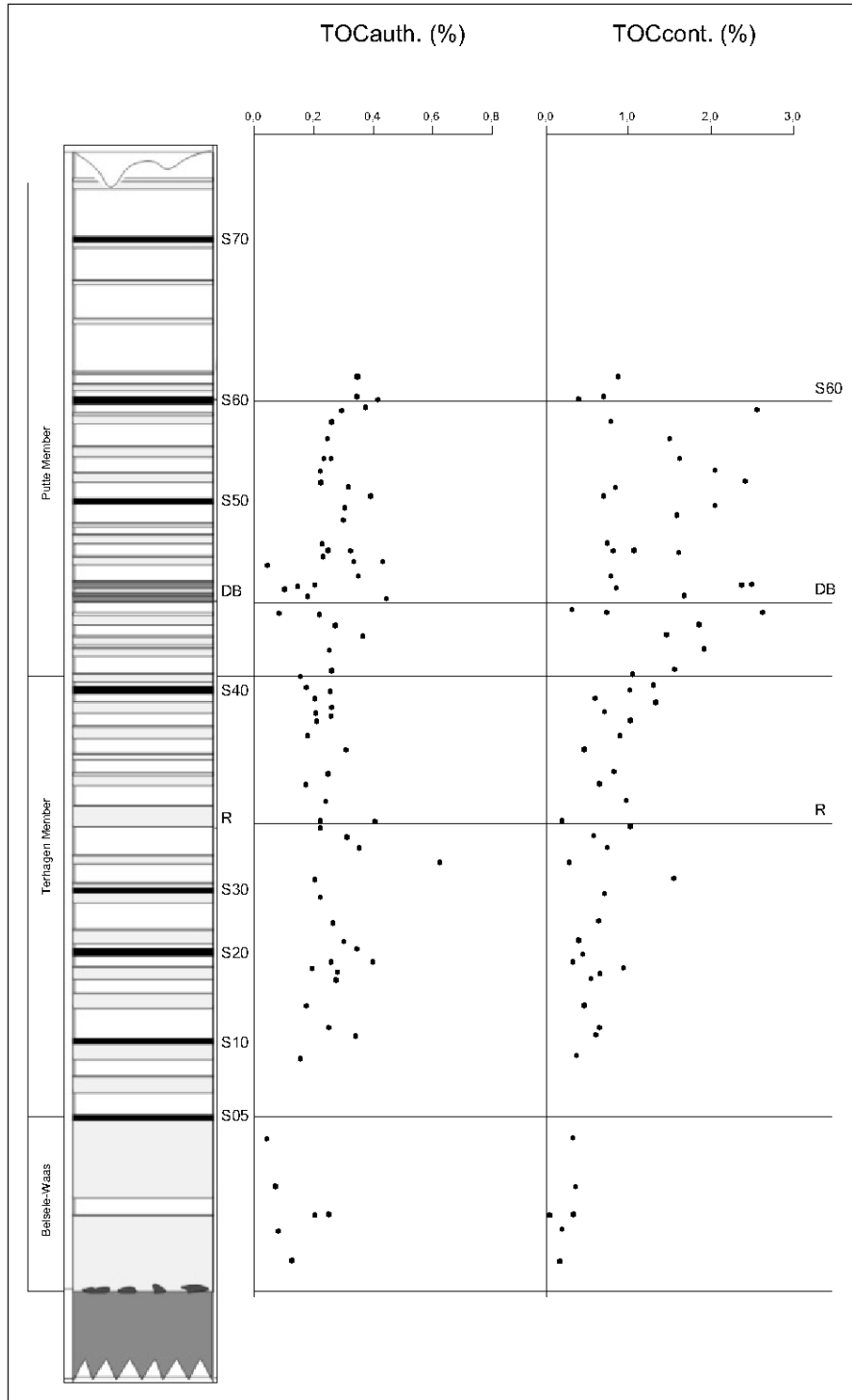
The black coloured bands in the clay contain more organic material (Figure 11). When present, such bands are systematically positioned right above the silt layer (see Figure 31), starting already in its top (Figure 11). This must mean that the formation mechanism of the organic rich layers is related to the climate driven grain size bands.

It is obvious from field observations and from analysis (Figure 11, Figure 29) that the occurrence of black organic rich layers is more developed in certain depth intervals than in others. The particular change from grey to black clays could even be used as a very widespread boundary between the Terhagen and Putte Members of the Boom Clay (see Figure 10 and Figure 11).

The particulate organic matter, the elemental C and N composition, the Rock Eval type pyrolysis and the molecular hydrocarbons analysis, all show that the black organic matter is dominantly made up of higher plant remains. This means that in the marine environment of the Boom Clay these organic components are detrital and land derived. However, these analyses also show that a fraction of autochthonous marine organic matter is always present in the clay, some being algal and some

bacterial in origin. Comparing the relative proportion of land derived to autochthonous marine organic matter (Figure 29) it is striking that more land derived organics also lead to somewhat more marine organics. This means that the reducing conditions created in the sediment by the more abundant land-derived organics lead to a better preservation of the less abundant but continuously produced marine organics. This phenomenon can also be observed at the level of individual layers.

Also at the level of the individual bands a systematic difference can be observed within the higher plant derived components. Molecules derived from the angiospermal plants occur more in the silty layers and resinous compounds with a gymnospermal origin are more abundant in the silt poor clay layers. Also the black layers have a larger contribution of gymnospermal molecules.



Figuur 29. Variations in marine (TOCauth.) and continental (TOCcont.) organic carbon content in the type section of the Boom Clay Formation (after Laenen, 1998).

4.1.3. Detrital particle provenance

Except for the small quantities of authigenic glauconite grains all sediment particles are detrital. Several of these particles have specific properties that point to a particular area of provenance around the North Sea basin (Laenen, 1997, 1998).

The transparent heavy mineral content can be subdivided in a group of ubiquitous minerals, an epidote-garnet-hornblende group, a group of parametamorphic minerals and the tourmaline grains. The epidote-garnet-hornblende group is generally linked to the erosion of the Scandinavian and the North Scottish land masses. The parametamorphic mineral group on the contrary is seen as eroded from Paleozoic massifs in France or Cornwall, or reworked from earlier Eocene deposits. Also the tourmaline minerals are thought to have a southern to southeastern origin. It can be concluded from the relative proportions of these groups that the arrival of fine sandy and coarse silty material brought by currents from the north was diluted by material swept in from the south, mostly from a tourmaline rich source area and to a lesser extent from the French Paleozoic Massifs.

Besides quartz that appears dominant, large mica and chlorite flakes occur in the light mineral fraction. However, the most striking is the presence of potassium feldspar, generally between 5 and 10 % of the bulk composition. It is difficult to imagine a southern source area delivering such an amount of feldspar and therefore the important northern Scandinavian-Scottish provenance as derived from the heavy minerals seems to be confirmed.

Both particulate and molecular organic components carry indications of provenance. In the macerals, coal particles were found showing characteristic low vitrinite reflectivities typical for British Carboniferous coals outcropping in Northern England (Vandenberghe, 1976). This confirms the existence of counterclockwise currents in the basin transporting particles from the north to the Belgian area (Figure 5). The molecular organic chemistry points to differences in source area: molecules derived from the angiosperms occur more in the silty layers and resinous compounds with a gymnosperm affinity are more abundant in the silt poor clay layers. In the North Sea Basin during the Early Oligocene, the gymnosperm cover points logically to a more northern provenance area than the angiosperm cover.

Although the clay mineral composition is remarkable constant (illite, illite-smectite random mixed layers, smectite, kaolinite and chloritic minerals) some minor variations that occur are pointing to different provenance areas (Figure 30). On a regional scale, smectite increases in the southeast where the smectite-dominated early Eocene strata probably outcropped; illite and chlorite content increases to the east where the Ardennes-Eifel massifs could have delivered these

minerals. Kaolinite was shown to periodically rise at the pace of cycles of a half to one million years (Figure 22). Kaolinite is also found to systematically increase slightly with the clay content in the section and therefore to covary with the gymnospermal compounds in the organic fraction; this suggests that also kaolinite has a more northern provenance.

A northern provenance would mean that the sediments are weathered and eroded from the dominantly silicic magmatic and metamorphic rocks in Scandinavia and northern Scotland. The trace elements that are typical for such rock types (Ba, Ta, Th, LREE) do indeed correlate with kaolinite content while other elements as Co, Cr and Fe correlate with the higher smectite and illite contents pointing to more southern and southeastern provenance contribution (Laenen, 1997, 1998).

4.1.4. Sedimentary model for the silt-clay layering

The combination of the grain-size properties, the absence of marked erosive features and the lateral continuity of the layering in the Boom Clay, leads to the definition of a probable sedimentation mechanism. The evolution across silt and clay layering can be understood as a cyclic change in the effect of sorting a continuous supply of sediment particles; the sorting mechanism must be effective over a wide area. The most logical process that corresponds to these constraints is wave activity.

The effect of the waves on the sorting of sediments was probably most effective at or close to the sea-bottom, as recent muddy sedimentation profiles show the sediment concentrations to increase drastically just above the sea bottom. The presence of wave erosion structures in some of the silty beds support this (Vandenberghe, 1978). Such varying wave turbulence intensity close to the bottom of the sea could have been caused either by periodically changing the wave length which determines the penetration depth of the wave turbulence or by periodically changing the water depth. The changing wave properties could most logically be linked to climatic variations. Cyclic changing water depth could be due to either eustatic sea-level changes or to tectonics influencing the relative sea-level in the depositional area; the tectonic possibility is less probable seen the great cyclic regularity of the layers and their lateral continuity. In fact the Milankovitch astronomical forcing which steers the alternation of silty clay and clay layers (3.8) clearly demonstrates a relationship of the layering with climate. Therefore, we prefer a genetic model with climate controlling the cyclically varying wave turbulence intensity at the bottom of the Boom Clay sea. In addition, the very widespread regularity in the layering favours a eustatically changing water depth bringing the sea bottom periodically in and out of the reach of the wave turbulence rather than a direct climatic control by wave property variation that could explain equally well the grain-size patterns.

The idea of eustatically changing sea-levels is furthermore strongly supported by the specific coupling of the grain-size banding with the black organic layers, that otherwise would be difficult to explain. Indeed, upon gradually rising the sea-level, the wave sorting near the sea bottom becomes less and less effective till the transgression proceeds rapidly and floods the coastal land mass. The vegetation cover of that submerged land is destroyed and the plants are transported into the basin where they are deposited as silt sized phytoclast particles (Vandenberghe, 1976). When the sea-level is approaching its highest position the maximal inundation of the land has occurred and the arrival of phytoclasts in the basin stops. The maximal water depth and hence maximal inundation is at the position of the lowest sorting degree of the sediment, namely in the middle of the clay layer. That is the reason that the black layers always occur just on top of the silty layers in the basal half of the clay layers.

Summarizing, an ideal silty clay – clay – silty clay evolution is represented in Figure 31, showing the gradual grain-size evolution with minimal sorting in the center of a clay bed and the maximal sorting in the middle of a silty clay bed, the co-evolving kaolinite and the position of the land derived organic matter bands. In the clay layers also somewhat more marine organic components are present with in particular more angiosperm compounds in the silty layer and more gymnosperm compounds in the clay layers. A simple eustatic variation model will situate the lowest sea-level position in the middle of a silt layer and the main sea-level height in the middle of a clay layer, distinguishing transgressive and regressive systems in a pattern of continuous repetition.

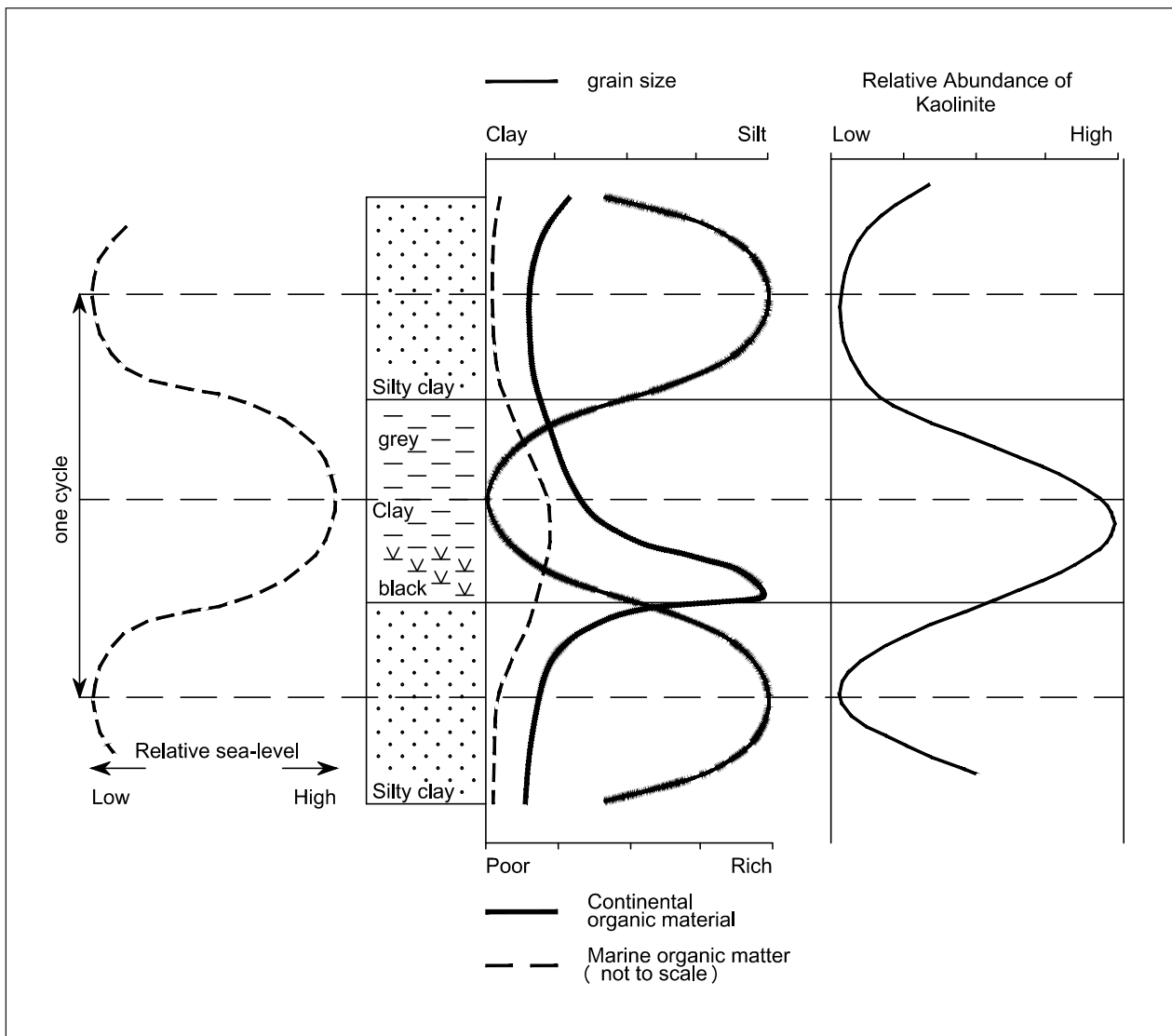
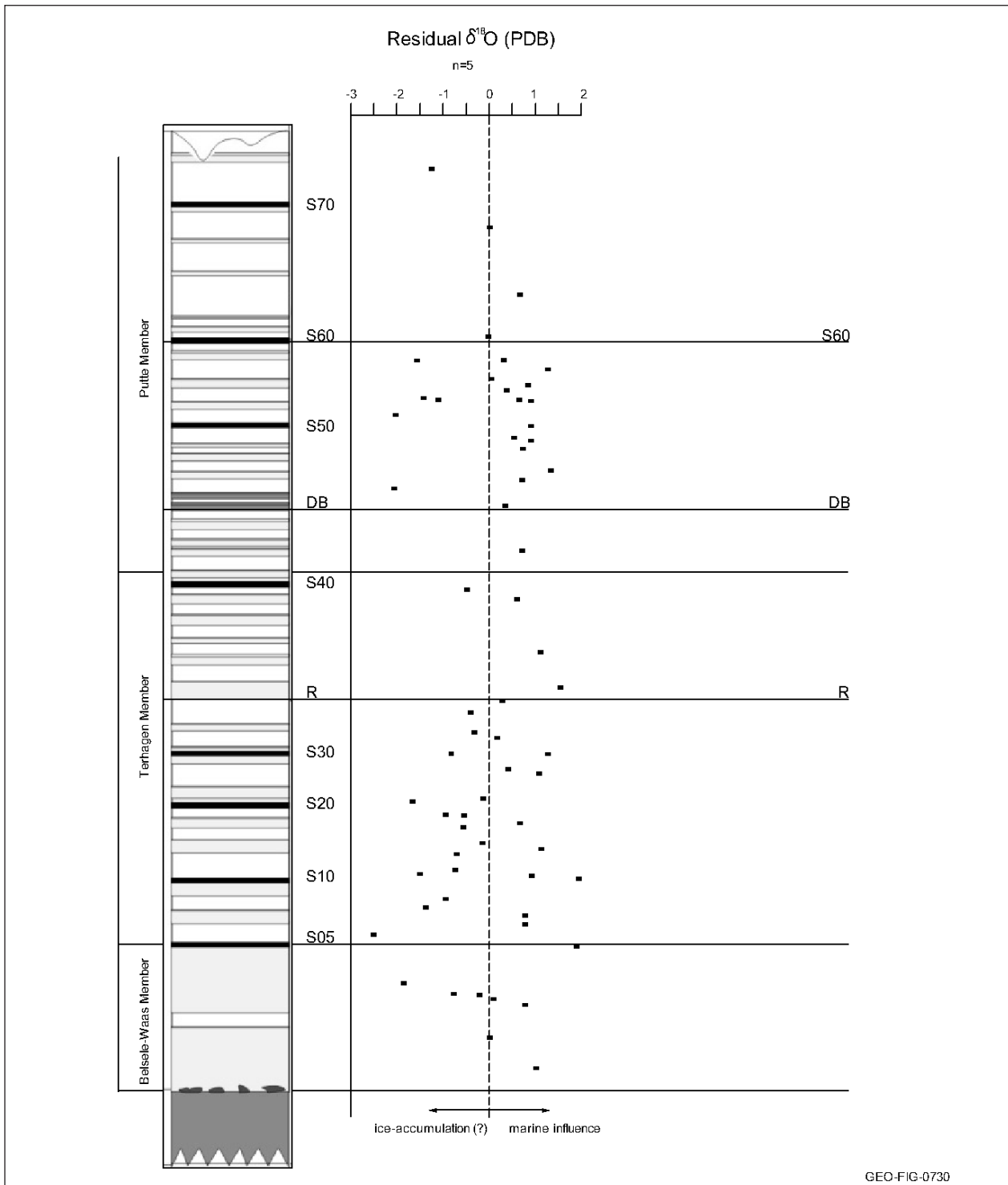


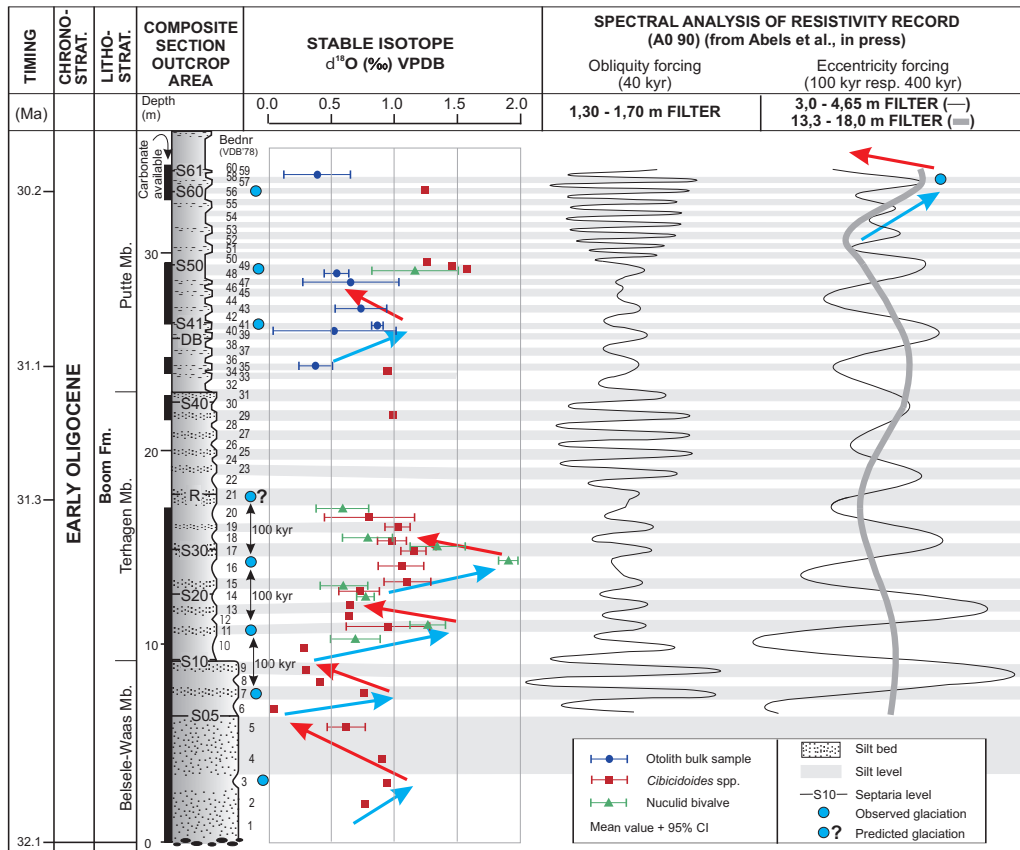
Figure 31. Schematic presentation of the variations in grain size and organic matter content (left side) and kaolinite content (right side) through a silt/clay couple. The diagram at the left shows the sequence stratigraphic interpretations of the silt/clay cycles (modified from Laenen, 1997).



Figuur 32. Relative oxygen isotope data in the outcrop area of the Boom Clay (after Laenen, 1998). Trends in the data are removed and the values are plotted on a relative scale, distinguishing values supposed to indicate ice cap growth from values supposed to indicate an ice cap free world.

Eustasy at the scale of Milankovitch scale as in the Boom Clay has been recognised during the Oligocene in ocean sediment cores (Wade & Pälike, 2004); based on oxygen isotope studies of the foraminifera shells, a glacio-eustatic mechanism was proposed with sea-level drops around 50 m. Oxygen isotopes studies in the Boom Clay did not have that resolution, but the

available data from Laenen (1998) and De Man (2006) show oxygen isotope variations at the level of layers or bundles of layers (Figure 32, Figure 33). Glacial eustasy during the Cenozoic in general has been discussed by Abreu & Haddad (1998 a,b).



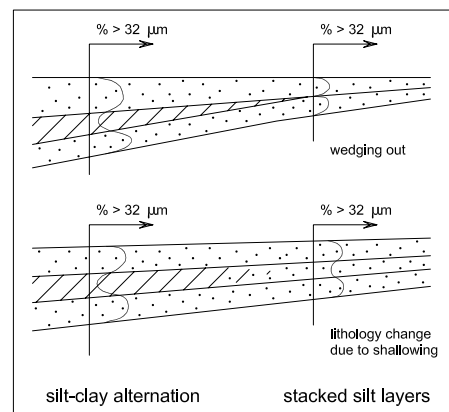
Figuur 33. Stable oxygen isotope results from the outcrop section of the Boom Formation plotted along a lithostratigraphic column and shown together with the obliquity and eccentricity signals derived from resistivity data. Blue arrows suggest glaciations trends and red arrows suggest deglaciation intervals. Blue dots indicate glaciation levels observed from heavy $\delta^{18}\text{O}$ values and predicted by assuming a 100 kyr pacing in between glacial episodes (from De Man, 2006).

4.2. Sedimentary model at larger scale

4.2.1. Lateral variations from basin to coast

Glacio-eustasy controls the vertical sorting of the main part of the Boom Clay sediment at orbital scale (4.1.4). Considering the evolution of the sorting in the Boom Clay laterally in a section perpendicular to the coastline, from deeper to shallower water, two types of lithological evolution can be expected (Figure 34). Towards the coast, the sediments are deposited in a gradually shallowing environment and consequently they will become more sorted and thinner layered. This can be observed when lithologies and bed thicknesses in outcrops are represented on a general basin to coast profile (Figure 35).

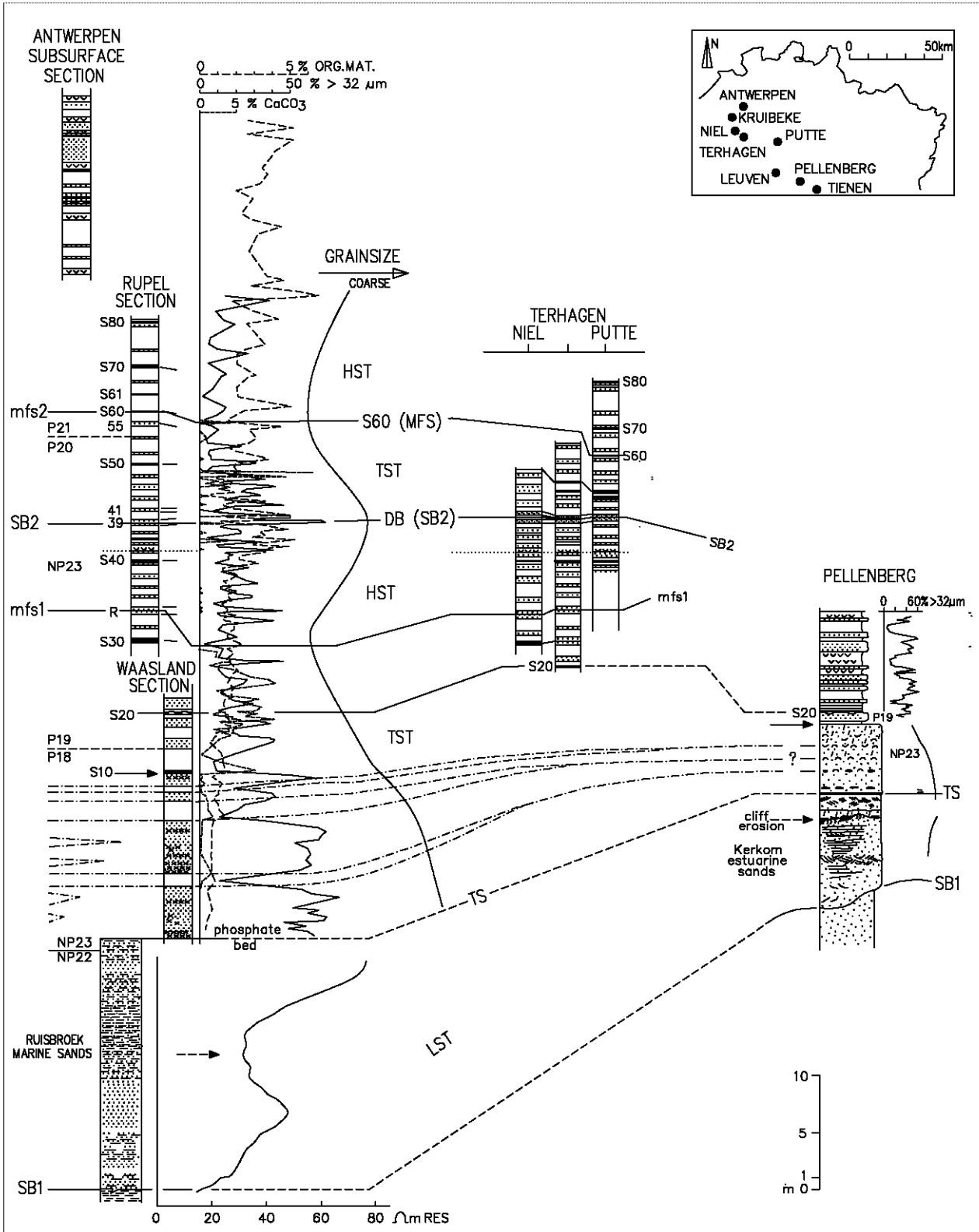
The first type of evolution is the wedging out of clay layers towards shallower water. A good example of this type of wedging out is the evolution of the clay layer between the two silty layers of the double layer (Figure 15). The consequence is the stacking of the 2 silt layers of the double layer into one silt horizon leaving only a faint horizon in between (Figure 36). When a series of stacked silty layers like in the Belsele-Waas facies evolve further to sandy coastal Berg Sand deposits,



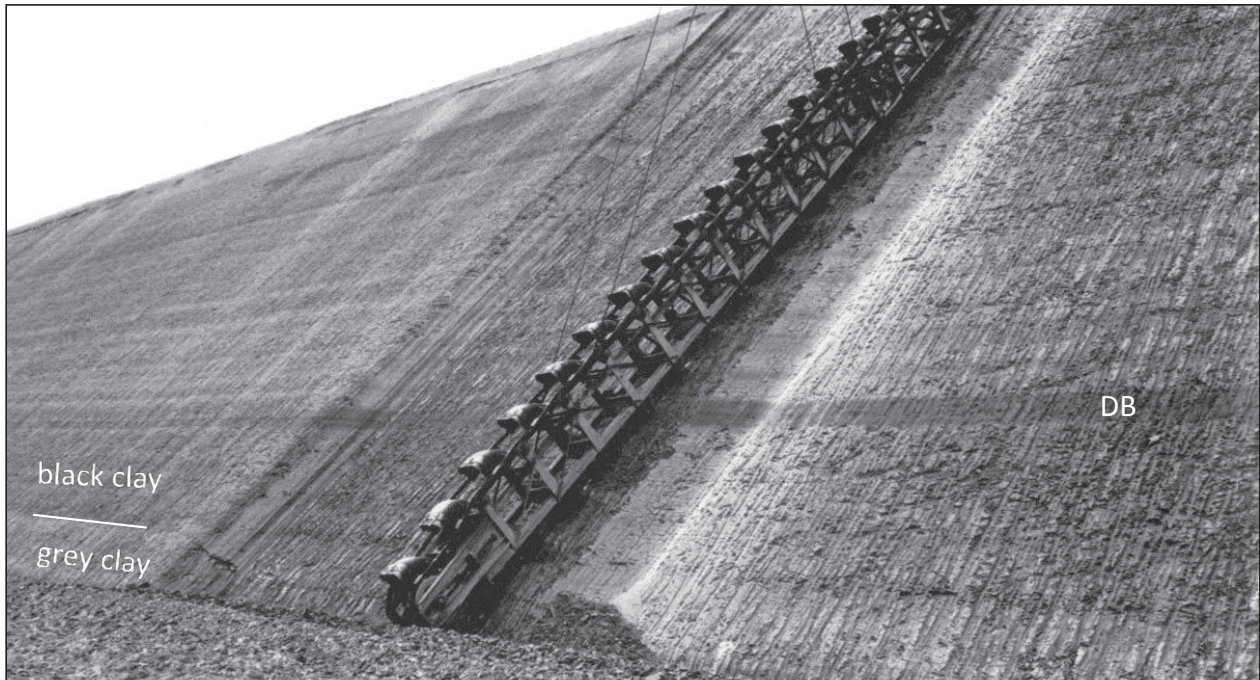
Figuur 34. Stacked silt layers can have two types of origin. In the upper case a clay layer is wedging out towards shallower water and in the lower case a clay layer is laterally evolving into silt towards shallower water. Both cases can be distinguished by the evolution of the grain size in the stacked silt. In the case of wedging out of a clay layer, the two size cycles in the silt will be stitched together on top of each other. In the case of lateral evolution of clay to silt, the normal cyclic size-evolution will be preserved as shown in Figure 31 but with less amplitude. Size evolution is expressed as $>32\mu\text{m}$ content.

the thickness diminishes and the full cyclicality is lost by incomplete preservation of the sediments (Figure 35). Still in the Berg Sands, cycles can be observed

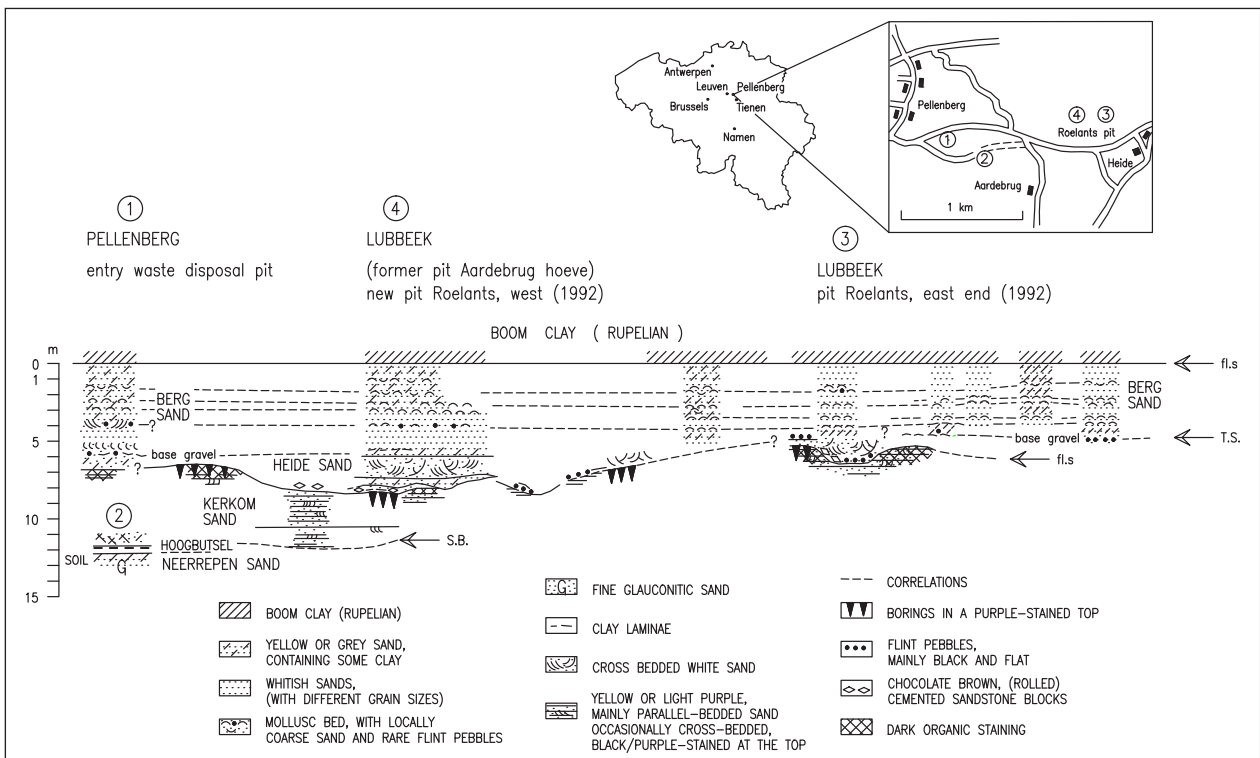
expressed as reworked shell layers even admixed with some rare pebbles (Vandenberghe and Gullentops, 2001) (Figure 37).



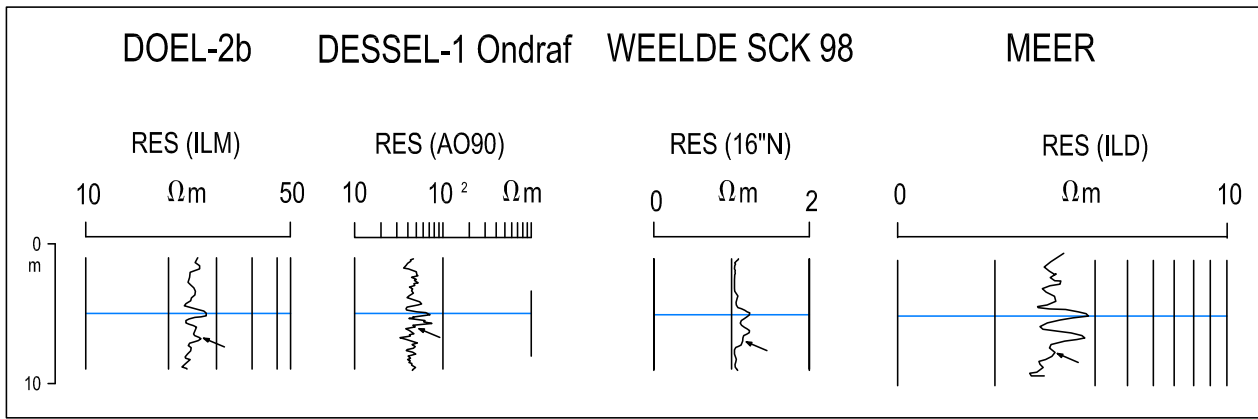
Figuur 35. Correlation between Rupelian sections in the type area, the Campine area and the Leuven-Tongeren area. The stacking of silty layers as at the base of the Waasland section and as at the DB level in Putte is explained by either the wedging out of clay layers or by the facies change from clay towards silt, when shifting from deeper to shallower water (see Figure 34). Layers annotated S are septaria layers (from Vandenberghe et al., 1998).



Figuur 36. Photograph of the Boom Clay in the Putte clay pit. The height of the excavation wall is 16.5 m. The prominent dark grey layer about 6 m above the base of the pit is the double layer (DB) consisting of only one layer with very high silt/clay fraction ratio having only a faint separation in the middle. The indicated boundary between grey and the black clay near the base of the pit is the limit between the Terhagen-Putte Members.

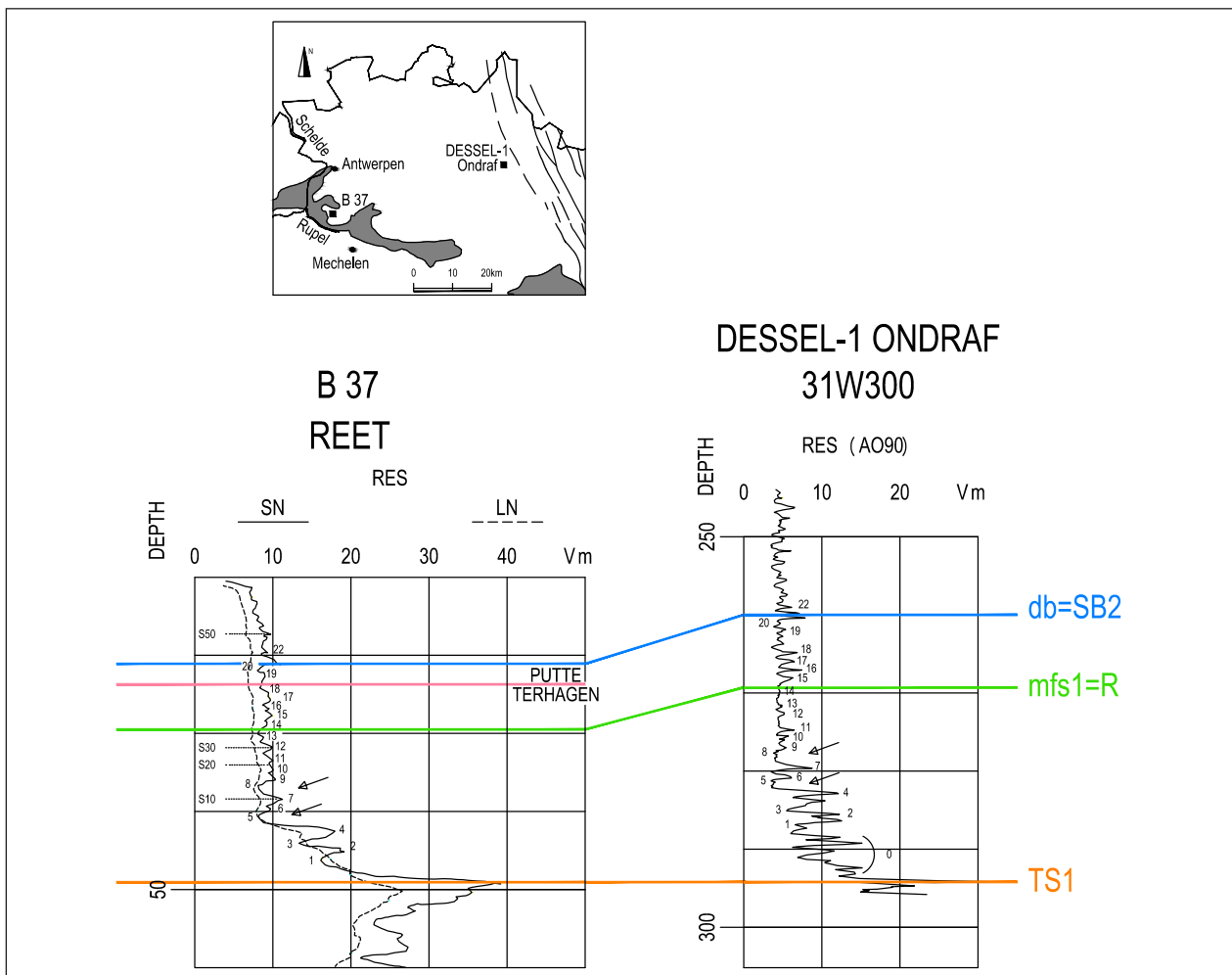


Figuur 37. Location, description and correlation of sections of the Pellenberg-Lubbeek sand pits in the hill north of the N3 Leuven-Tienen road. The Neerrepesand (upper member of the marine Sint-Huibrechts-Hern Formation, Tongeren Group), Kerkom Sands (member of the continental Borgloon Formation, Tongeren Group), Heide Sand (a thin white sand member between the Kerkom Sands and the Berg Sand), coastal Berg Sand (member of the marine Bilzen Formation, Rupel Group) and the marine Boom Formation (Rupel Group) are the lithostratigraphic units identified in the section. The organic impregnation occurs at the eroded top of the Kerkom Sand (from Van Riessen & Vandenberghe, 1996).



Figuur 38. a. The two thick silt layers of the Belsele-Waas Member composed of several sub-units, suggesting that the water was too shallow to develop clay layers (from Vandenberghe & Van Echelpoel, 1987). The significance of the grain-size evolution in the different sub-units is discussed in the text.

b. Examples of the detailed resistivity log response of the DB in the Doel-2b, ON-Dessel-1, Meer and Weelde wells. The blue line is at the level of the upper coarse layer of the DB couple of coarse layers. Note that the lower layer of the couple is complex and can be underlain (arrows) by a less well expressed (Meer, Weelde) or additional (Doel-2b, ON-Dessel-1) coarse layer. The complex nature of this lower layer is also expressed in the detailed grain-size analysis (Figure 28 layer 39) and in the original field logging in the Kruibeke clay pit (31 m level in Vandenberghe, 1983).



Figuur 39. Detailed correlation of the Lower Rupelian sequence between the Dessel-1 and the Reet wells. The corresponding peaks are numbered and the arrows indicate the equivalent position of the Kleine-Spuuwen Clay which develops as an individual unit more to the east (from Vandenberghe et al., 2001).

A second type of lithology evolution is when the full orbital cyclicity remains preserved but evolves from more clayey to more silty sediments. In such case, the grain-size cyclicity or geophysical well-log cyclicity can still be entirely correlated. For example a clay layer, in-between two silt layers, evolving to a silt - because of the shallowing environment - should still show a grain-size cycle with a minimal amount of coarser particles in its center as shown in Figure 31, and not a maximal amount of coarse particles in its center as is the case in the regular silt layers. This situation is well observed in the middle silt layer subunit of the upper stacked thick silt layer in the Belsele Waas Member (Figure 38); depositional depth is estimated to be only a few tens of meter (see 4.1.1). The grain size evolution in the lower stacked thick silt layer of the Belsele Waas Member in Figure 38 rather suggests stacking by wedging out of clay layers as discussed in the first type of lithology evolution. This not surprising as it was demonstrated already in Vandenberghe et al. (2001) that between the Dessel and the Reet boreholes several clay layers had disappeared (Figure 39) leading to a stacked silty appearance of the Belsele-Waas Member in the outcrop area. The very shallow water depth during the Belsele-Waas deposition is further indicated by a gutter erosion gully observed in the lower silt layer (Vandenberghe et al., 2002).

The presence of a short and small secondary cycle on a silty grain-size wiggle is more difficult to clarify. Such a typical secondary cycle can be observed e.g. in the lower silty layer of the double band in boreholes e.g. Poppel, Brasschaat (annex 11 & 12 in D'hooge et al., 1991) and e.g. Doel 2b, Meer, Weelde (fig. 6 in Vandenberghe et al., 2001; Vandenberghe, 1999) (Figure 38b). It could be interpreted as the subtle indication of a disappeared clay layer as discussed above but it could more probably be the indication of a precession cycle superposed on an obliquity cycle. Examples of such precession cycles are shown in Figure 52.

4.2.2. Vertical low frequency variations

The low frequency vertical trends in grain size (Figure 35), already discussed earlier in the description of the sequence stratigraphy of the Boom Clay (3.9), can also be interpreted in terms of changing water depths as was done for the Milankovitch controlled high frequency cycles (see 4.1.4). In the total section of the Boom Clay, at least four sequences can be recognised. This is based on the relation between grain-size trends, expressed as resistivity changes on borehole logs (Figure 23), and changing water depth. The discussion on the origin of these sedimentary sequences of longer duration was however related mostly to the outcrop sections where a low frequency grain-size trend

was recognised as an envelop linking the silt contents of the individual Milankovitch cycles (Figure 40). The double layer marks the boundary of two cycles. The trend was interpreted as 3th order stratigraphic sequences, reflecting glacio-eustatic sea-level trends thought to be recognisable world-wide (Vandenberghe & Van Echelpoel, 1987; Stover & Hardenbol, 1994; Vandenberghe et al., 1997). Unfortunately, the outcrop section of the Boom Clay represents only part of the Rupelian, and in fact in an updated chart of the sequence stratigraphy (Hardenbol et al., 1998), more sequences were recognised in the Rupelian (Figure 41).

The oxygen isotopic record, in support of the glacio-eustatic origin of the sea-level fluctuations (Abreu et al., 1998a,b), shows four major cooling events during the Rupelian (Figure 41). More recent compilations and interpretations of oxygen isotope records (Zachos et al., 2008; Cramer et al., 2009) show three major cooling events in the Rupelian with additional minor cooling events. However, the oxygen isotope data in the Boom Clay at the double band level, supposed to represent a major glacio-eustatic sea-level drop, do not convincingly show a cooler climate (Figure 32, Figure 33). The origin of these sea-level variations will be further discussed in 4.6 and 4.7 when the tectonic history of the area is also taken into account.

Other intermediate duration cycles with lengths between 0,5 and 1 million years have been reported by Laenen (1997, 1998). These intermediate cycles are expressed in the clay mineralogical and geochemical data (examples in Figure 22, Figure 29, Figure 30) and in combined geochemical parameters expressing weathering intensity (Figure 22). The signals are not always clear but a convincing support for the existence of the cycles is the occurrence of significant changes in kaolinite content in the middle of such cycles (Figure 22). As the cycles have been interpreted as climatically driven, the increase in kaolinite could point to the higher sea-level bringing more northern provenance particles as was discussed for the silt-clay couplets (4.1.4).

Truly climatically driven cycles of longer duration than the silt-clay couplets have been recognised in the spectral analysis of the resistivity data of the Dessel-1 borehole (Figure 21). The analysis was very convincing and showed that the 40 ka obliquity driven couplets are arranged in packages of 100 ka eccentricity and in trends of 400 ka eccentricity cycles. The key horizons R, DB en S60, discussed in the section on sequence stratigraphy (3.9) seem to be related to the 400 ka cyclicity rather than to 3th order sequences of longer duration, as discussed above. There seems to be no particularly striking lithological trends

corresponding to the 1,2 Ma obliquity period which is of the order of duration of 3th order sequences (Figure 21). The more outspoken presence of fine sandy deposits of the Eigenbilzen Formation to the

east (Figure 14) is most probably related to local tectonics and will be discussed in the Rupelian local tectonic section (4.6).

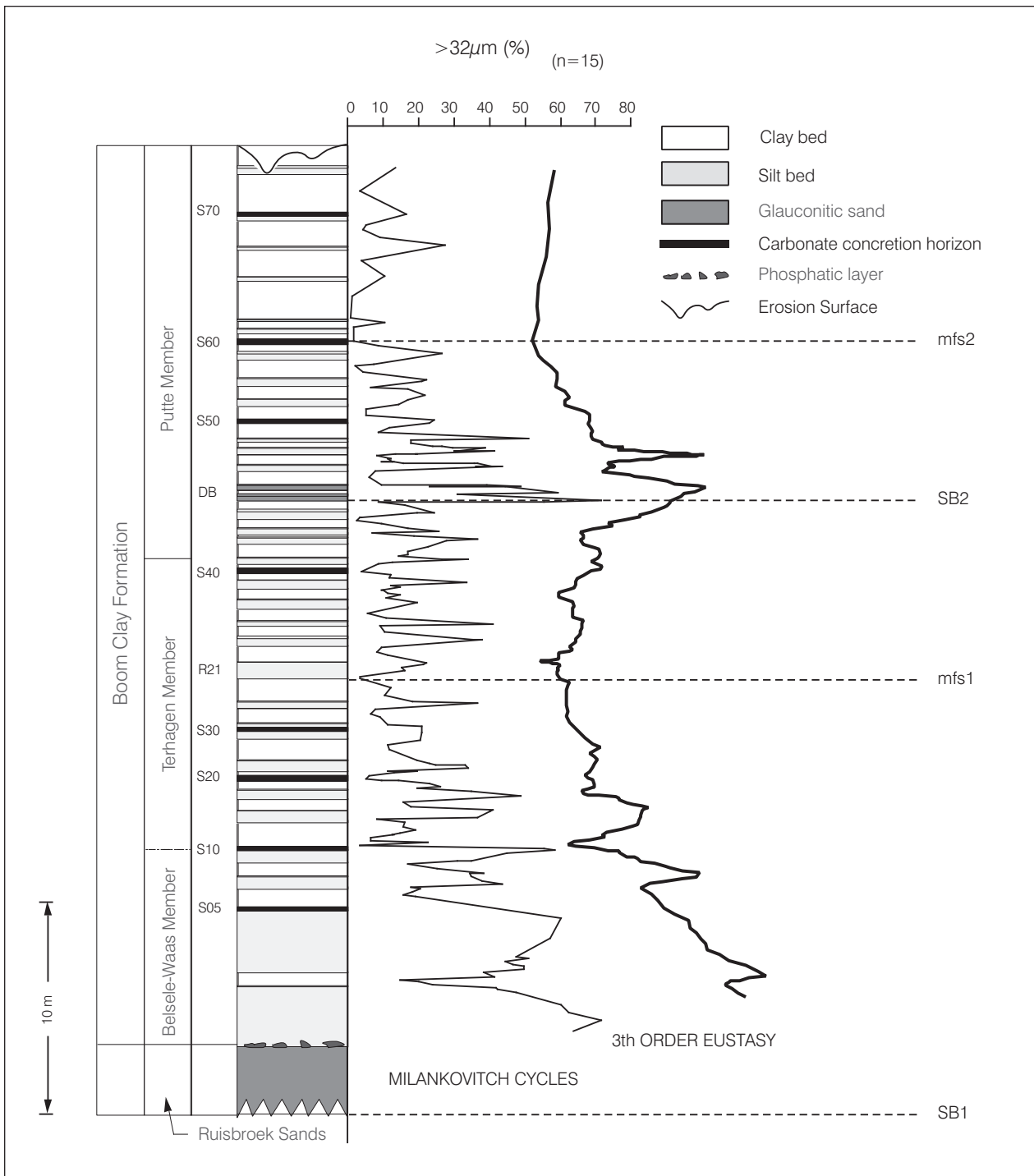


Figure 40. Composite lithologic log of the type section in the outcrop area of the Boom Formation showing the lithostratigraphic subdivision and the variations in grain size (>32 µm fraction) of the high frequency Milankovitch controlled cycles and of the lower frequency envelope traditionally interpreted as 3th order eustasy-controlled sequences (from Laenen, 1997, 1998).

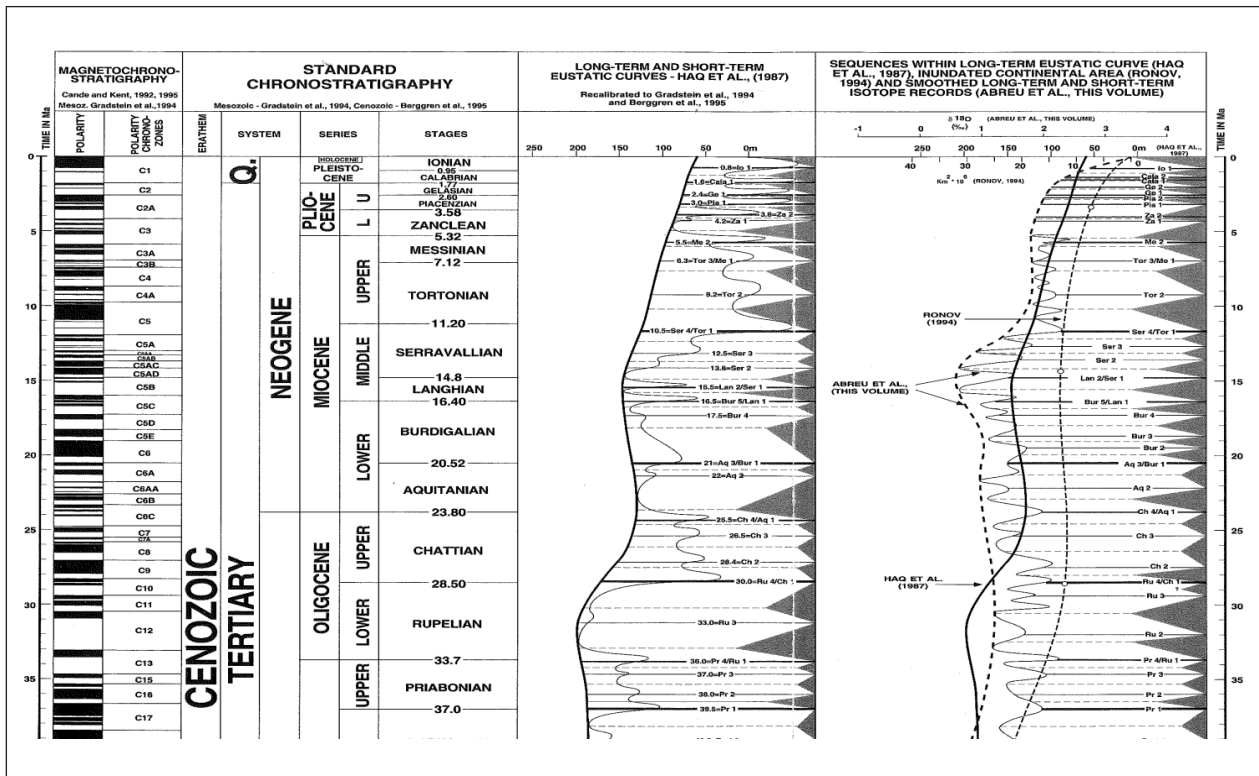


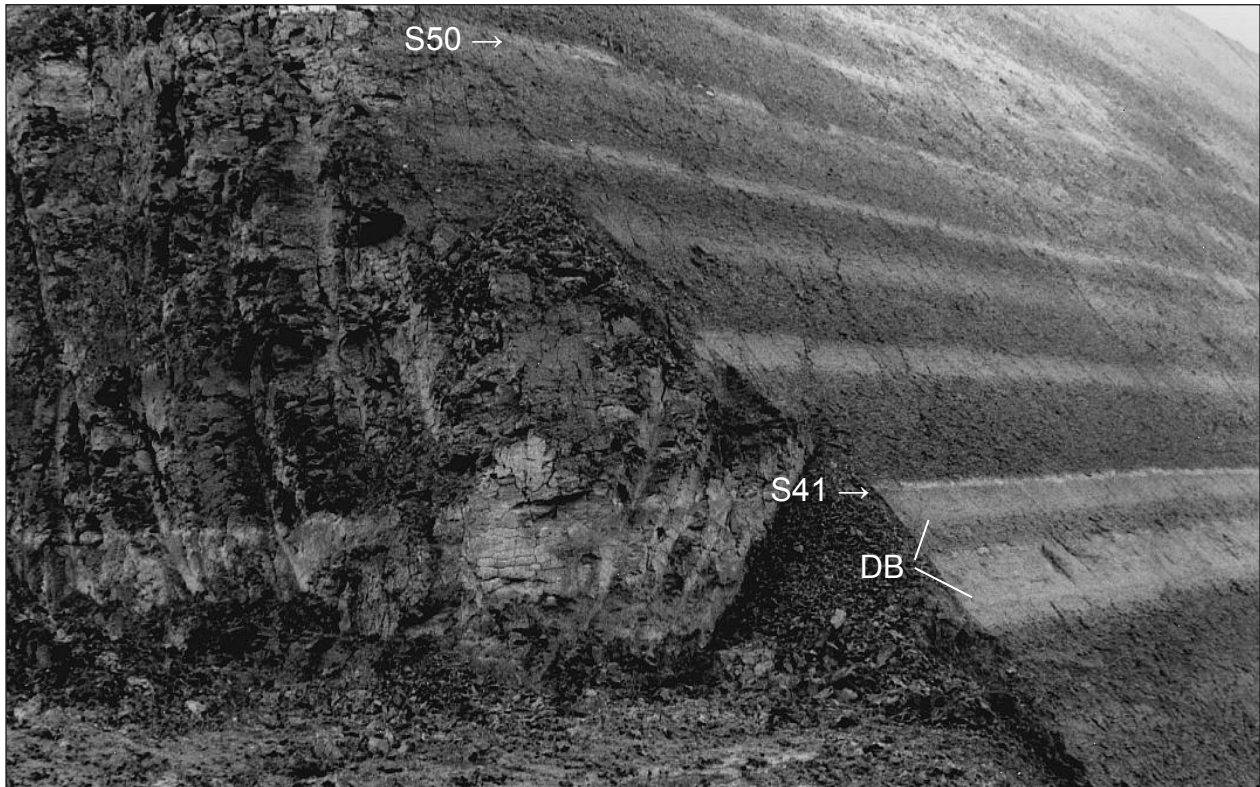
Figure 41. Part of the Cenozoic sequence chronostratigraphic chart (part of Chart 1 from Hardenbol et al., 1998). The left sequence column shows the time-recalibrated chart of Haq et al. (1987) with two sequences in the Rupelian (the two 3rd order sequences indicated on Fig. 30); the right column shows the renewed sequence chart of Hardenbol et al. (1998) comprising three Rupelian 3rd order sequences. In the right column, the fluctuating left border curve, and its envelope (Abreu et al., 1998), represents the oxygen isotope evolution as a proxy for the temperature.

4.3. The carbonate-rich/marly horizons and the development of carbonate concretions in the Boom Clay

In the outcrop area, only the lower part of the Terhagen Member, below the R horizon, has a more or less continuous carbonate content (Figure 11; Vandenberghe, 1978; De Man, 2006). Below and above, the carbonates are present in marly bands (originally a few cm's to dm's thick; Figure 42), in which septarian carbonate concretions have developed during early diagenesis (often some dm's thick; De Craen, 1998; De Craen et al., 1999a,b; Van Tassel, 1966; Vandenberghe & Laga, 1986). These originally marly horizons, now containing septarian carbonate concretions, are the so-called 'septaria' layers, indicated by S on the profiles in Figure 11 and Figure 12. It is suggested that, originally, more continuously dispersed carbonate was present but that it has been dissolved in the slightly acidic pore waters, especially where much organic matter was present. This original presence of marly horizons seems to be confirmed by a few carbonate content spikes and by the recovery of some carbonate-walled foraminifera in otherwise no-carbonate containing clays (Figure 11, Figure 43).

The origin of these marly horizons is not well understood, although it is clear that it is not diagenetic but sedimentary because they always occur in beds parallel to the major grain-size stratification planes. The most remarkable fact is that the marly horizons show no relationship with the lithologies in the silt-clay and organic matter banding. The marly horizons occur in both silty clay and in clay layers. Within these silty clay and clay layers, the marly horizons may occur in the center of the layer (most often), at the top or at the base of the layer. No periodicity could be detected in their position. Therefore, the marly horizons must have formed independently of the Milankovitch climatic steering mechanism as demonstrated for the formation of the grain-size and organic matter couplets.

It is not excluded that the chemical composition of the sea water varied from time to time due to the influx of more saline water derived from the opening of the generally closed-off Rhine Graben or to a further closing of the already semi-enclosed North Sea Basin (Figure 5, 6) or to climatic changes unrelated to astronomical periodicities. The effect of changing water composition could be either a direct chemical precipitation of carbonate or the blooming of calcareous plankton leading to the accumulation of calcareous microfossil debris in the sediment.



Figuur 42. Thin white layer in the top of the double band, corresponding to a marly horizon containing a rich and diversified microfauna (S41). At the top of the photograph, S50 can be observed. The carbonate in the marly horizons S41 and S50 is calcite. Quarry at Terhagen (from De Craen, 1998).

The latter possibility is suggested by the increased abundance of calcareous microfossils in the septaria levels compared to their abundance in the clay above and below the septaria layer (Moorkens et al., 1997; De Craen, 1998; De Man, 2006). Macrofossil molluscs seem also to be more abundant in the septaria layers: for example in S50, the double shelled lamellibranchiate mud feeder *Nucula deshayesiana* is commonly present, whereas elsewhere in the clay only single shells of this mollusc are found. Calcareous microfossils, particularly planktonic foraminifera, are also more abundant. Therefore, the accumulation of calcareous microfossil debris in the sediment was possibly caused by the blooming of calcareous plankton. These blooming events must have been active over the entire basin as the marly horizons are amongst the lithological features that can be correlated over large parts of the basin (Figure 14; Vandenberghe et al., 2001).

Very soon after the deposition of the marl, early-diagenetic processes resulted in the development of carbonate concretions within these marly horizons (Figure 44). The early formation of carbonate concretions is well known in many muddy sediments (Curtis and Coleman, 1986; Coniglio and Cameron, 1990; De Craen, 1998; Dickson and Barber, 1976; Duck, 1995). In the Boom Clay, the very early formation of the carbonate concretions is shown by the undisturbed preservation of fine structures such as thin shells, faecal pellets and worm burrow traces (De Craen, 1998).

The fundamental process controlling the diagenesis of Boom Clay – and the formation of the carbonate concretions – is mainly related to the degradation of the primary organic matter during progressive burial (De Craen, 1998; De Craen et al., 1999 a, b; Laenen & De Craen, 2004).

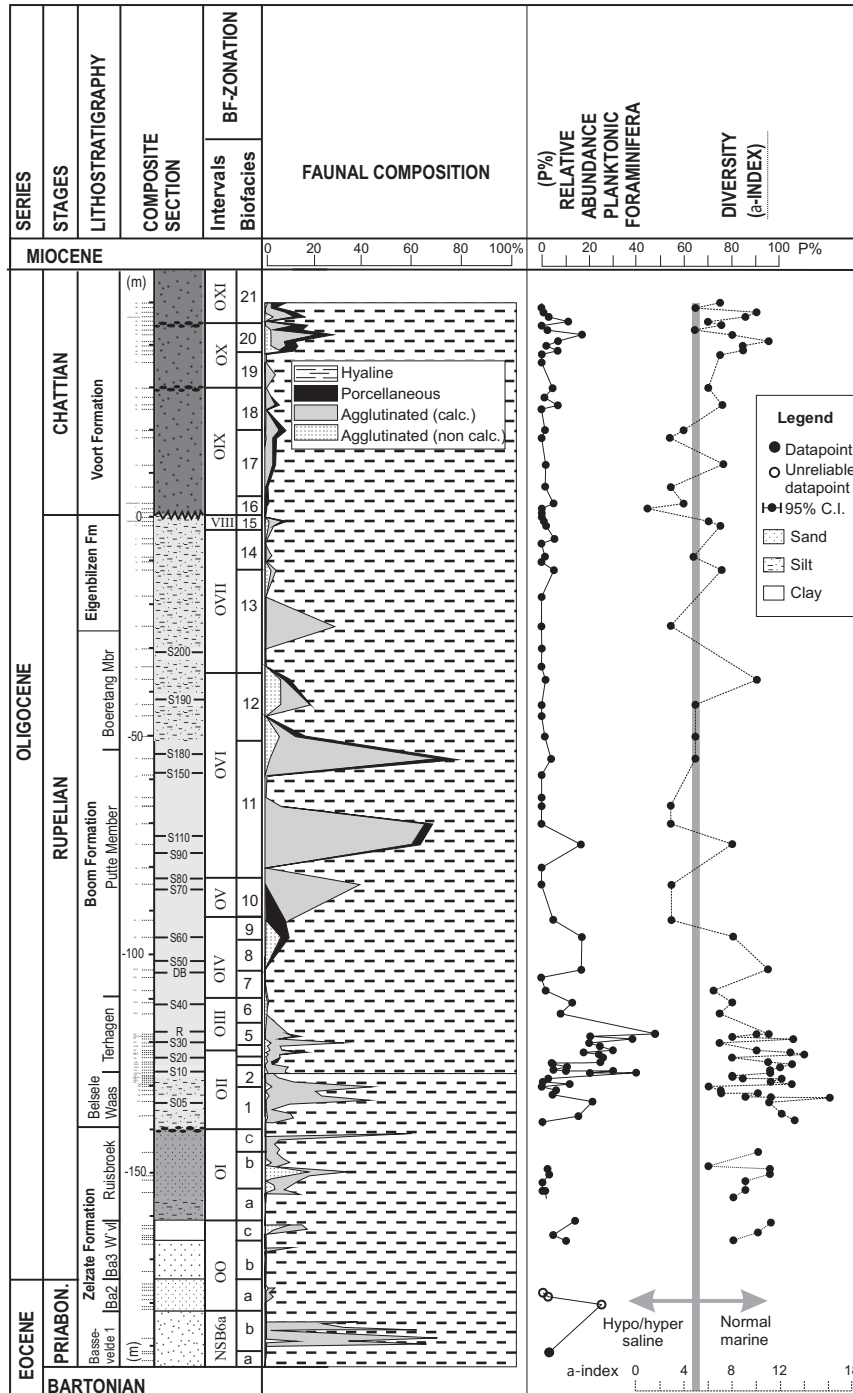
In the shallow burial realm, degradation of the primary organic matter mainly occurs through bacterial sulphate reduction reactions, releasing dissolved H^+ , HCO_3^- and HS^- into the pore water (typically occurring within the first 10 m of burial). These processes encourage the precipitation of pyrite and carbonates. If the sulphate reduction exceeds the iron reduction, the carbonate phase is iron-poor. Otherwise, ferroan carbonates (ferroan calcite, ferroan dolomite, ankerite, siderite) co-precipitate with pyrite.

In Boom Clay, the concretions are composed of carbonates and various amounts of pyrite; the carbonate phase mostly consists of calcite to ferroan calcite (Figure 45).

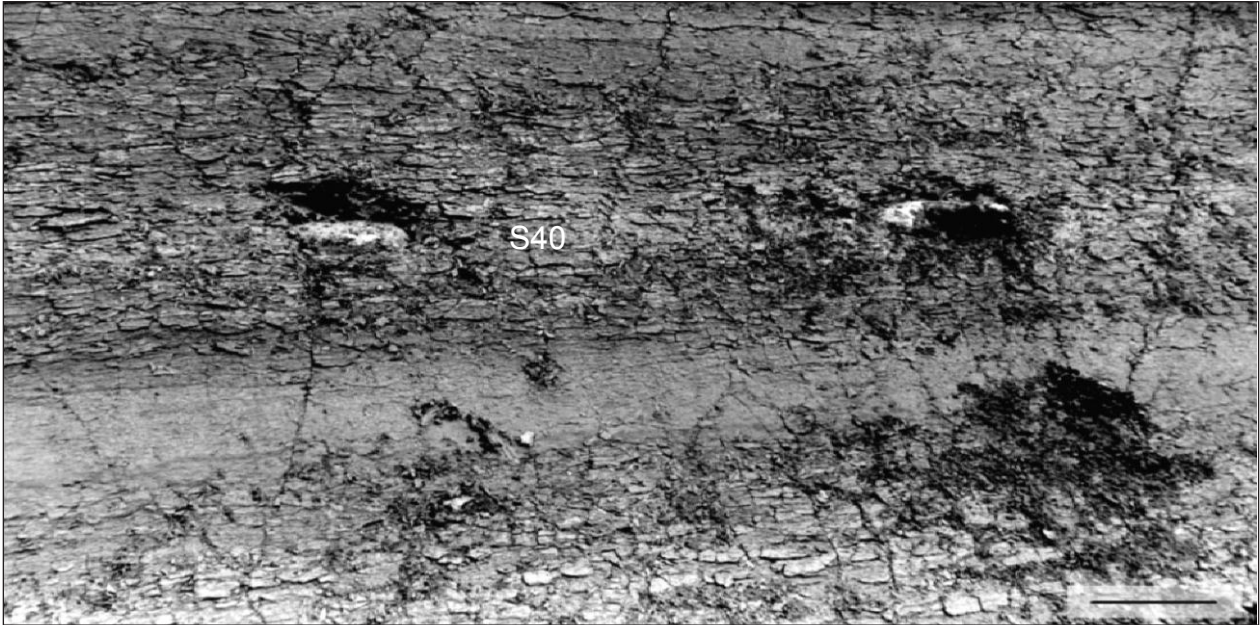
However, in stratigraphic level S60, the concretions also contain siderite (Figure 46). In the sequence stratigraphic analysis, S60 is a level considered to correspond to a maximum relative sea-level position. The sedimentological and chemical zoning, and the high degree of bioturbation in the clay, is indicative for low sedimentation rates. Furthermore, the enclosing clay is strongly enriched in iron, manganese and phosphorus (Figure 47), three elements that are known to be enriched in the uppermost

aerobic zone of marine sediments during slow sedimentation rates (Bonatti et al, 1971; Deming and Baross, 1993; Curtis, 1995). Concentration of iron was the prerequisite for the formation of the siderite-containing concretions. It is thought that the formation of concretions in this layer already started in the slowly accumulating thin sub-aerobic top layer of the sediment, where iron reduction exceeds sulphate reduction, typically resulting in the precipitation of sideritic concretions. The co-precipitation with pyrite

is an argument for a formation in the sulphate reduction zone, and is indicative for a high rate of iron reduction. The latter was due to the rapid changes in sedimentation rates, and hence rapid burial of the iron-enriched layer below the redox boundary (Laenen & De Craen, 2004). Vochten et al. (1975) have reported sideritic concretions around trace fossils with high phosphate content in their center from a clay pit north of Aarschot, Herselt, at a level that probably correlates with the S60 horizon.



Figuur 43. Foraminiferal parameters for the Upper Eocene and Oligocene southern North Sea Basin succession reflecting the continuous occurrence of carbonate deeper than the R horizon and the discontinuous occurrence above (from De Man, 2006; De Man & Van Simaey, 2004). The position of the Boeretang and Eigenbilzen units has been added based on the Weelde well as most data in the figure were obtained from this well.



Figuur 44. Example of carbonate concretions occurring in an originally marly horizon (S40) within a clay layer. Quarry at Terhagen. Scale bar = 50 cm. (from De Craen, 1998).

In general, concretion growth in the Boom Clay occurred in the sulphate reduction zone. The important role of sulphate reducing bacteria in the production of bicarbonate, leading to the precipitation of the carbonate concretions in the Boom Clay, was suggested by the presence of framboidal pyrite and by the typical signature of the carbon isotopes. The presence of sulphate reducing bacteria has furthermore been visualised under the electron microscope, and has been confirmed by organic geochemical studies (De Craen, 1998, De Craen et al., 1999a,b).

Sulphate reduction processes result in the acidification of the pore water. The acid pore waters dissolve the finely distributed carbonates and saturate the pore waters with calcium and bicarbonate. As the lithological composition of the sediment is not homogeneous, some more basic micro-environments may have a sufficiently high pH to precipitate calcium and carbonate; these are the nuclei for

starting the concretion growth in the upper few meters, or even shallower, of the buried clay. Once the precipitation has started it will continue, as usual in concretion growth, because the precipitation creates a chemical gradient around the nucleus. This process of concretion growth will continue till either the chemicals are exhausted or the permeability in the sediment prevents the migration of the elements to the growing concretion. The growing in the clay of the carbonate concretion, that originally starts as a pore filling precipitation, takes place by further displacive and replacive cementation (De Craen, 1998). Calcite contents even higher than 80% were reported in the center of the concretions, diminishing only slightly to the rims. The elemental and isotopic variations towards the edge of the concretions show a progressive evolution of the pore water chemistry during the formation of the concretions, reflecting carbonate precipitation during progressive burial in the shallow-burial realm (De Craen, 1998).



Figuur 45. Carbonate concretion from the S20 level within the Boom Clay, composed of calcite, with the development of septarian fractures, covered with orange-brown ferroan calcite cements. Quarry at Terhagen.

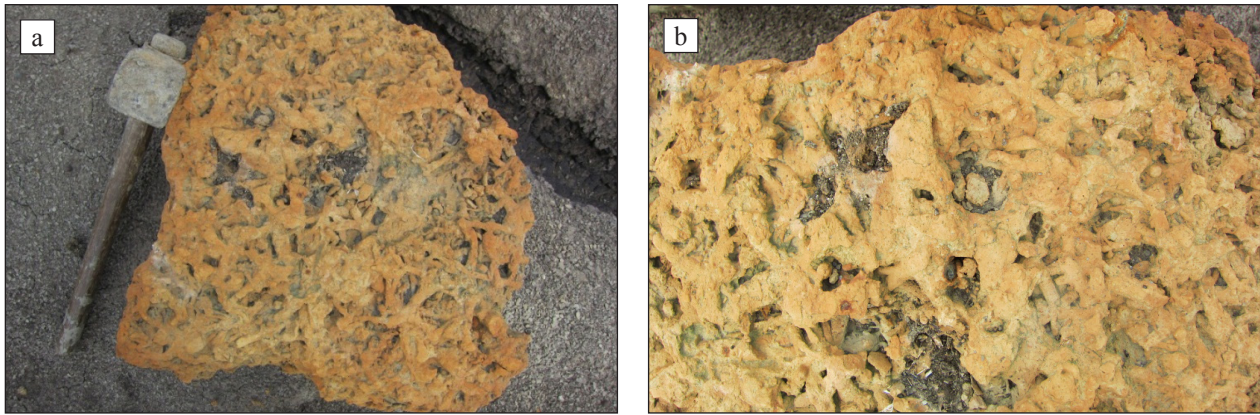


Figure 46. a. Dense network of bioturbations preserved on siderite concretion from the S60 level within the Boom Clay. Quarry at Kruikebe (shovel handle is 60 cm). b. detail of a.

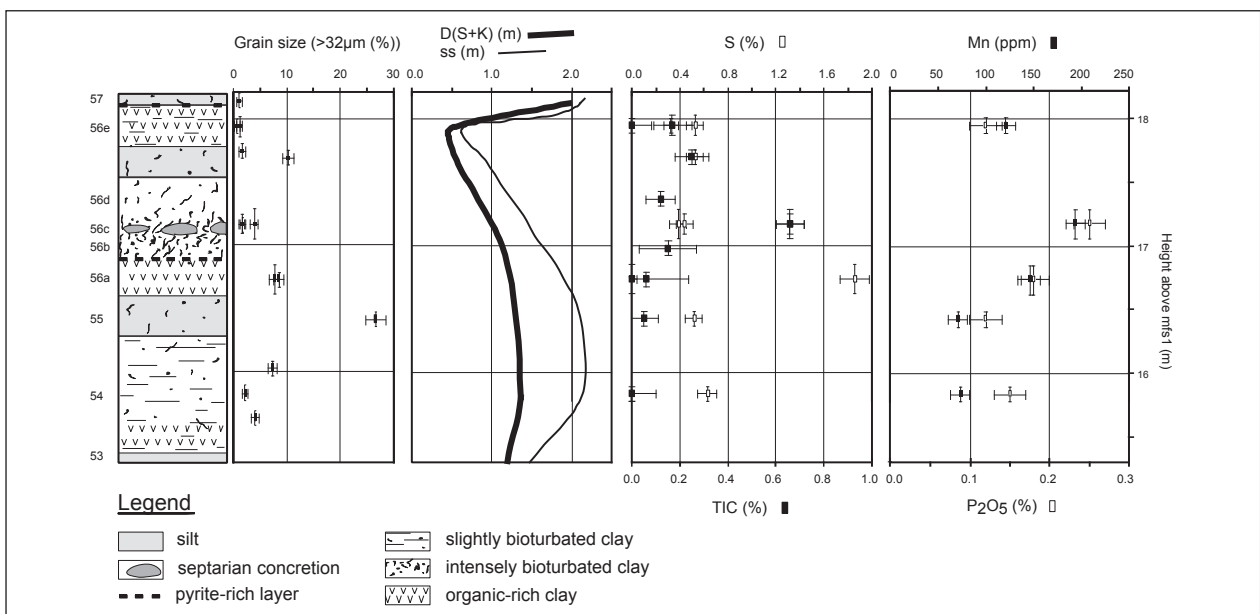


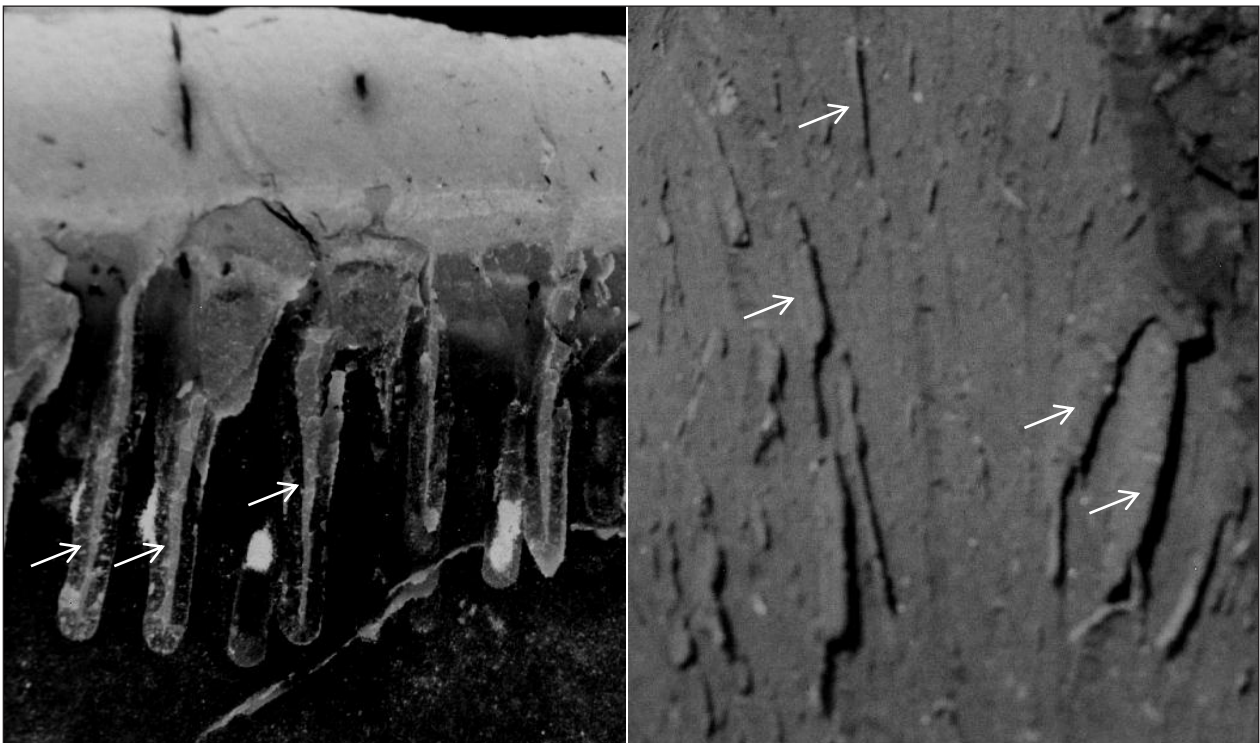
Figure 47. Variations in grain size, sediment supply (represented as the thickness of a silt/clay microsequence, D(S+K)), inorganic carbon content (TIC), sulphur content, manganese concentration and amount of P₂O₅ across stratigraphic level S60. The bed numbers shown left of the litholog are according to Vandenberghe (1974); the depths indicated at the right-hand side are metres above the maximum flooding surface, horizon R, of the first third-order relative sea-level cycle (from Laenen & De Craen, 2004).

Upon further burial of the Boom Clay, but still early in diagenesis, septarian fractures were formed within the carbonate concretions (Figure 48). With burial, the carbonate concretions dehydrate much more rapidly than the enclosing clay. As a consequence, when the concretions solidify, they have an excess of space. This is only for a very limited amount compensated by further compaction of the concretion as the hardened carbonate concretions are now sufficiently strong and react to the overburden stress by cracking. The cracks are vertical as the overburden is the cause of maximal stress and in horizontal view the cracks show a somewhat concentric pattern cut by irregularly radial cracks; this horizontal pattern is probably conditioned by the equal horizontal stress in all directions. Fractures in the inner concretion body are generally characterized by a

rectilinear appearance, and may cut through fossil shells. These are typically brittle fractures that formed when the inner part of the concretions was already well-lithified. The vertical cracks are more open in the center and thin towards the outer limit of the concretion where they disappear; these vertical cracks are also somewhat bulging out towards the outer boundary of the concretion. Furthermore, in the outer rim of the concretions, ‘tapering flakes’ are often observed, a feature occurring when a stiff clay is pulled apart (Figure 49), and septarian fractures often follow the fossil outlines. This suggests that the outer part of the concretion was not yet well-lithified when the septarian fractures formed. These properties are interpreted as the effect of a very early diagenetic start of septarian fracturing, and continuing during further cementation of the carbonate concretions.



Figuur 48. Septarian fractures in a carbonate concretion from the S20 level within the Boom Clay. The vertical cracks are wide open in the center and thin and bulge out towards the outer boundary of the concretion where they disappear. Quarry at Terhagen (from De Craen, 1998).



Figuur 49. ‘Tapering flakes’ at the outer rim of a concretion (left), a typical feature occurring when a stiff clay is pulled apart (right), (from De Craen, 1998).

Once the cracks are formed, the permeability of the concretion remains sufficiently high to allow the passage of pore waters from the surrounding clay towards the water-filled septae in the concretions. The associated precipitation of various cement phases on the walls of the septae, typically carbonates (fibrous calcite with increasing iron content, rhombic calcites, needle-shaped calcites), pyrite or both (Figure 50), typically represent the evolving geochemical conditions in the clay. As indicated by their chemical and isotopic composition and also by the crystal shape, the successive cement phases reflect the evolution of the diagenetic reactions during progressive burial, initially dominated by sulphate reduction processes, but with an increasing influence of methanogenesis with increasing burial depth (De Craen, 1998). Thus, while the concretions were formed due to carbonate precipitation in the sulphate reduction zone (typically leading to ferroan calcite concretions), the cements on the septae walls are indicative of further burial towards the transition zone

sulphate reduction – methanogenesis (becoming progressively more ferroan). This zone is known as the zone of anaerobic methane oxidation, at the boundary between the sulphate reduction zone and the zone of methanogenesis, at about 10 m depth, and being a few tens of cm's thick (Curtis, 1995, 1987; Hoehler et al., 1994; Orphan et al., 2002; Raiswell, 1987, 1988). Due to anaerobic methane oxidation, dissolved HCO_3^- and HS^- is released into the pore water. The carbonate produced in this zone precipitates as ferroan carbonate phases (ferroan calcite, ferroan dolomite, ankerite, siderite). Pyrite precipitation may also occur. Anaerobic methane oxidation may be in agreement with the late formation of pyrite crystal precipitation in the septae of the Boom Clay concretions; the methane generated by the degradation of organic matter in the sediment could have reduced remaining sulphate, or reacted with primary pyrites and in this way produced sulphide anions that could reprecipitate as newly formed crystalline pyrite on top of the calcite cements in the septae.

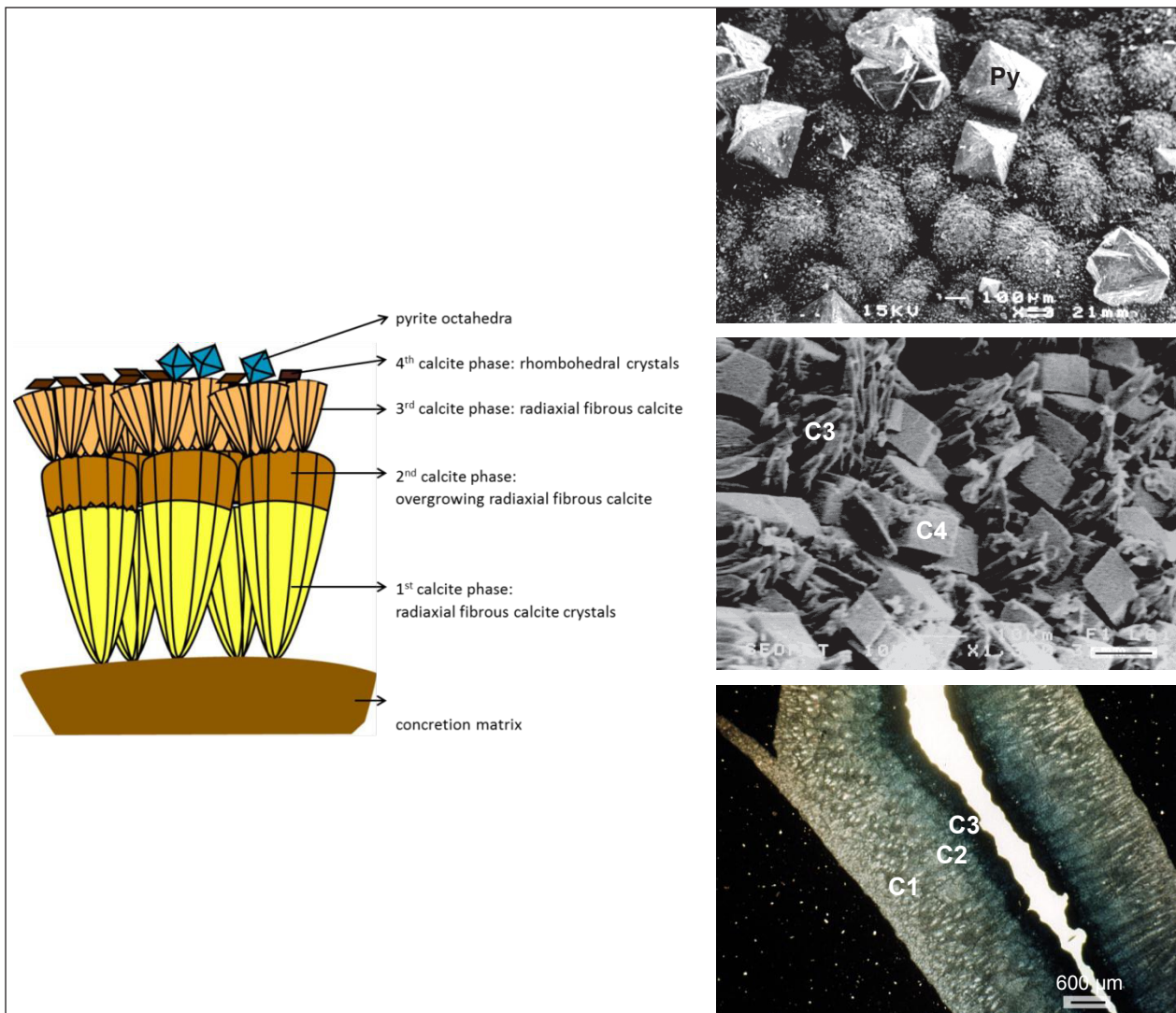


Figure 50. Left - Schematic representation of the various cement generations recognised in the septarian fractures of concretion from the S40 level within the Boom Clay. Right – Subsequent generations of cements filling up the septae: C1-C3: successive phases of fibrous calcite cements, progressively becoming more ferroan, C4: rhombohedral calcite crystals, Py: pyrite octahedra (after De Craen, 1998).

Upon further burial, methanogenesis becomes the dominant process, releasing dissolved HCO_3^- and CH_4 , and encouraging the precipitation of siderite. It is not clear if cementation of the septae of the Boom Clay concretions continued in the zone of methanogenesis.

At present, the water inside septarian carbonate concretions has a similar chemical composition as the present pore water composition of the clay (NaHCO_3 type water at the Mol-site).

It can be concluded that the carbonate concretions in the Boom Clay started to form rapidly after burial of the sediment, slightly below the water-sediment interface. During low accumulation rates, concretion growth already started in the thin sub-aerobic top layer of the sediment (S60), but generally, concretion growth occurred in the sulphate reduction zone, typically within the first 10 m of depth. The completion of the concretion growth, the septae formation and the precipitation of new cements in the septae was already finished when the burial brought the sediment with its concretions in the top of the methanogenetic zone. This means that only about 10 meters of burial were required to reach the final stage of the formation of the septarian carbonate concretions (De Craen, 1998). The septaria loaf shape and their size are determined by the thickness of the marl horizon, the maximal carbonate content located in the center of the horizon and the total amount of carbonate originally in the marl.

In the Antwerp area, fragments of fully formed septaria were found at the base of the Burdigalian Edegem Sands confirming a very early formation of the concretions.

4.4. The oxygen conditions of the water in the Rupelian sedimentary basin

The common occurrence of black clay layers (sometimes with organic matter content up to 5 %; Figure 31), the very typical presence of pyrite nodules (sometimes up to cm sized), the presence of pyrite layers, and the relatively poor mollusc content of the clay are all indications of an oxygen deficit in the sedimentary basin.

Regarding the macrofossils, the fauna is dominated by the benthic molluscs *Nucula deshayesiana* and *Gemmula selysii*, but in fact a whole list of less commonly occurring molluscs exists (Glibert, 1955, 1957; Glibert & de Heinzelin, 1954). In the septaria horizons apparently more molluscs are generally present than in other parts of the clay. Burrowing is very common in the clay. Many of the fish species identified have a benthic mode of life. Benthic microfossils such as foraminifera are present, but their abundance is always low (Figure 43), with higher abundances in the septaria horizons.

Therefore, the fossil content suggests a fairly hostile environment for life, but life was not impossible. The bottom water might generally have been close to suboxic. A suboxic zone of several meters can occur between the oxic and anoxic zones in a sedimentary basin and is characterized by very low oxygen and sulphide contents (Murray et al., 1995). It has been suggested that the higher abundances of fossils in the carbonate layers is related to the presence of more oxygen in the bottom waters (De Man, 2006).

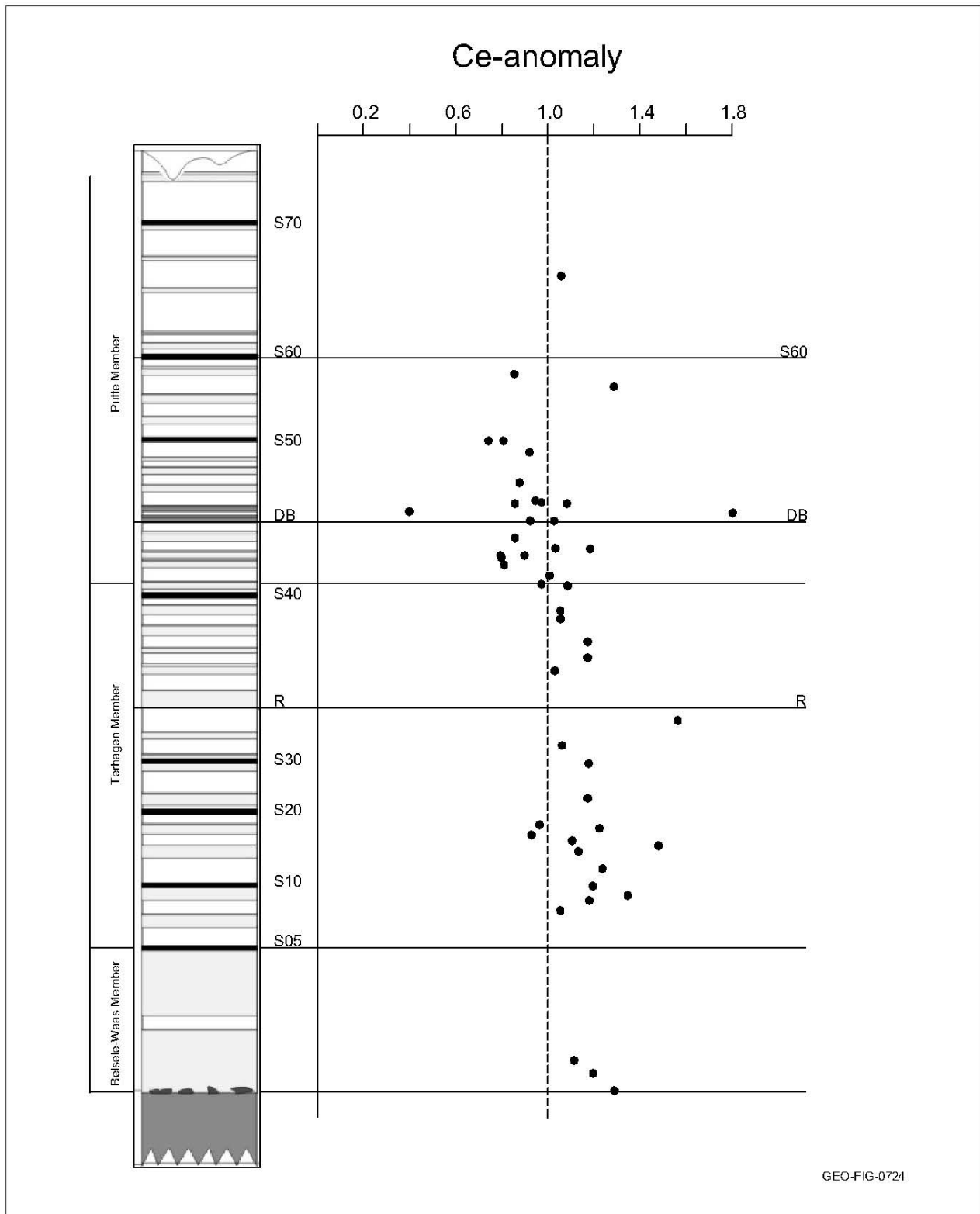
The abundance of pyrite is obviously related to an early diagenetic process. The pore waters very rapidly became reducing and the common formation of pyrite is caused by the hydrogen sulphide, produced by bacteria thriving on organic matter and reducing the sulphate in the marine pore waters, combined with the bivalent iron, brought into dissolution by reduction from the oxidised iron coatings attached to the detrital clay minerals. The framboidal nature of many early pyrites is the result of this bacterially-mediated origin (Berner, 1984, 1985; Sawlowicz, 1993; Folk, 2005). The bacterial origin is also the reason that pyrite is so commonly related to organic forms such as mollusc fossils, burrow traces and wood fragments. This type of pyrite formation can continue as deep as sulphate can migrate from the sea water into the sediment; some 10 m deep.

The observed layered pyrites (base R, Figure 11), probably have a very early diagenetic origin in the sediment. At least four pyrite layers have been reported in the outcrop area (Figure 11) of which the thin whitish weathering layer at the base of the R horizon is the most conspicuous one in the field. The last example is certainly independent of variations in organic matter content in the section and could be an original ferric oxide layer which became transformed into pyrite when burial reached the reduced conditions of the sulphate reduction zone (Vandenbergh, 1978). The other layered pyrites are situated in the black organic rich Putte Member and could eventually be due to early diagenetic migration of sulphide and precipitation of pyrite at the boundary between black and grey clay. Organic molecule studies (Laenen, 1997), and also the higher pyrite quantities in the black layers, have shown that the rate of sulphate reduction was highest during the deposition of the black layers.

The common but reduced presence of benthic life at the Boom Clay sea bottom shows that the bottom waters were not anoxic and at the worst suboxic. This is also supported by organic chemical compounds in the Boom Clay. Buried Boom Clay mud sediments very quickly became reduced as most clearly shown by the omnipresence of pyrite. An indication on the depth of the redox boundary in the sediment is given by the Ce chemistry of the shark teeth commonly preserved in the clay (Laenen, 1997, 1998; Figure 51). Shark teeth change their organic-phosphorus compounds into mineral

apatite at the very start of their burial. During this crystallisation, trace elements are taken up by the apatite as a function of their availability in the pore waters (Laenen et al., 1997). This is also the case for Ce which

is a redox sensitive lanthanide. In the oxic zone, Ce is fixed in the iron and manganese oxides-hydroxides and only becomes available in the pore water near the redox boundary where these oxides-hydroxides are dissolved.



Figuur 51. Ce-content in shark teeth collected from the clay plotted along the composite lithologic log of the type section of the Boom Formation. The values are normalised with respect to the value at the boundary between the Terhagen and the Putte Member (value 1). Note the change in Ce content occurring at this boundary (after Laenen, 1997).

Relative higher concentrations of Ce can be absorbed by teeth crystallisation at this redox boundary, and in fact only at that position. Indeed, in the reduced zone, Ce can only be further brought into solution by dissolving organic and mineral compounds, leading to very low Ce concentrations in reduced pore waters. Therefore, the reduced pore waters will be characterized by very low concentrations of Ce. Assuming that the crystallisation of the shark teeth is almost completed at 1 to 2 m depth, the higher Ce contents in the shark teeth of the clays of the Terhagen Member, pointing to their mineralisation around the redox boundary, show that the redox boundary in the Terhagen Member was probably situated around 1 m depth; the sharp rise in Ce content at the Terhagen/Putte Members boundary reflects the sudden separation of the crystallisation level and the redox boundary by bringing the redox boundary close to the sediment water interface, but not in the sea water itself as discussed above. Therefore, the clay of the Putte Member contains shark teeth with low Ce contents as the higher contents were produced in the very top of the sediment and were already evacuated by the time of the crystallisation of the teeth apatite. The sudden rise could be due to a sudden increase in organic matter; however, the estimation of the amount of organics destroyed by oxidation in the clay of the Terhagen Member is unsure and therefore it is difficult to be certain about the difference in the amount of organics brought into the basin during the Terhagen and the Putte Members regimes. The fact that also in the Upper Rhine graben this transition to black clays occurs at exactly the same time (Grimm & Steurbaut, 2001) may point to a major event explaining the sudden arrival of more organic matter or the sudden better preservation conditions upon burial.

4.5. Climatic conditions during the Boom Clay deposition

Fossils have been the classical source of information to derive climatic conditions in the geological past. Since no major latitudinal changes have occurred in the southern North Sea area since the Eocene, information from the fossil record can reasonably be obtained by comparison with modern analogues. Fish remains in the Boom Clay have been reported to show a subtropical to warm temperate climate (Steurbaut & Herman, 1978). Palynology has shown the vegetation during the Rupelian to evolve from warm and humid at the base to colder and probably drier at the end (Roche & Schuler, 1979). A similar conclusion was reached from the trend in the stable oxygen isotope data (Figure 20) and the weaker weathering towards the end of the Rupelian (Figure 22).

A detailed study of the benthic foraminifera (De Man & Van Simaëys, 2004) shows a cold temperate climate with bottom water paleotemperatures never exceeding

10°C (Figure 16). The temperatures are again distinctly higher in the upper Oligocene Voort Sands.

The cooling of the climate since the middle Eocene is also demonstrated by the study of the stable oxygen isotope composition of calcareous fossils (molluscs, foraminifera, fish otoliths). In fact the temperature has fallen stepwise, particularly since the beginning of the Priabonian and a major cooling occurred at the base of the Ruisbroek Sands and the Borgloon Formation; this is shortly after the beginning of the Oligocene and at the base of the stratigraphic sequence that brings the Boom Clay over the area (Figure 20; see also 3.9). It is this major cooling that is usually associated with the start of the growth of larger ice caps on Antarctica (Miller et al., 1991; Zachos et al., 2001).

Study of the fish otoliths (small oval calcareous concretions in the inner ear of vertebrates) with clear growing rings even allows to detect the seasonal temperature differences; for the Boom Clay waters in the North Sea Basin the mean annual cooling is associated with a strong reduction in the seasonality as well. Also the palaeotemperature differences obtained from benthic and from planktonic foraminifera allow to estimate a 5 °C difference between bottom and surface waters in the Boom Clay sea (De Man, 2006).

At the more detailed stratigraphic level, oxygen isotopes show no clear relation with the astronomical cyclicity (0). However, interestingly the averaged resistivity values in the ON-Dessel-1 borehole show a clear asymmetrical signal varying at the 100 ka eccentricity pace (Figure 52). Slowly increasing resistivity or silt content, which means a slowly lowering sea-level, is followed by rapidly decreasing values, meaning a rapid rise of the sea-level. This is exactly the sea-level fluctuation steered by climatic conditions during the glaciations of the last 800 ka. Therefore, this pattern in the Boom Clay is interpreted as a strong support for the existence of waxing and waning ice caps and consequently for eustatic sea-level variations. Obviously, these are not directly related to the climate at the latitude of the North Sea, but are confirming the general cooling also observed in the Boom Clay of the North Sea area. In ocean drilling cores, similar studies using oxygen isotope composition of calcareous microfossils have also shown the orbital forcing on glacio-eustatic variations and calculated a value of 50 to 65 m for the major 1,2 Ma obliquity driven eustatic sea-level change; these levels occur approximately between the R and DB horizons (Oi2 on Figure 21), above S130 (Figure 12, Oi-2* on Figure 21) and in the Eigenbilzen Formation (Oi-2A on Figure 21). No good indicators exist in the Boom Clay to evaluate the 40 ka obliquity driven sea-level changes associated with the silty clay-clay alternations but logically they are less than the 50 m estimated for the largest oxygen isotope changes.

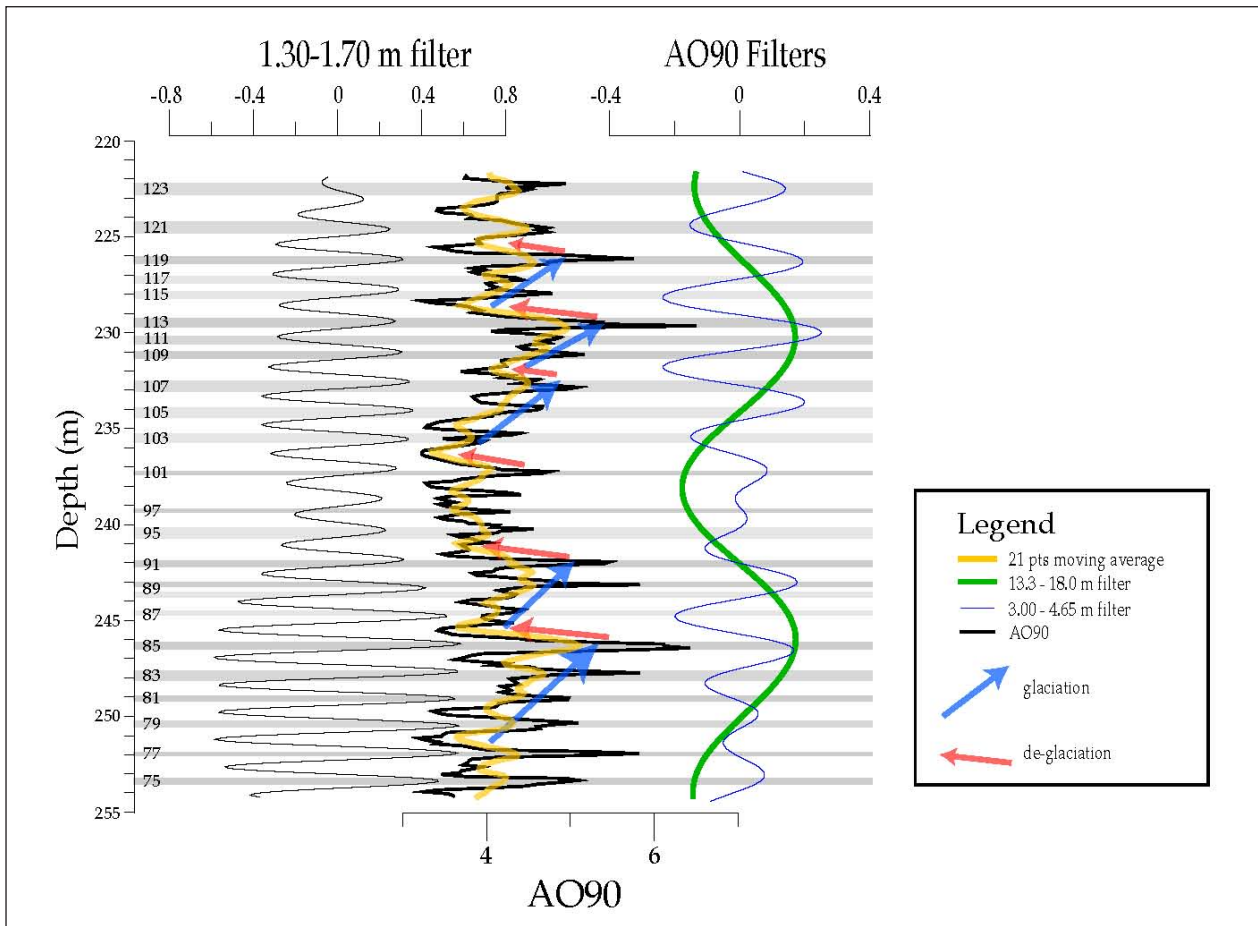


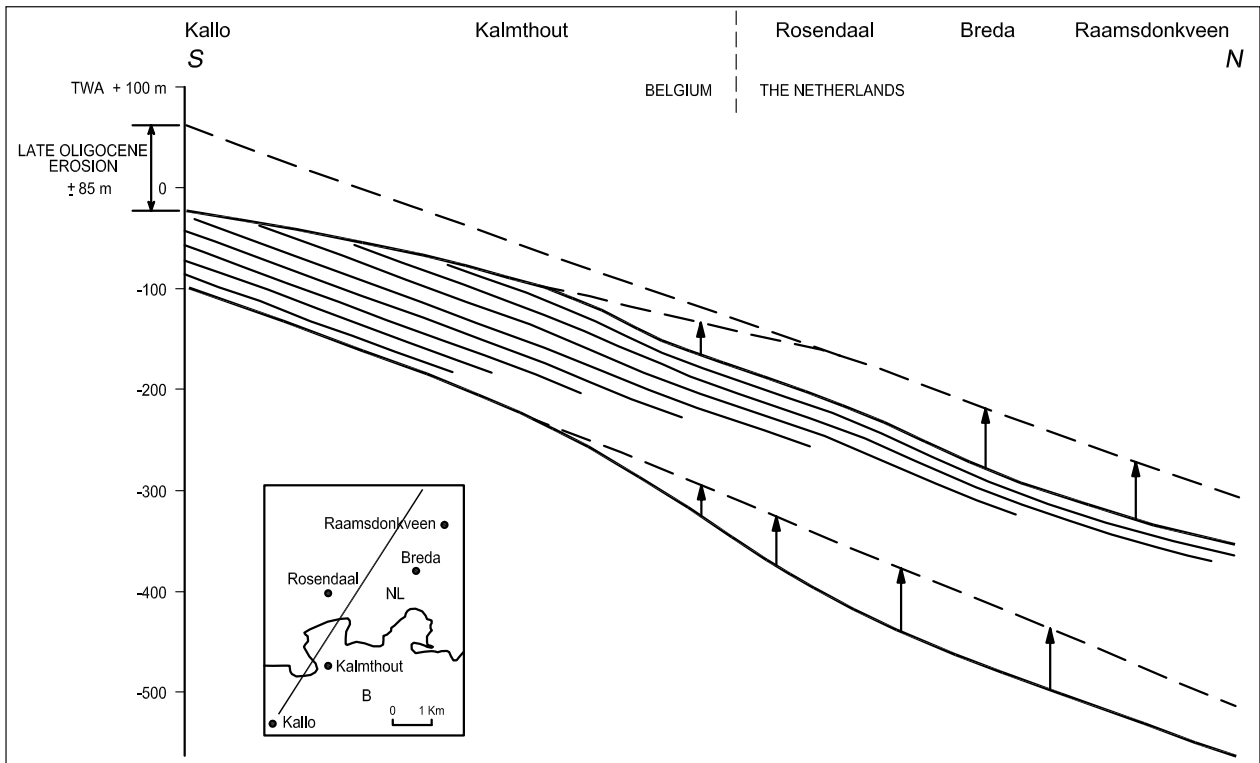
Figure 52. Detail of the Boom Clay stratigraphy in the Dessel-1 borehole showing the AO90 resistivity record (proxy for grain size), its 21-point moving average, and the 1.30-1.70, 3.00-4.65 and 13.3-18.0 m filters of the record. Blue (or dashed red) arrows indicate gradual increasing (or decreasing) grain size. A pattern of gradual increasing ice volume and fast deglaciations can be recognised, due to the interplay of obliquity and the 100 ka and 405 ka eccentricity (from Abels et al., 2007). Note that around 240m depth about 4 grain size cycles are present compared to the expected 2 obliquity cycles: this could be the indication of the presence of precession cycles already detected in the Boom Clay by Van Echelpoel and Weedon (1990).

4.6. Tectonic activity during the Rupelian

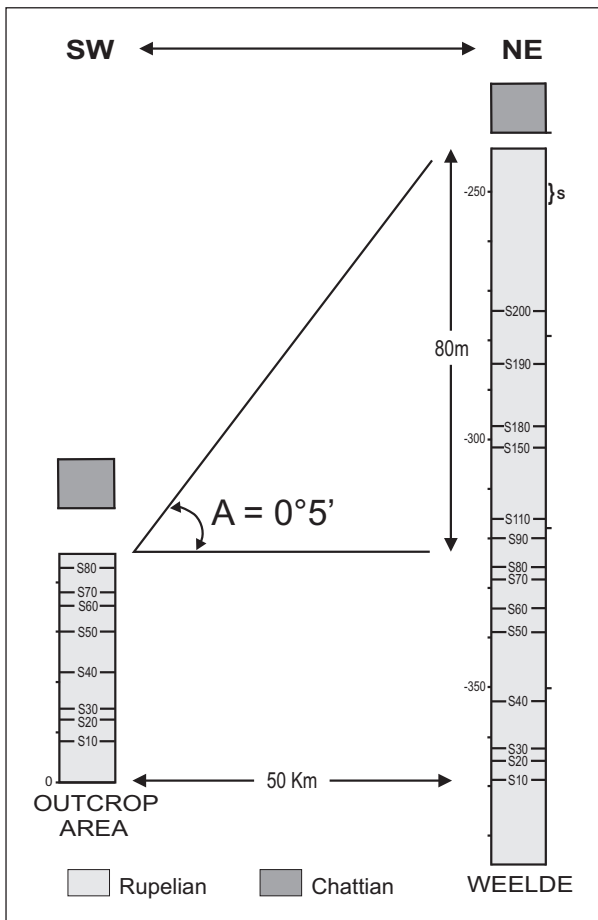
The Boom Clay is exposed in Belgium along the river Rupel where it has a maximum thickness of 80 m, whilst in the subsurface of northern Belgium its thickness reaches a maximum of 135 m. The lower thickness in the outcrop area results from erosion, as can be derived from a geometrical reconstruction in which the base of the Boom Clay is straightened into its pre-Neogene-differential-subsidence shape (Figure 53). The erosion must have taken place before the early Chattian, more precisely before the second Chattian sequence at the NP24/25 boundary, as deposits of that age have been found on top of the Boom Clay in the Antwerp harbour area. The start of this erosion occurred already during the latest Rupelian as this erosion event has been related to the sudden influx of reworked Cretaceous microfossils a few meters from the top of the Rupelian deposits in the Campine area (De Man et al., 2010)(Figure 54). The lower part of the clay preserved in the outcrop area can be correlated layer by layer to the Campine subsurface

(3.2.2) where about 80 m of younger Rupelian, Boom Clay and Eigenbilzen Formation overlies the lower outcrop part of the Boom Clay. This thickness corresponds to the 80 to 90 m of now eroded overburden estimated for the Boom Clay in the Antwerp area (Schittekat et al., 1983). Neogene sediments never were that thick over the area (see Figure 64-Kruikebeke). Therefore it is concluded that the almost complete Rupelian section present in the Campine area was also present in the Antwerp area and that 80 m of it was eroded in the west during the latest Rupelian to earliest Chattian at a rate of at least 6 mm/100 yr. Remarkably, some 25 km to the east, almost no erosion took place (Figure 54).

Tectonic activity during the Rupelian in the provenance area around the basin can be deduced from the sediment supply evolution which is reflected by the thickness of the silt-clay couplets which all formed during the same time interval (0) (Vandenberghe et al., 2005; Vandenberghe and Mertens, 2013).

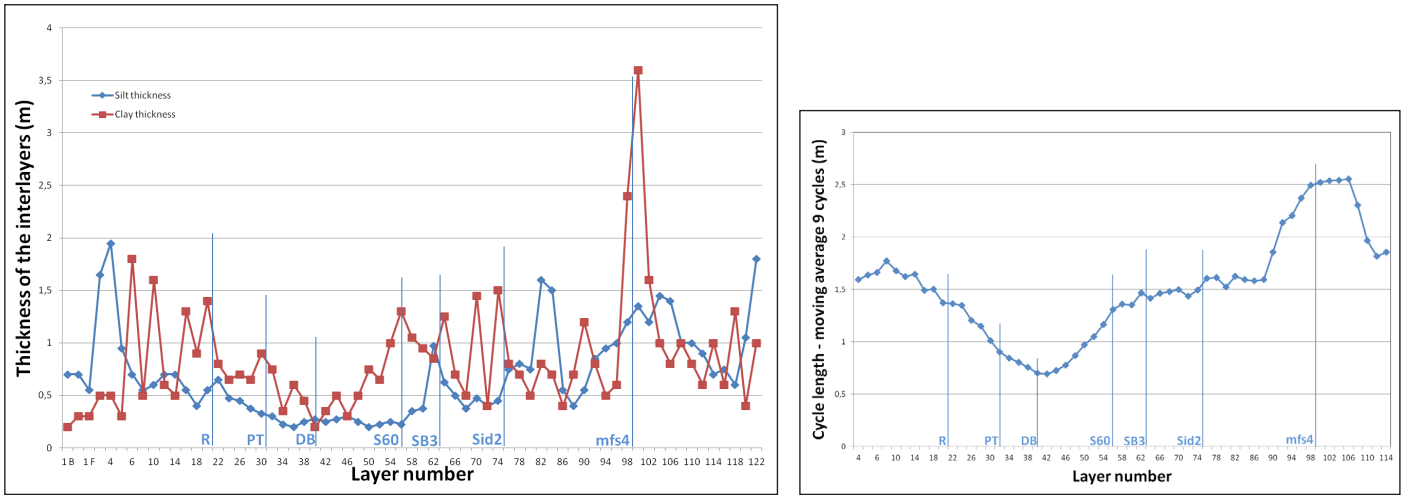


Figuur 53. Reconstruction of the eroded part of the Boom Clay at the Rupelian-Chattian sea level drop (from Vandenberghe et al., 2003). The reconstruction is based on the elimination of the post-Rupelian bending of the clay layer and the presence of internal layering in the clay parallel to its base. The timing of the erosion is constrained by the presence of Chattian deposits on top of the Boom Clay in the Antwerp area.



In a vertical section in the outcrop area, the thickness of the silty clay layers and the silty clay/clay bed thickness ratio reflect the duration of the turbulence impact (0). As these thicknesses do not vary considerably (Figure 55 top), it can be assumed that the turbulence impact on total thickness was not important. Therefore, the total thickness of the silty clay/clay couplets (Figure 55 bottom), and the thickness of the clay layers in particular, do reflect the sediment supply. Hence, they are indicators of the vertical tectonic movement intensity and erosion in the area surrounding the basin. For the outcrop area, tectonic uplift was larger at the base, lowest in the middle part and again higher towards the top. The former is probably related to the presence of many reworked microfossils in the Ruisbroek Sand just below the Boom Clay and the latter can be the announcement of the uplift and later erosion of the basin itself in the Antwerp area.

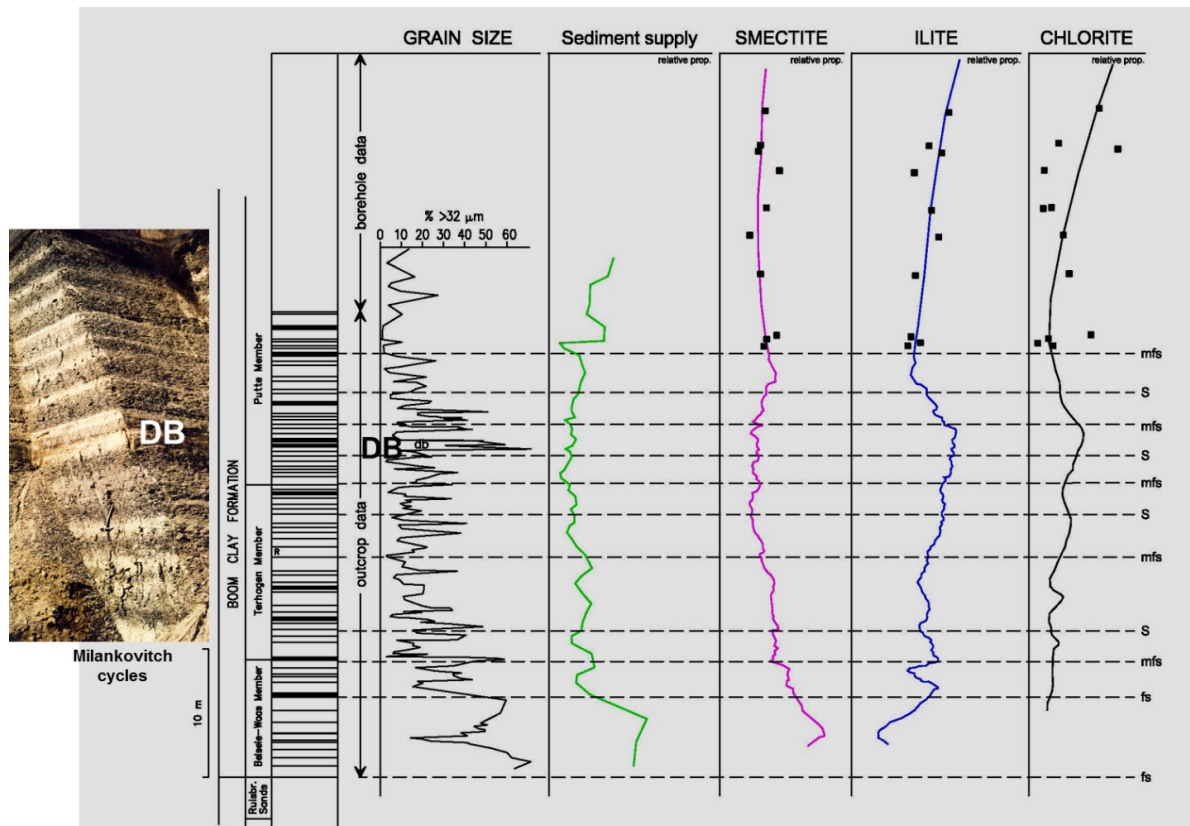
Figuur 54. Schematic illustration of the tectonic tilting in North Belgium during the Rupelian-Chattian transition. The same Rupelian clay section as now preserved in the Campine area (Weelde borehole) is now present in Antwerp (outcrop area) at the end of the Rupelian and was eroded before the deposition of the middle Chattian sequence (Vandenberghe et al., 2004). The time the erosion started corresponds in the Weelde borehole to the level with an influx of reworked silicified Upper Cretaceous Heterohelicidae foraminifer (level 's' in Weelde borehole) (from De Man et al., 2010).



Figuur 55. Left: The thicknesses of the individual silty clay and clay layers plotted along the horizontal Boom Clay section (bed numbers in 12). The thickness variation of silty clay - clay obliquity couples is dominated by the variations in their clay bed thicknesses (courtesy J. Mertens); Right: Total cycle thickness evolution along the horizontal Boom Clay section (from Vandenberghe & Mertens, 2013). The key stratigraphic layers are the red horizon (R), the Putte-Terhagen limit (PT), the double layer (DB), septaria level S60 , sequence boundary SB3, upper siderite horizon and main flooding surface mfs4 (see figures 23,24).

The higher sediment supply at the base of the Boom Clay is accompanied by a relative increase of well-crystallised and low-charge smectite with a southern provenance, pointing to the uplift of the Artois-Brabant Massif. The increased sediment supply at the top of

the Boom Clay is characterized by higher proportions of illite and chlorite, apparently due to the uplift of the Ardennes-Rhenish Massif (Figure 56). This uplift of the Ardennes-Rhenish belt precedes the reactivation of the Lower Rhine graben system in the Chattian.



Figuur 56. Grain-size variations, sediment supply based on cycle thickness, and variations in smectite, illite and chlorite in the outcrop type section of the Boom Clay Formation and extended upwards by analyses in boreholes (after Laenen, 1997).

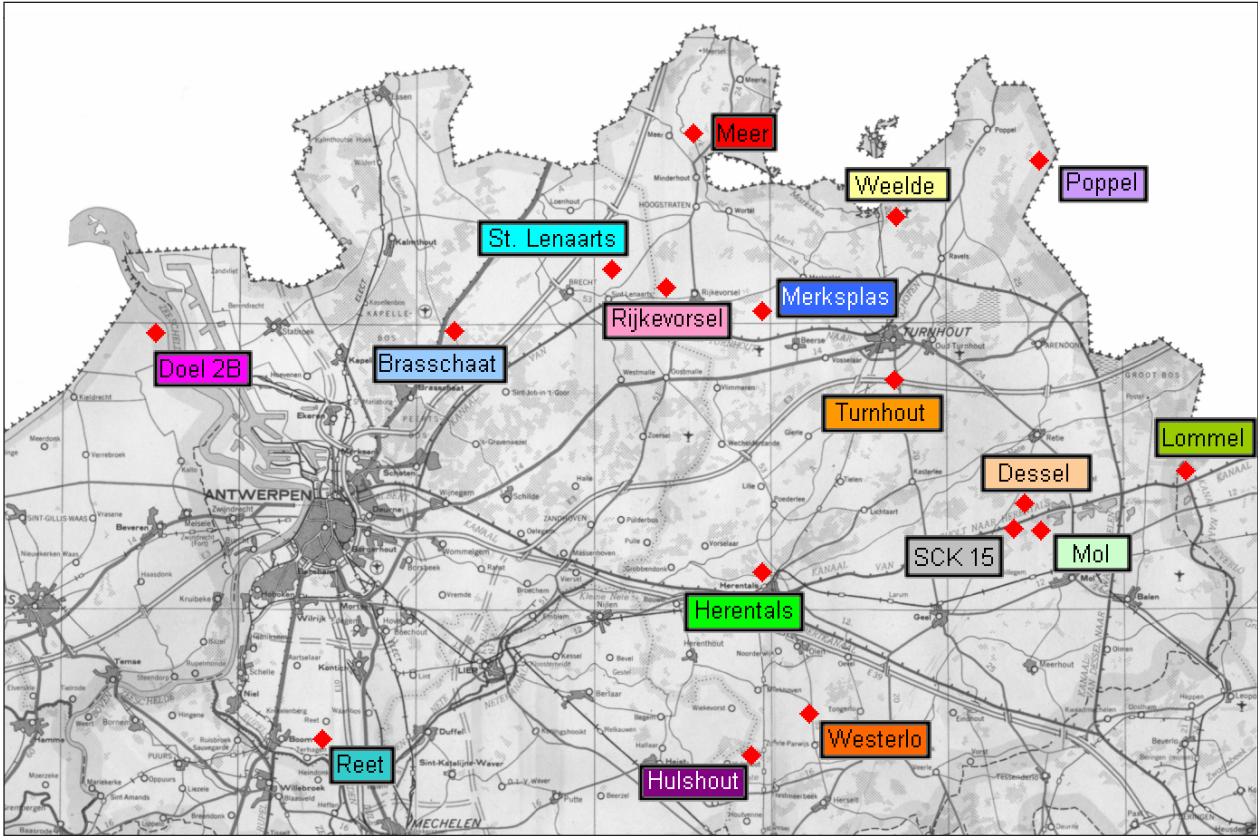


Figure 57. Location of the investigated boreholes in order to study lateral variations and the internal layering of the Boom Clay in northern Belgium (from Mertens, 2005b).

The alternating silty clay and clay layers of a few tens of centimeter thickness can be precisely identified and characterized by the resistivity log in boreholes. Correlation of the individual layers between the wells in the area is hence well established. It is therefore also possible to precisely measure the thicknesses of the individual layers and compare these thicknesses between wells spread over the Campine area (Figure 57). In case that, not the absolute thicknesses, but the thickness differences of a particular layer compared to the thickness in a reference well are considered (Figure 58), the influence of eustasy is eliminated. The remaining parameters explaining such thickness differences are local tectonism and sediment supply.

Maps constructed for the lower outcropping part of the Boom Clay, displaying the cumulative differences as explained in Figure 58, show that initially, from the base of the clay till about the double band, the western part of the Campine Basin is receiving less sediment than the Herentals, Turnhout, Weelde axis and the rest of the Campine Basin (Figure 59A-E). Somewhat later at the position of the S60, the extension of the clay deposition towards the west is shown by the cumulative thickness map (Figure 59F). On cumulative thickness maps showing the evolution between the double band and the levels 45 and 55 (=S60) (Figure 59G-H), the start of the stronger subsidence of a northern part of the Campine Basin stretching from Doel to Poppel is observed. In the south, the present Rupel area links up with the southern Antwerp Campine area as a relatively

less subsiding area (Figure 59H). More remarkably, the block east of the Mol and Dessel area becomes also relatively less subsiding at that time (Figure 59F-H), probably announcing the uplift of the whole eastern area as shown by the development of the more sandy facies of the Eigenbilzen Formation in that area approximately from that time onwards (Figure 14). In fact, this is the area where the renewed subsidence of the Roer Valley Graben during the Chattian will activate a series of northwest-southeast faults. Uplift of an area before it becomes rifted is common.

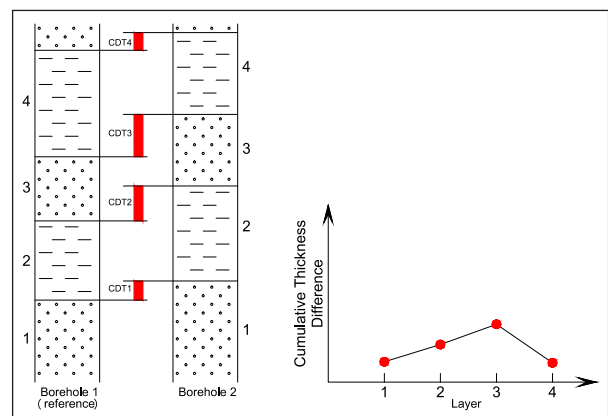
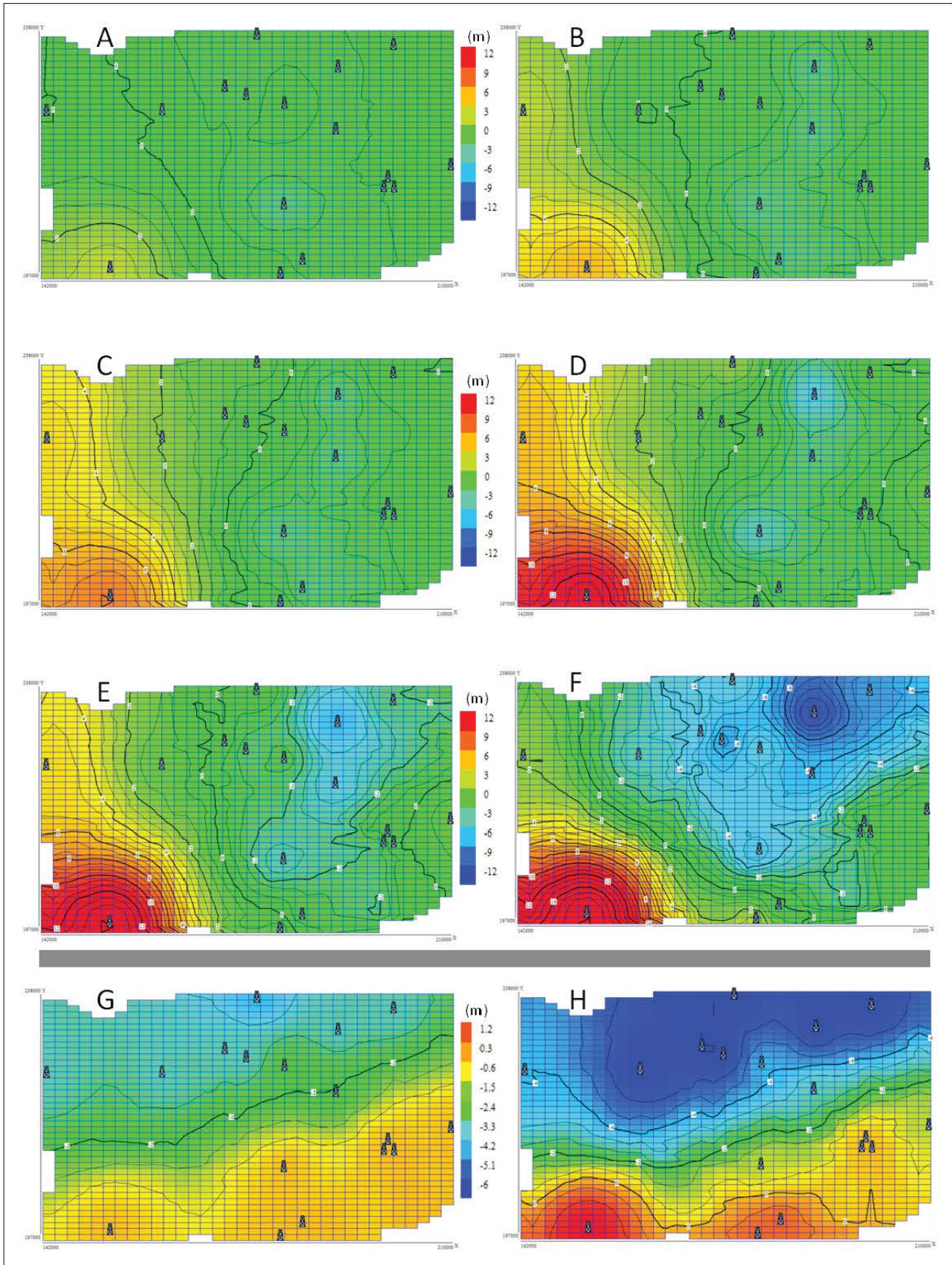
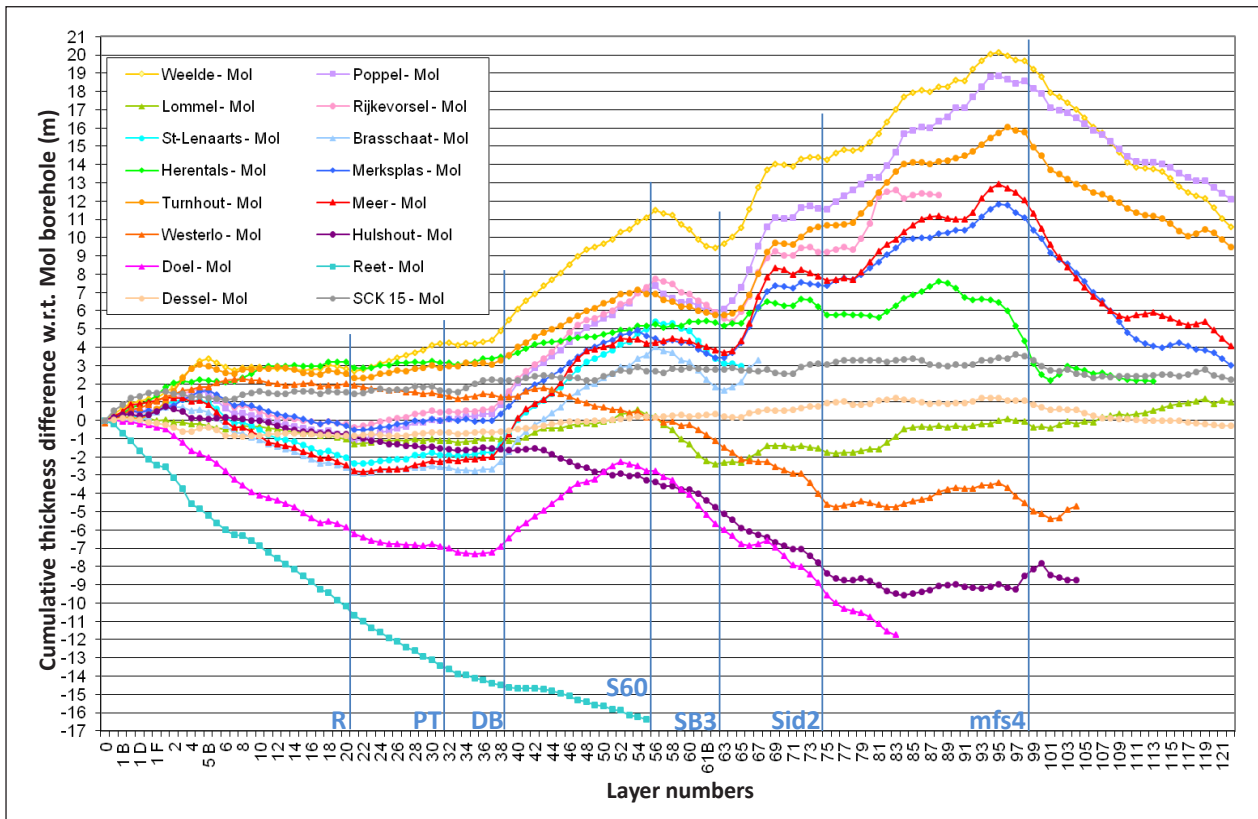


Figure 58. Illustration of the principle of the Cumulative Thickness Difference (CTD). Borehole 1, which is the reference borehole, is compared to borehole 2 (from Mertens, 2005b; Vandenberghe & Mertens, 2013).



Figur 59. Maps of areal distribution of differential sedimentation rates. The maps are produced by contouring the cumulative thickness differences of the individual layers with the Mol well as reference. Maps A to F show the differences from the base of the clay till the level 2(A), 8(B), 16(C), 32(D), 40(E) and 55(F); maps G and H show the differential evolution between the DB level and level 45 (G) and DB and level 55 (H). For situation of levels with respect to reference horizons (R, DB, SID,...) see Figure 12 (from Vandenberghe & Mertens, 2013).



Figuur 60. Cumulative thickness differences of individual wells with the Mol-1 borehole as a reference. Some of the bends positions where slope changes occur can be linked to features as maximum flooding surface (R, S60, mfs4) sequence boundaries (DB) etc. (from Mertens, 2005b; Vandenberghe & Mertens, 2013).

The patterns obtained in the Figure are remarkable as they represent local subsidence differences subsequently compensated by a difference in suspension sediment supply. Most logically, the sediment winnowed from the deeper areas is transported in suspension to the deeper areas, leading to increased sediment thickness in the more subsiding parts of the basin. However, it is not excluded that also gravitational movement of a dense suspension layer forming during sedimentation just above the bottom, a fluid mud layer (Wright & Friedrichs, 2006), has directed the fluid mud slowly to the deeper parts explaining the subtle but real thickness differences within a same layer over the Campine Basin.

Representing the cumulative differences as determined in Figure 58 over the entire sediment column in a single borehole (Figure 60) is equally instructive as are the map patterns (Figure 59). As long as a particular area continues to deviate in the same way from the reference area, the trend of the cumulative curve obtained from a particular borehole will be the same and a change in trend means the thickness evolution compared to the reference area has reversed. The cumulative curves show a remarkable coherence between the different wells (Figure 60). Surprisingly, the main turning points in the trends, representing turning points in the tectonic relative subsidence evolution occur precisely on the R, DB, and S60 levels long considered as eustatic

sequence surfaces (3.9). Because of this coincidence between these particular levels and the changes in thickness evolution, these levels must be related to tectonic events rather than glacio-eustasy related.

On a regional scale, the Rupelian tectonics of the area are controlled by important subsidence during the Rupelian, probably as a reaction to the compressive strains in the Alpine front such as the Pyrenean pulse at the Bartonian-Priabonian boundary recognized as a low-angle unconformity in the area and by renewed and strong subsidence of the Lower Rhine Graben at the beginning of the Chattian.

4.7. The post-Rupelian tectonic evolution of the area affecting Boom Clay

Fault-related post-Rupelian tectonics affected the eastern Campine and therefore also influenced the present geometry of the Boom Formation (Figure 62). The renewed subsidence of the Roer Valley Graben since the early Chattian acted along earlier faults. The western boundary faults of the graben affected northeast Limburg and also the Mol area with, a.o., the well known fault of Rauw.

The history of the subsiding Roer Valley Graben may have started in the Paleozoic, but the outline of the fault

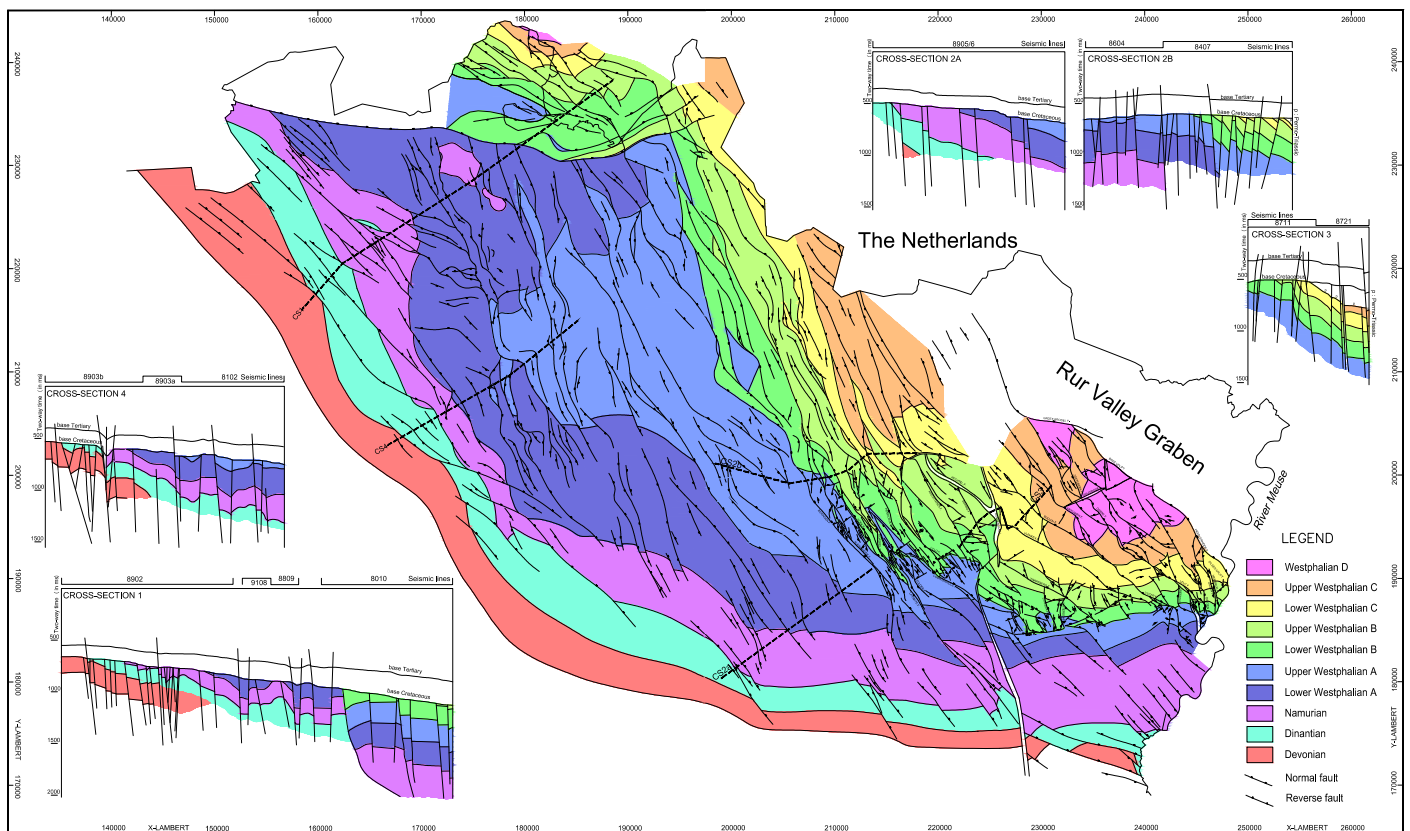
system as seen today developed during the Middle and Late Jurassic: it was inverted into an uplifted block due to Alpine movements during the Late Cretaceous and, after a period of quiescence in the main part of the Paleogene, renewed subsidence started in the beginning of the Chattian at the end of the Paleogene. Subsidence rates peaked during the Chattian and the Pliocene as can be derived from the thicknesses of the strata compared to those in the Campine Basin.

Mapping faults needs to consider also at which stratigraphic level faults were active. Therefore, the map showing the faults affecting the base of the Miocene can be different from maps showing the faults in the same area at the top of the Paleozoic or at the present surface. The Cenozoic faults are reactivations of Paleozoic faults, which develop upwards in the less consolidated sediments under different angles and sometimes also splitting into several branches. Fault maps at the top of the Paleozoic and at the base of the Cretaceous, Paleocene, Miocene and Pliocene are shown in Figure 591 and Figure 602 respectively, the latter based on the DOV website (see also Van Baelen and Sintubin, 2006).

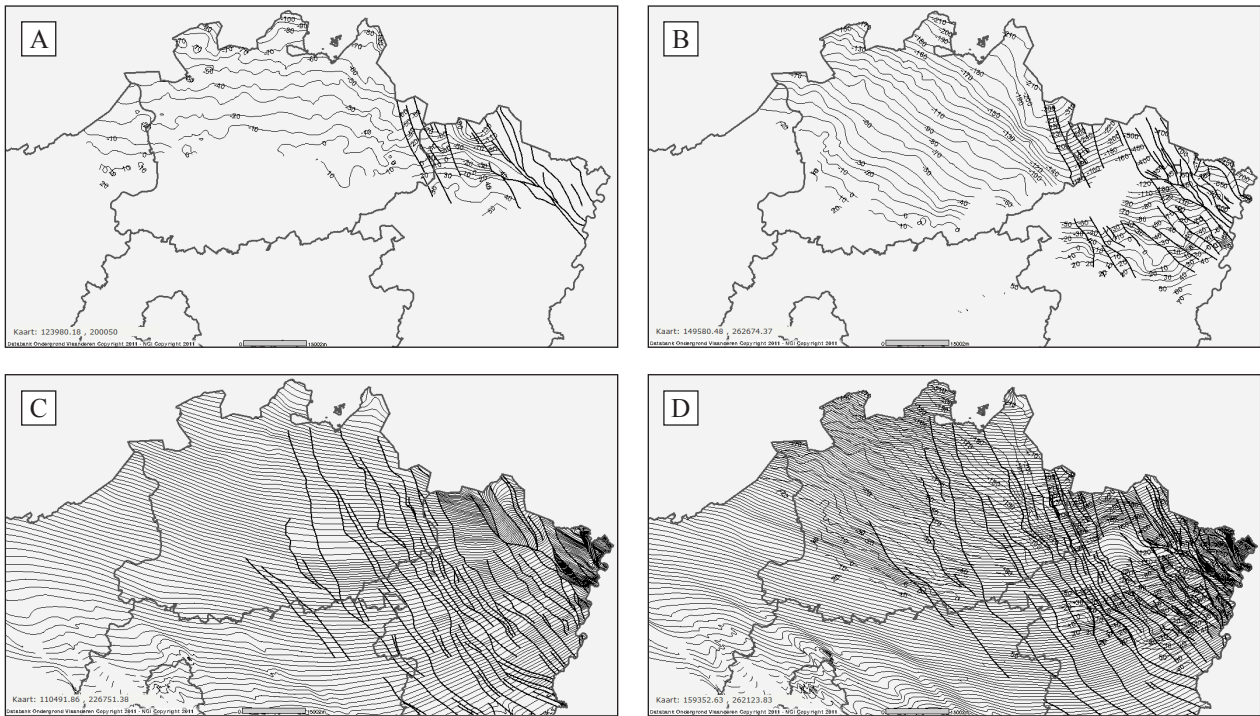
Reactivated basement faults that do not reach to the surface may bend overlying soft sediments, a case relevant for the Boom Clay in the western part of the Roer Valley Graben (see also Baeye and Sintubin, 2008).

In the Campine Basin, the Neogene and Quaternary subsidence has bent the Boom Clay (Figure 63). The top of the Boom Clay is still near the surface south of Antwerp, but already around 200 m depth near the Dutch border (Figure 7).

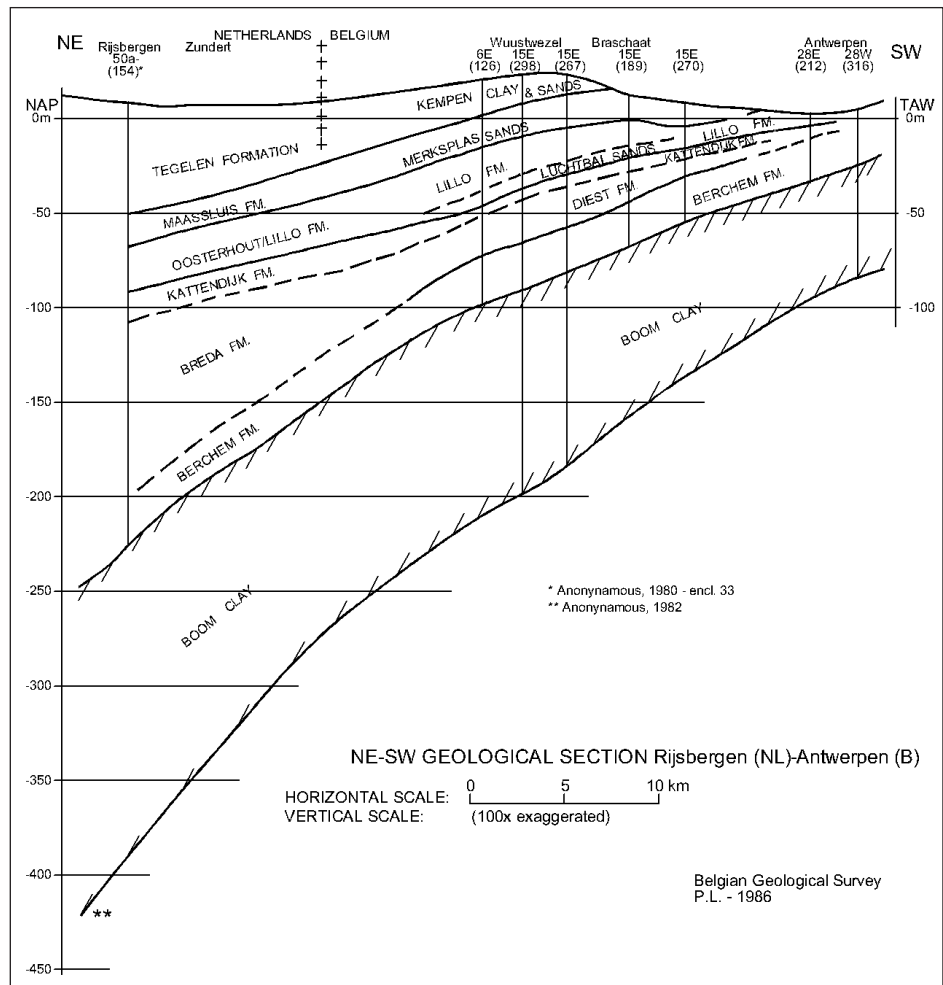
The subsidence history of the Boom Clay can be represented on a burial graph. The burial curve of the Boom Clay at the Mol site shows that, after its deposition which started some 32 Ma ago, the top of the Boom Clay was never again eroded (Figure 4-Mol). The top of the Eigenbilzen Formation just reached the surface and might have been slightly eroded at the Rupelian-Chattian transition as shown on Figure 4-Mol. The Chattian Voort Sands are also partly eroded at the beginning of the Miocene (23 Ma ago; Figure 4-Mol). The beginning of the Miocene is known to be a major hiatus, explaining the absence of Aquitanian deposits. Burdigalian and Langhian deposits are present and a major subsidence occurs during the Tortonian when the Campine Basin is filled with the Diest Sands. The Pliocene subsidence with deposition of the Mol Sands is clearly visualised on the burial graph. During the late Quaternary, differential erosion between the Campine Plateau area (consisting of Middle Pleistocene fluvial gravel and coarse sands and approximately bordered in the west by the Mol Rauw fault), and the area to the west of the Plateau (consisting of more easily erodible Cenozoic sands) has resulted in relief inversion with the former fluvial sediments forming the elevated Campine Plateau (Figure 5).



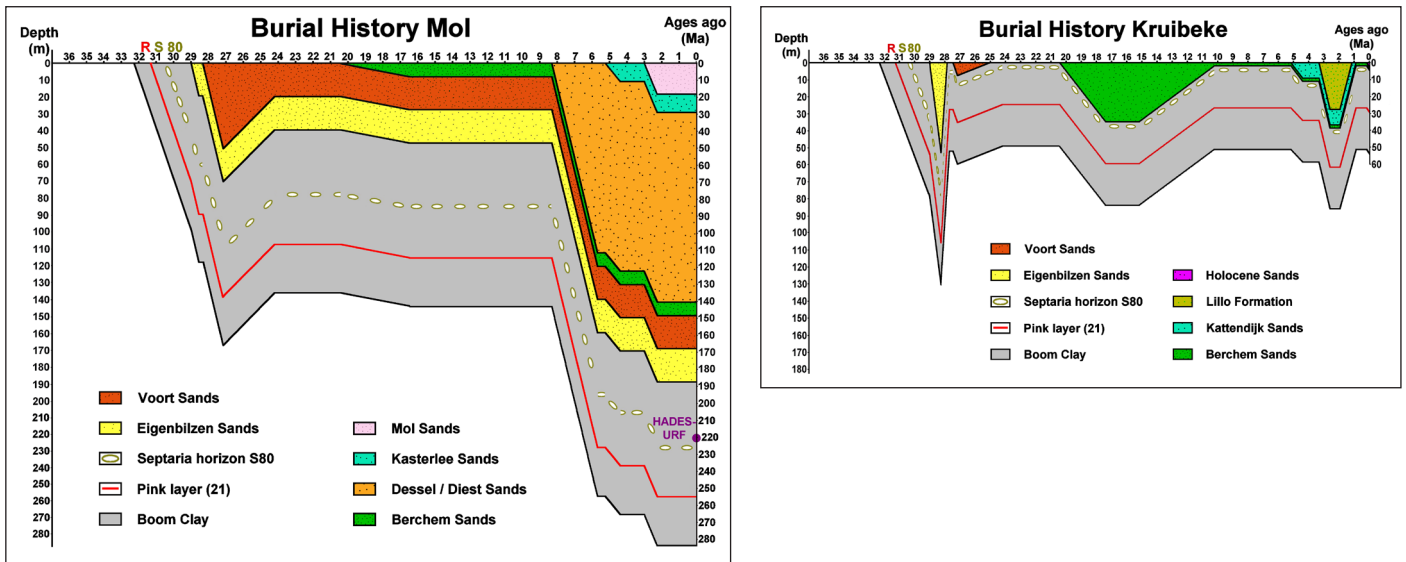
Figur 61. Geological and structural map of the Devono-Carboniferous subcrop of the Campine, Belgium part of the Roer Valley Graben (from Langenaeker, 2000).



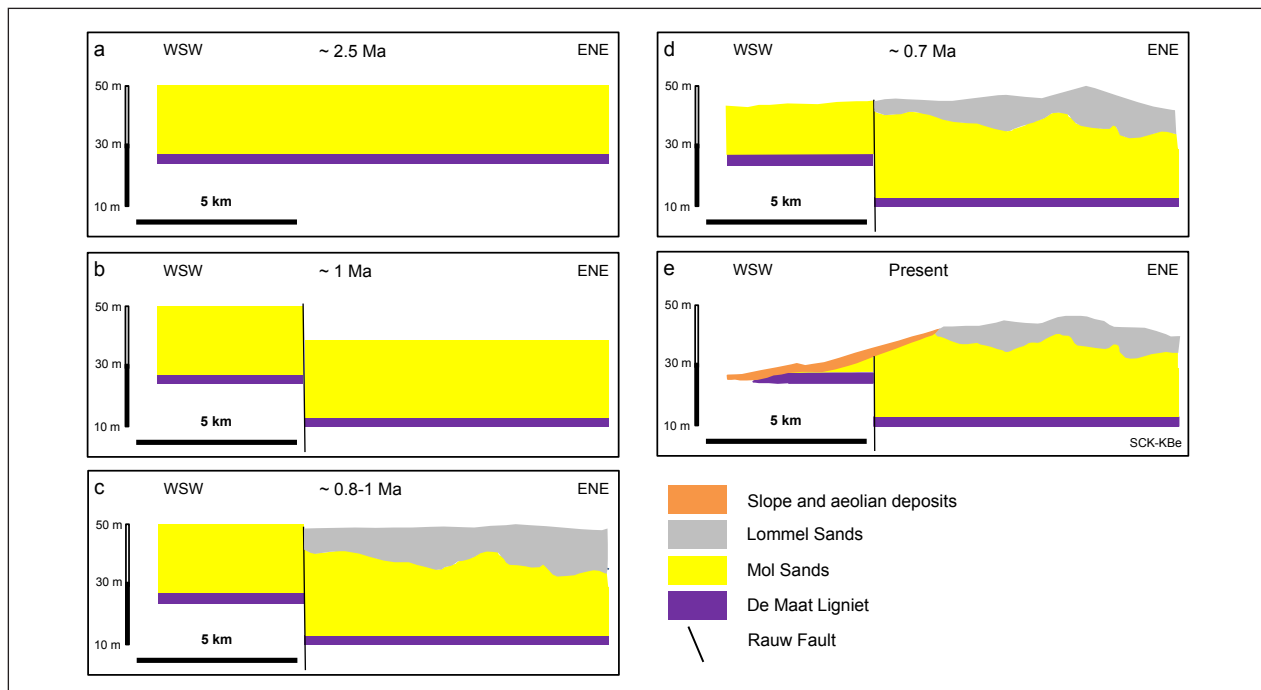
Figuur 62. Fault and isohypse map of the base of the Pliocene (A), the Miocene (B), the Paleocene (C), and the Cretaceous (D) in northern and northeastern Belgium including part of the Roer Valley Graben. The maps are mainly based on boreholes (From Databank Ondergrond Vlaanderen, consulted in May 2012, <http://dov.vlaanderen.be>).



Figuur 63. NE-SW Geological Section of the Oligocene, Neogene and Quaternary between Rijsbergen (the Netherlands) and Antwerp (Belgium) (from Vandenberghe & Laga, 1986).



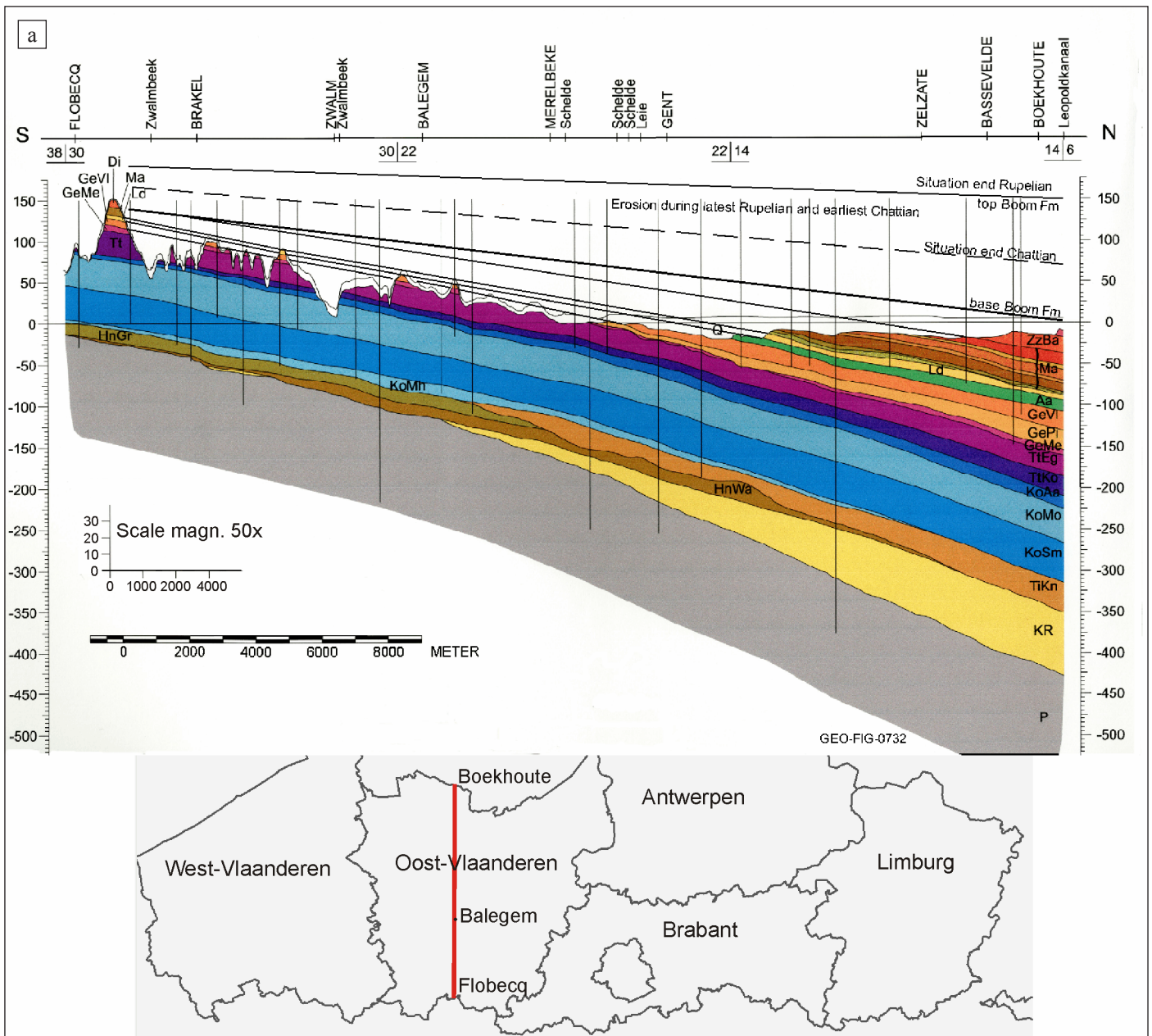
Figuur 64. Burial history of Boom Clay and younger layers in Kruibeke (Rupel area) and in Mol (Antwerp Campine area) (Mertens, 2005a). Initially, the Boom Clay was rapidly subsiding and at the end covered by the Eigenbilzen Sands. At the end of the Rupelian, a large tectonic uplift/tilting of the entire Campine Basin took place. This tilting consisted of an uplift of the western part of the Campine Basin and a subsidence of the eastern part. As a result of this tectonic activity, the burial history in the Rupel area (in the west) and in the Mol-Dessel area (in the east) is slightly different since then. Note that in the Mol area, west of the Rauw Mol fault (Figures 2,65) the detailed history reconstruction (Beerten et al., 2013) suggests that original Mol Sand was about 20 m thicker and that it was eroded during the last 0,7 Ma.



Figuur 65. Landscape development and evolution of the western edge of the Campine Plateau east of the Mol area, showing a typical case of relief inversion due to differential erosion. Early Pleistocene activation of the Rauw fault causes offset of the Mol Sands (Maatheide Member) and the De Maat Lignite of about 15 m (a-b). Further subsidence forces the Rhine to divert its course to the west and deposit the Lommel Sands (c). Around the Middle Pleistocene transition, the depocenter of the Rhine shifts to the east and erosional processes start to play a dominant role (d). Differential erosion of the loose and relatively fine Mol Sands causes pronounced lowering of the topography west of the coarse Lommel Sands which stand out as a positive relief known as the Campine Plateau (e) (from Beerten et al. (2013), modified after Van Mechelen (1982) with age control from Vandenberghe et al. (2004) for the Mol Sands and Gullentops et al. (2001) for the Lommel Sands).

A similar burial graph of the Antwerp area (Kruibeke) is shown in Figure 4. The major differences with the Mol area are on the one hand the earlier discussed uplift at the end of the Rupelian and the associated erosion removing

the entire Eigenbilzen Formation and the upper part of the Boom Formation, and on the other hand the continued near surface presence of the eroded top of the Boom Clay, indicating a limited subsidence during the Neogene.

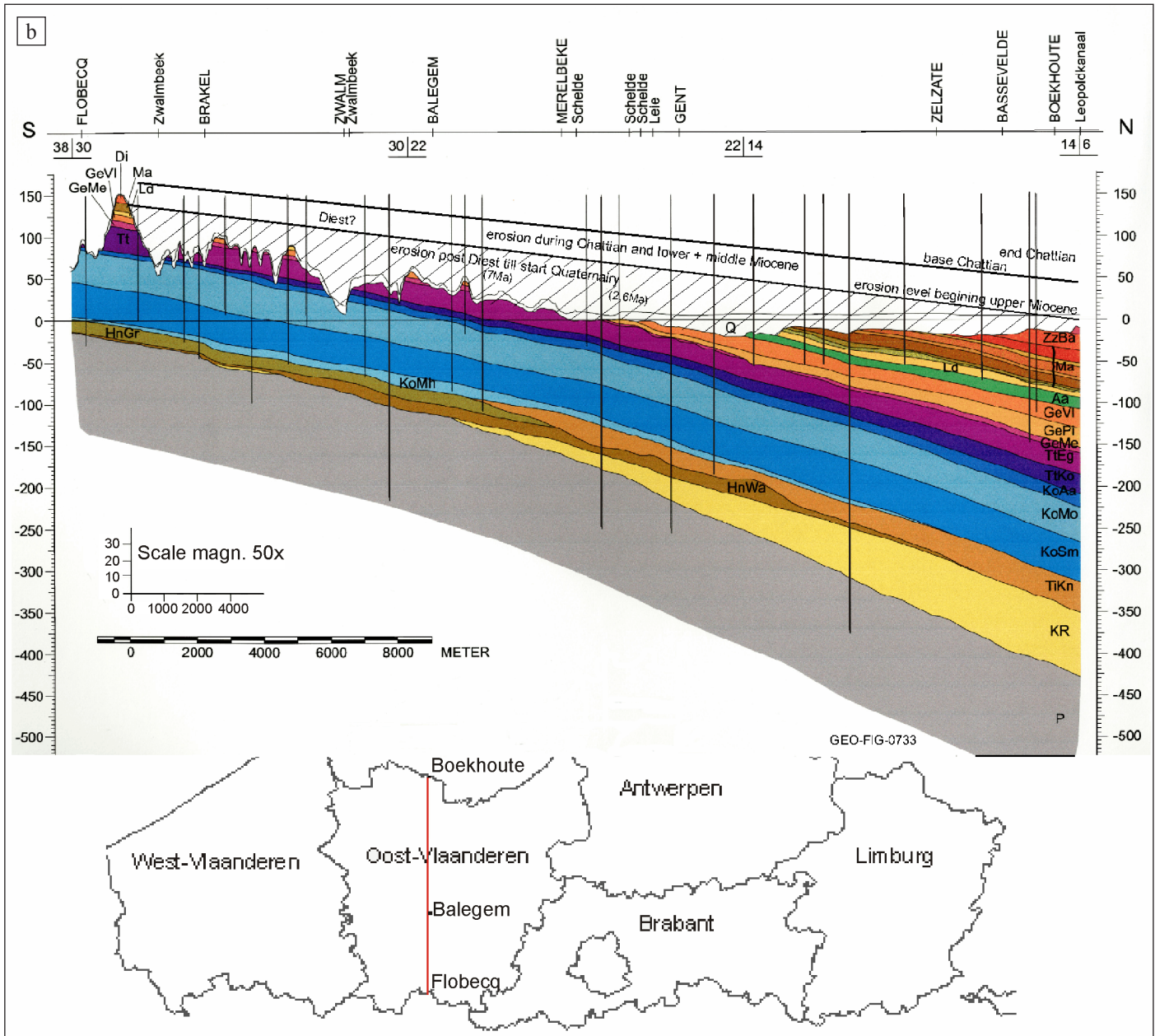


Figuur 66. Landscape development since the Oligocene represented on a north south geological section from the Flemish hills in the south to the Belgian-Dutch border in the north. The geological profile is provided by the Geological Survey of Belgium (courtesy K. Welkenhuysen)

a. In the north the position of the base of the Boom Clay is reconstructed at the end of the Rupelian, based on the known thickness of the Bassevelde (ZzBa), Watervliet and Ruisbroek Members in the area. The position of the top of the Boom Clay is based on its reconstructed thickness before and after erosion in the Antwerp area (Schittekat et al., 1983; De Man et al. 2010). Chattian sediments in the area have had a limited thickness (Van Simaey, 2004). The units of the Maldegem (Ma) and Zelzate (Zz) Formations between Asse Clay (close to base Ma) and Boom Clay are supposed to wedge out towards the south based on their mainly shallow water and sandy nature. The appearing slight angular unconformity below the Boom Clay represents the Pyrenean unconformity (2.2.2). The thin earliest Oligocene sequence containing Bassevelde3 sand (Ba3, see Figure 23) can have been present over the hill area. The thickness of the Boom Clay Formation diminishes towards the south at the same pace as derived in Figure 15.

The evolution of the landscape to the west and south-west of the Boom Clay outcrop area can be reconstructed based on the earlier discussed depositional and erosion history of the Boom Clay, on the position

of the base of the Tortonian Diest-Deurne Sands in the Antwerp area and in the Flemish Ardennes hills, and on the position of the present landscape and the base of the Quaternary (Figure 6 a&b).



b. The Lower and Middle Miocene erosion can be estimated from the position of the Late Miocene Diest Formation. This formation is traditionally mapped in the top of the Flemish hills (see also Houthuys, 2014) and its base there can be correlated with the base of the Deurne Sand Member in the Antwerp area occurring around 0 m TAW. The dip of this surface shows that the northern part of the profile was subsiding relative to the southern part after the start of the Upper Miocene, as is also the case for the Campine area. The volume between the end Chattian surface and this base Diest Formation has been eroded during Lower and Middle Miocene times; the thickness of sediments of this age, first deposited and then eroded is unknown. The thickness of the Diest Formation over the area is not known but was probably limited seen the shallow water facies of the pebble containing Diest Sands of the Flemish hills and the fossil rich Deurne Sands. Since the end of the Miocene this thickness of Diest Formation sediment and the volume between the base of the Diest Formation surface and the present base of the Quaternary has been eroded during the Pliocene and the Quaternary. The present volume of Quaternary sediments shown on the profile only compensates for a very limited amount this large eroded volume.

4.8. Natural discontinuities in the Boom Clay: the physical expression of the Boom Clay regional geological evolution

4.8.1. The discontinuity surfaces in the Boom Clay

a) Subvertical joints

A ‘hard rock’ type regular nearly vertical joint pattern is macroscopically the most striking feature in the outcrop area of the Boom Clay. Two families of coeval, smooth, unpolished, surfaces occur, almost perpendicular to each other and spaced at several dm to m distance from each other. No displacement occurred along the surfaces except from the tiny opening of the joints pointing to a tensional origin. Slickensides are never observed on these surfaces but in some cases microscopic shear bands near the fracture surface can be observed.

These joints developed when the concretions were already formed but not yet fully hardened (Mertens et al., 2003), a situation occurring by the very end of the Rupelian, and possibly also the Chattian, as fragments of eroded, fully lithified concretions are found already at the base of Burdigalian lower Miocene glauconitic sands (Edegem Member of the Berchem Formation) just above the Boom Clay. As discussed above, this is the time of a major uplift and erosion of the Boom Clay in the western outcrop area (Figure 54), creating the overconsolidation conditions (Figure 4-Kruibeke).

The orientation of the joint pattern has a prevailing direction of N130°E, the other main direction is N30°E. This orientation is measured in all clay pits and is independent of the orientation of the quarry faces. This orientation is even similar in clay and lithified layers of Eocene deposits more than 100 km away in central Flanders to the SW from the Boom Clay outcrop area, suggesting a relationship with regional stress conditions and stress history (Mertens et al., 2003).



Figure 67. The fault zone in the Boom Clay at Kruibeke; this is the only fault zone ever observed in the outcrop area of the Boom Clay.

a. In the picture at the top, arrows indicate the position of the normal faults with a slight throw; the throw at the left fault is about 1 m.

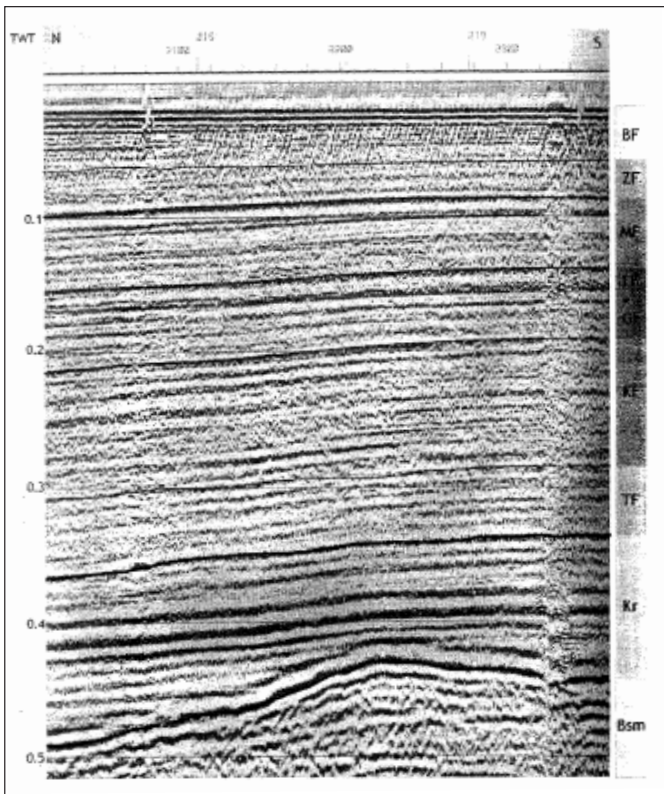
b. The picture at the bottom shows sampling of the fault zone for petrophysical measurements; the arrows indicate the throw of the fault (Dehandschutter, 2005a).

b) Slickensided surfaces

Polished slickensided surfaces are common in the clays. They are generally small, cm scale, planar and have moderate to steep dips in directions varying from the SW to the NE. The strike and dip directions are similar to the tensional joints discussed above, and therefore related to these joints. However, the polishing and striations point to a shear mechanism for their formation. Also, the spread in the striae azimuth, and the microtectonic and paleostress analysis show the slickensided surfaces to have occurred under more radial than pure tension conditions (Dehandschutter et al., 2004, 2005b). The slickensides have been observed also in borehole cores, sometimes from more than a couple of hundred meter deep, in which the more vertical joints are not observed and apparently are lacking.

c) Faulting

From all outcrops of the Boom Clay, only one clay pit has been found displaying a meter-scale fault zone (Dehandschutter et al., 2005a). It is a normal fault zone in the Kruibeke clay pit (Figure 67). It is related to minor differential regional tectonic tilting occurring in the late Oligocene, as indeed the base of overlying lower Miocene Edegem Sand is not faulted. The fact that this fault is located in Kruibeke is explained by the outspoken relief and bending in the Paleozoic basement at that location (Figure 628). The fault surfaces are composed of slickensided slip surfaces. Petrophysical measurements show an associated bulk volume loss and therefore relates this type of faulting to polygonal fault systems that occur in reaction to early stage dewatering of the clays. The faults rotate septaria, confirming that the septaria had already formed in the Late Oligocene. Jointing is observed to postdate the faulting.



Figuur 68. High-resolution seismic section recorded along the Scheldt river (recorded by RCMG, University Gent, in Dehandschutter et al., 2005a) close by the faulted zone in the Kruikebe Clay pit (Figure 67) which is located on the left bank of the Scheldt. On the seismic section, between 0.4 and 0.5 sec, a relief in the top of the Caledonian subsurface can be observed above which the Kruikebe fault zone is located. On a lower resolution land survey, located on the right bank of the Scheldt (recorded by TU Delft students), the same structural anomaly in the Caledonian basement is observed and bounded by a pre-Cenozoic normal fault dipping to the north (Dusar & Lagrou, 2007). The structure in the top of the Caledonian is supposed to have determined the location of the normal fault zone in the Boom Clay in the Kruikebe pit (Dehandschutter et al., 2005a).

d) Conchoidal fractures

The very clay-rich parts of the Boom Clay can develop conchoidal fractures in a similar way as very homogeneous and fine-grained materials can do.

e) Bedding planes

Bedding planes in the Boom Clay have not developed into discontinuity planes, neither in silty clay nor in clay-rich beds. However, in outcrops, the development of fine bedding fissility as a consequence of recent weathering has been observed in black Boom Clay layers which are rich in detrital organic matter particles.

4.8.2. Discussion on the origin of faulting, jointing and the slickensided surfaces

Based on paleostress and SEM texture analyses, a comprehensive evolution of and relationship between joints and the slickensides has been proposed by Dehandschutter et al. (2005b).

The low angle slickensides form as shear bands in the plastic domain at the maximal burial depth of the clay deposit, attained already during the Rupelian. The orientation of the slickensides is governed by the northeast trending extension during the Oligocene, related to the formation of the Roer Valley Graben. The wide range in dip azimuth of the striations is explained by the low horizontal stress anisotropy at that time.

As at the regional scale continuing uplift is associated with some tilting of the strata (Figure 54), still governed by the northeast-southwest extension regime, the horizontal stress anisotropy logically increases and consequently the now formed slickensides have a more preferred dip azimuth. As during uplift, the effective stress levels decrease, the dips of the microplanes steepen. The progressive change in grain texture during uplift due to the shear band development causes progressive strain hardening and hence slight changes in the geomechanical properties of the clay leading during uplift to the development of always new slickensides which consequently remain small in size, in contrast to the observed underground excavation-related large slickensides which originate in a very short time.

As uplift continues, the tectonic anisotropy increases and the fault planes of the Kruikebe zone are developed perpendicular to the NE extension direction. With even more continuing uplift, lower effective stress levels are reached, approaching the tensile regime where the joints develop. At first, the joints are hybrid, tensional and shear; bending of clay grain shear bands can be observed at the boundary with the joint surface. With even further uplift, the total effective stress becomes so low that pure tensile joints are now developed.

It is a common observation that overconsolidation of uncemented clays induces brittleness and can therefore produce dilatant fractures. This observation is corroborated by the absence of such joints in non-overconsolidated Pleistocene clays (Campine/Tegelen) outcropping in the clay pits of North Belgium, the Netherlands and Germany. However, under normal circumstances in the situation of overconsolidation, the horizontal stress is higher than the vertical one near the surface, normally preventing tensional jointing. A supplementary tensional stress needs to be invoked. For example, dehydration shrinkage of the clay by 1 or 2 % water loss in a regional anisotropic stress field has been proposed (Mertens et al, 2003). Such a mechanism, however, would probably also lead to a decreasing joint intensity with depth which is not observed over the depth of

the clay exposed in deep pits. Note that the decrease in the horizontal and mean effective stress, necessary for vertical tensile joint development, are in the scheme of Dehandschutter et al. (2005a,b) due to layer parallel contraction, tilting and uplift of the Boom Clay as a consequence of the regional geological history of the area.

Recognizing that in the Mohr diagram a low maximal normal stress is required for tensional failure rather than shear failure to occur, the value of the maximal stress allowing tensional failure was calculated in terms of cohesion and internal friction by Mertens et al. (2003). These authors have simulated the situation of normally consolidated clay for which the maximal stress is the vertical one; they calculated the cohesion needed for tensional failure at each depth and compared these values to the experimentally determined cohesion-depth relationship for the Boom Clay (Wildenborg et al., 2003). Based on this logic, the maximal depth above which tensional joints can occur in the Boom Clay was calculated to be 40 to 50 m.

The different burial histories as appearing from the burial graphs (Figure 4), with strong overconsolidation at Kruikeke and almost no overconsolidation at Mol, could explain the difference between the ubiquitous jointing observed in the outcrop area and the apparent absence of jointing in the subsurface reconnaissance of the Boom Clay in the Mol area.

A geomechanical modelling study simulated the mechanical properties evolution during the different phases of the sedimentation-burial-uplift-erosion history of the clay in an area between Antwerp, Weelde and Mol (Dizier, 2011; Dizier et al., 2008). Stress state, void ratio and water pressure are simulated in the Boom Clay at successive time steps of its history. The evolution of the stress path of the clay is calculated in a multi-mechanism elasto-plastic model envelope. A difficulty is the lack of reliable data on the geotechnical parameters of the Boom Clay as a function of the compaction–uplift history. Also, the model is simplified by not considering the tilting of the clay and therefore excluding horizontal deformation (Dizier, 2011), which is an essential component in the model proposed by Dehandschutter et al. (2005a,b).



Figuur 69. The picture at the top shows a Pleistocene periglacial frost wedge penetrating into the top of the Boom Clay; the growth of the ice wedge has laterally compressed the clay into microfolds (Pellenberg, sand pit Roelants). Detailed photographs show these microfolds on both sides of the wedge.

The 1D modelling for the Boom Clay in Mol shows that no failure can develop at any stage of its history. Similar modelling for the Boom Clay in Kruike leads to the same conclusion. Introducing a lower cohesion value for the Boom Clay in Kruike results in a possible frictional failure condition during the late Oligocene erosion. However, the observed jointing in the outcrops is tensional. The modelling has also simulated the influence of the regional context of the stress history induced in the Boom Clay. For this objective, the stress path in the Boom Clay since the deposition of the Boom Clay has been calculated in a clay body along a 54 km section Kruike-Oelegem-Zoersel-Weelde, using the reconstructed geological evolutionary history at these 4 sites. It turns out that, with the normal cohesion value of 0.3 MPa, the calculated stress path stays far off the frictional failure criterion in the top of the Boom Clay. If however a decreasing cohesion is introduced in the equations from deep to undep, frictional failure can be introduced at the surface over some meters depth in a limited area where the clay outcrops or at very shallow depth.

4.8.3. Permafrost induced deformation

During the Quaternary glacials the area of North Belgium has been subject several times to permafrost formation up to depths of at least 20 to 30 m (Vandenberghe, 2001; Govaerts et al., 2011). Large frost wedges, deforming the clay along its border, and continuing as small cracks deeper into the clay have been observed in the Boom Clay where it occurs near the surface (Figure 9).

4.8.4. Valley bulging

Plastic deformation of the Boom Clay has been observed for the first time by Laga (1966) in the excavations for the railway track along the Kennedy tunnel under the Scheldt at Antwerp. These structures were interpreted as diapiric uprisings in the top zone of the Boom Clay. Later seismic work, using an echo sub-bottom profiler and high frequency reflection seismics, confirmed the presence of diapir structures in the Boom Clay underlying the Scheldt river south of Antwerp (Wartel, 1980; Henriët et al., 1983; Schittekat et al., 1983). Such deformations are only found in this particular situation and never in the numerous clay pits in the outcrop area. The updoming seems to start at about 25-30 m depth and never achieves more than 10 m displacement (Figure 70).

Remarkably, these structures only occur at places where the Scheldt river eroded into the top of the Boom Clay. These features are similar to valley bulging features seen in the UK, typically occurring at places where river incisions reach soft sediments (Shaw et al., 2011). As this is similar to the observations made in the Boom Clay, the observed plastic deformation in Boom Clay should better be indicated as 'valley bulging' rather than 'diapirism'.

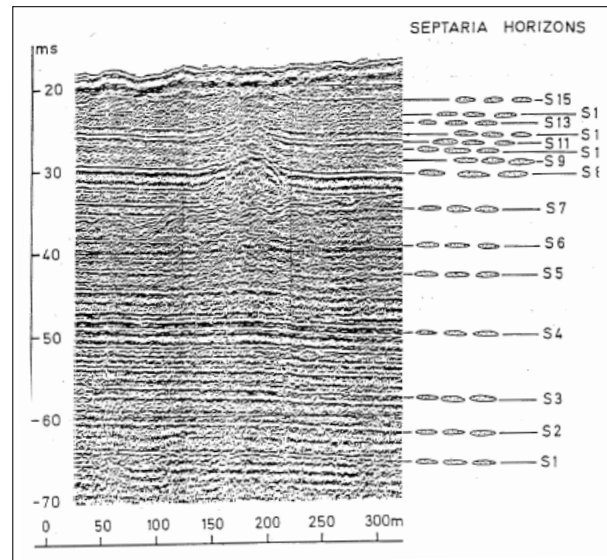


Figure 70. Valley bulging structure in the Boom Clay under the Scheldt river, upstream Antwerp, previously indicated as diapiric structures (from Henriët, 1986).

The origin of valley bulging can be explained as follows: firstly, a local decrease in the overburden load occurred due to denudation and river incision. Secondly, the horizontal stress inherited from past burial conditions largely exceeded the (reduced) vertical stress after removal of the overburden (river incision and erosion), which resulted in the vertical upward movement of the clay. Therefore, it is thought that the origin of this clay deformation in Boom Clay is related to the incision of the Scheldt river, which occurred some 10-15 ka ago in the Antwerp area (Adams et al., 2002).

5. Conclusions

At present, the Boom Clay in Belgium crops out in a several kilometers wide zone, stretching northwest to southeast from the Waasland to the southeast of Limburg. The outcrop zone is interrupted in the Hageland by the deeply incising upper Miocene Diest Formation. The Boom Clay dips slightly to the north-northeast and its top occurs at a depth of 200 to 250 m near the border with The Netherlands. Its thickness in the subsurface is in the order of 100 to 150 m.

The Boom Formation is a clay deposited in an open marine environment at the southern border of the epicontinental North Sea Basin during the Rupelian (Early Oligocene). The paleoecology of the fossils and the estimated wave properties in the basin point to water depths periodically varying between some tens of meter and well over hundred meter. The shallowing of the basin to the south is expressed by the disappearance of clay-rich layers and the stacking of silt-rich clay layers. Fossils of terrestrial vertebrates, insects and drifted wood furthermore point to the vicinity of the coast. Very shortly after the start of the Rupelian, a worldwide sharp cooling of the climate occurred that could

also be recognised below the Boom Clay base. Some fossil groups in the Boom Clay point to a temperate climate and oxygen isotopes show a marked cooling with respect to the Eocene temperatures. Seasonality was reduced and bottom waters remained below 10 °C.

Boom Clay is composed of silty clay and clayey silts. The components of its mineralogical composition are constant; variations are related to the varying proportions of clay minerals, consisting mainly of illitic, smectitic and kaolinite minerals, and of coarser grains, mainly quartz and feldspars. It has a water content of about 20 weight % and is still plastic but described as firm to stiff because considerable force is needed to mould the clay. Based on its lithological properties the Boom Formation has been subdivided from base to top into a silty Belsele-Waas Member, a grey Terhagen Member, a black Putte Member and a silty Boeretang Member. On top of the Boom Formation in the Campine subsurface west of the Mol Rauw fault, a thin silty to fine sand occurs known as the Eigenbilzen Formation; its relation with the equivalent formation east of the Mol Rauw fault needs further study.

The most striking characteristic of the Boom Clay is its regular stratigraphic layering. It is directly visible in outcrops and indirectly by geophysical well logging in the subsurface. The layering results from periodic variations in grain size, organic matter content and carbonate content. Some layers and boundaries between layers have distinct properties that can be recognised in outcrops and indirectly established by subsurface logging. Amongst these marker beds are a 'pink' horizon (R), a sharp boundary between grey and black clay (boundary between Terhagen and Putte Members), two subsequent very silty layers called the double layer (DB) and septaria horizons with particular shape and size properties. The systematic recognition of these horizons, and the extension of this approach to the subsurface parts of the Boom Clay, has led to a microstratigraphy of the total Boom Clay, consisting of all individual layers, that could be followed over long distances. The recognition of this microstratigraphy was essential for the sampling programs to study the stratigraphy, the sedimentology, the mineralogy, the geochemistry, the fossil content and other petrophysical and mechanical properties of the clay.

The Boom Clay Formation and its fossil content has been intensively studied since the 19th century for scientific and engineering objectives. It is the original unit stratotype of the Rupelian age/stage (Early/Lower Oligocene) in the International Chronostratigraphic and Time Scale. The North Sea Basin was at least intermittently connected through a northern European branch and a Rhenish graben system to the Paratethys and Tethys realms. The currents in the North Sea Basin were transporting the main mass of sediments from its northern part, picking up sediments and organic particles along the British coast. The Boom Clay is the first major deposit in the North Sea Basin to develop after the sudden cooling and the installation of the climatic

icehouse we are still living in today. The characteristic grain-size and detrital organic matter layering of the Boom Clay is the result of the starting Antarctic glaciation-deglaciation history. This history is steered by the astronomical periodicities with obliquity as the dominant influence; the climatic periodicity is expressed in the North Sea Basin as sea-level fluctuations of several tens of meters. A layering of originally marly horizons, now evolved into large carbonate septaria levels, is unrelated to the obliquity driven grain-size and organic-matter layering and the origin of this layering is still not understood. Generally the water at the bottom of the sea was poor in oxygen explaining the relatively poor fossil content. Already at very shallow depth below the sediment-water interface the sediment was in a reduced state as shown by the abundant pyritised organic traces in the clay. The carbonate concretions started to form slightly later but still very soon after sedimentation. The septaria were already in a final shape at about 10 m burial depth at the transition between the sulphate reduction zone at the top and the methanogenesis zone below. In this zone, new carbonate and pyrite precipitations inside the septae voids formed. Fragments of fully developed septaria are found at the base of the overlying lower Miocene sediments. In the western area, it was demonstrated that half of the Boom Clay thickness deposited in that area was eroded already during the latest Rupelian and earliest Chattian. Vertical tectonic differentiation in the Belgian part of the basin development is furthermore demonstrated by comparing thicknesses of the individual sediment layers. Such comparison also suggests that the low frequency grain-size cycles of the order of some tens of meters could be related to water depth variations caused by varying vertical tectonic uplift rather than by 3th order glacial-eustasy as is commonly proposed. The uplift and erosion of a large part of the Boom Clay in the western outcrop area, together with the continued relative subsidence of the Campine area during the post-Rupelian Cenozoic, are also responsible for the common development of joints observed in the clay pits and explain their absence in the subsurface of the still buried clay in the eastern area.

The wide range of subjects discussed in this synthesis document, and the long reference list documenting the state of know-how related to the geology of the Boom Clay, indicate that this Formation was and still is intensely studied. The scientific attraction of the clay deposit inspired many master and doctoral theses on fundamental questions related to the origin and evolution of the Boom Clay. Furthermore, the need for research on the qualities of the Boom Clay as a potential host rock for the geological disposal of high level and long-lived radioactive waste has stimulated and encouraged detailed studies on its properties. In contrast to the knowledge of the Boom Clay geology in the outcrop and the Campine areas, many uncertainties remain regarding the occurrence and characterisation of its more silty and sandy stratigraphic equivalents east of the Mol Rauw fault. Establishing a more detailed stratigraphy in that area will also lead to a better understanding of the fault history in the area.

6. Acknowledgments

The Geological Survey of Belgium, ONDRAF/NIRAS and SCK•CEN are thanked for the kind access to many data and samples all over the years. Clay-pit owners are thanked for authorising access to the pits. All colleagues and students that worked with the authors on specific items of the Boom Clay are sincerely thanked for their contribution, often referred to in the present review paper. Greet Willems and Frans Slegers are thanked for drafting many figures in the paper. Stephen Louwye, Boris Dehandschutter and Wim Westerhoff are sincerely thanked for reviewing the paper and suggesting many improvements.

7. References

- Abels, H.A., Hilgen, F.J., Krijgsman, W., Kruk, R.W., Raffi, I., Turco, E. and Zachariasse, W.J., 2005. Long-period orbital control on middle Miocene global cooling: integrated stratigraphy and astronomical tuning of the Blue Clay Formation on Malta. *Paleoceanography*, 20, PA4012.
- Abels, H.A., Van Simaey, S., Hilgen, F.J., De Man, E. & Vandenberghe, N., 2007. Obliquity-dominated glacio-eustatic sea level change in the early Oligocene: evidence from the shallow marine siliciclastic Rupelian stratotype (Boom Formation, Belgium). *Terra Nova*, 19, 65-73.
- Abreu, V.S. & Haddad, G.A., 1998a. Glacial eustasy during the Cenozoic: Sequence stratigraphic implications. *American Association Petroleum Geologists Bulletin*, 82, 1385-1400.
- Abreu, V.S. & Haddad, G.A., 1998b. Glacioeustatic fluctuations: the mechanism linking stable isotope events and sequence stratigraphy from the early Oligocene to Middle Miocene. In: De Graciansky P.C., Hardenbol J., Jacquin T., Vail P.R. & Farley M.B. (eds), *Mesozoic-Cenozoic Sequence Stratigraphy of European Basins*, SEPM Special Publication 60, 245-259.
- Abreu, V.S., Hardenbol, J., Haddad, G.A., Baum, G.R., Droxler, A.W., Vail, P.R., 1998. Oxygen isotope synthesis: a Cretaceous ice-house? In: De Graciansky, P.C., Hardenbol, J., Jacquin, T., Vail, P.R., Farley, M.B. (eds), *Mesozoic-Cenozoic Sequence Stratigraphy of European Basins*, SEPM Special Publication 60, 75-80.
- Adams, R., Vermeire, S., De Moor, G., Jacobs, P., Louwye, S., Polfiet, T., 2002. Toelichting bij de Quartairgeologische kaart, kaartblad 15 Antwerpen. Vlaamse Overheid, Dienst Natuurlijke Rijkdommen. Brussel.
- Baeye, M. and Sintubin, M., 2008. Monoclines: a bibliographic state-of-the-art; NIROND-TR 2008-41.
- Batjes, D.A.J., 1958. Foraminifera of the Oligocene of Belgium. *Koninklijk Belgisch Instituut Natuurwetenschappen, Verhandelingen*, 143, 188p, 13 Pl.
- Baut, J.-P. & Génault, B., 1999. Les Elasmobranches des Sables de Kerniel (Rupélien), à Gellik, Nord Est de la Belgique. *Geological Survey of Belgium Mémoire*, 45, 61 p.
- Beerten, K., De Craen, M., Wouters, L., 2013. Patterns and estimates of post-Rupelian burial and erosion in the Campine area, north-eastern Belgium. *Physics and Chemistry of the Earth, Parts A/B/C*. In press, available online <http://dx.doi.org/10.1016/j.pce.2013.04.003>
- Berggren, W.A., Kent, D.V., Swisher, C.C. & Aury, M.P., 1995. A revised Cenozoic Geochronology and Chronostratigraphy. In: Berggren, W.A., Kent, D.V., Aubry, M.P. & Hardenbol, J. (Eds.) *Geochronology, Time Scales and Global Stratigraphic Correlation*, Society of Economic Paleontologists and Mineralogists, Special Publication, 54, 129-212.
- Berner, R.A., 1984. Sedimentary pyrite formation: An update. *Geochimica Cosmochimica Acta*, 48, 605-615.
- Berner, R.A., 1985. Sulphate reduction, organic matter decomposition and pyrite formation. *Philosophical Transactions Royal Society London*, A315, 25-38.
- Blanchart, P., 2011. Influences de l'oxydation et de la biodégradation anaérobie sur la matière organique de l'argile Oligocène de Boom (Mol, Belgique): Conséquences sur la formation d'espèces organiques hydrosolubles, Institut National Polytechnique de Lorraine, Université de Nancy.
- Blow, W.H., 1969. Late middle Eocene to Recent planktonic foraminiferal biostratigraphy. In: Brönnimann P. & Renz H.H. (Eds.), *International Conference Planktonic Microfossils*, Proc. 1st., v. 1, Leiden (E.J. Brill), 199-422.
- Bohaty, S. & Zachos, J.C., 2003. Significant Southern Ocean warming event in the late Middle Eocene. *Geology*, 31/11, 1017-1020.
- Bonatti, E., Fisher, D.E., Joensuu, O. & Rydell, H.S., 1971. Postdepositional mobility of some transition elements, phosphorus, uranium and thorium in deep sea sediments. *Geochimica Cosmochimica Acta*, 35, 189-201.
- Bruggeman, C. & De Craen, M., 2012. Boom Clay natural organic matter – status report 2011. External Report of the Belgian Nuclear Research Centre, Mol, Belgium: SCK•CEN-ER-206, 149 p.
- Coniglio, M., Cameron, J.S., 1990. Early diagenesis in a potential oil shale: evidence from calcite concretions in the Upper Devonian Kettle Point Formation, southwestern Ontario. *Bulletin of Canadian Petroleum Geology*, 38, 64-77.

- Cramer, B. S., Toggweiler, J. R., Wright, J. D., Katz, M. E. and Miller, K. G., 2009. Ocean overturning since the Late Cretaceous: Inferences from a new benthic foraminiferal isotope compilation, *Paleoceanography*, 24, doi: 10.1029/2008pa001683.
- Curtis, C.D., 1987. Mineralogical Consequences of Organic Matter Degradation in Sediment: Inorganic/Organic Diagenesis. *In: Leggett, J.K. & Zuffa, G.G. (eds), Marine Clastic Sedimentology*, Graham and Trotman: 108-123.
- Curtis, C.D., 1995. Post-depositional evolution of mudstones 1: early days and parental influences. *Journal of the Geological Society, London*, 152, 577-589.
- Curtis, C.D., Coleman, M.L., 1986. Controls on the precipitation of early diagenetic calcite, dolomite and siderite concretions in complex depositional sequences. *In: Gautier, D.L. (ed.), Roles of Organic Matter in Sediment Diagenesis*, SEPM Special Publication, 38, 23-33
- De Craen, M., 1998. The formation of septarian carbonate concretions in organic-rich argillaceous sediments. PhD-thesis, K.U. Leuven, 330 p.
- De Craen, M., Swennen, R., Keppens, E.M., 1999a. Petrography and geochemistry of septarian carbonate concretions from the Boom Clay Formation (Oligocene, Belgium). *Geologie en Mijnbouw*, 77, 63- 76.
- De Craen, M., Swennen, R., Keppens, E.M., Macaulay, C.I. & Kiriakoulakis, K., 1999b. Bacterially mediated formation of carbonate concretions in the Oligocene Boom Clay of Northern Belgium. *Journal Sedimentary Research*, 69, 1098-1106.
- De Koninck, L.G., 1837. Description des coquilles fossiles de l'argile de Basele, Boom, Schelle, etc. *Nouveaux Mémoires de l'Académie Royale des Sciences de Belgique*, XI, 37 p.
- Dehandschutter, B., Vandycke, S., Sintubin, M., Vandenberghe, N., Gaviglio, P., Sizun, J.-P. & Wouters, L., 2004. Microfabric of fractured Boom Clay at depth: a case study of brittle-ductile transitional clay behaviour. *Applied Clay Science*, 26, 389-401.
- Dehandschutter, B., Gaviglio, P., Sizun, J.P., Sintubin, M., Vandycke, S., Vandenberghe, N. & Wouters, L., 2005a. Volumetric matrix strain related to intraformational faulting in argillaceous sediments. *Journal of the Geological Society*, 162, 801-813.
- Dehandschutter, B., Vandycke, S., Sintubin, M., Vandenberghe, N. & Wouters, L., 2005b. Brittle fractures and ductile shear bands in argillaceous sediments: inferences from Oligocene Boom Clay (Belgium). *Journal of Structural Geology*, 27/6, 1095-1112.
- De Man, E., 2006. Benthic Foraminifera biofacies analysis and stable isotopes of the middle Eocene to Oligocene successions of the southern North Sea Basin: tools for stratigraphy and for reconstruction of extreme climate changes. Doctoral Thesis Geology, K.U. Leuven, Belgium, 375 p.
- De Man, E. & Van Simaey, S., 2004. Late Oligocene Warming Event in the southern North Sea Basin: benthic Foraminifera as paleotemperature proxies: *Netherlands Journal of Geosciences/Geologie en Mijnbouw*, 83/3, 227-239.
- De Man, E., Ivany, L. & Vandenberghe, N., 2004. Stable oxygen isotope record of the Eocene-Oligocene transition in the southern North Sea Basin: positioning the Oi-1 event. *Netherlands Journal of Geosciences*, 83/3, 193-197.
- De Man, E., Van Simaey, S., Vandenberghe, N., Harris, W.B. & Wampler, J.M., 2010. On the nature and chronostratigraphic position of the Rupelian and Chattian stratotypes in the southern North Sea basin. *International Union of Geological Sciences, Episodes*, 33/1, 3-14.
- Deming, K.W. & Baross, J.A., 1993. The early diagenesis of organic matter: Bacterial activity. *In: Engel M.H. & Macko S.A. (eds.), Organic Geochemistry* Plenum Press, New York, 119-144.
- Deniau, I., Derenne, S., Beaucaire, C., Pitsch, H. & Largeau, C., 2001. Morphological and chemical features of a kerogen from the underground Mol laboratory (Boom Clay Formation, Oligocene, Belgium): structure, source organisms and formation pathways. *Organic Geochemistry* 32, 1343-1356.
- Dethy, B. & Neerdael, B., 1983. Correlations entre diagraphies et caractéristiques géotechniques d'une argile raide Tertiaire. *Bulletin International Association Engineering Geology*, 26-27, Paris, 49-57.
- D'hooge, L., Laga, P., Vandormael, C., 1991. Opsporen van geschikte sites voor de diepe berging van radioactieve afval B & C in de streek van Mol-Dessel. Unpubl. Report for NIRAS, ASBL Belgian Geological Engineering V.Z.W., Geological Survey of Belgium, Brussels.
- Dickson, J.A.D., Barber, C., 1976. Petrography, chemistry and origin of early diagenetic concretions in the Lower Carboniferous of the Isle of Man. *Sedimentology*, 23, 189-211.
- Dizier, A., 2011. Caractérisation des effets de température dans la zone endommagée autour de tunnels de stockage de déchets nucléaires dans les roches argileuses. Thèse doctorale, Département ArGENCo, Université de Liège, 299p.

- Dizier, A., Collin, F., Radu, J.-P., Charlier, R. & Vandenberghe, N., 2008. Provisional Report Discontinuities modeling in the Boom Clay Formation. ArGenCo U.Lg for ONDRAF/NIRAS, 65 p.
- Doré, A.G., Cartwright, J.A., Stoker, M.S., Turner, J.P. & White, N. (eds), 2002. Exhumation of the North Atlantic Margin: Timing, Mechanisms and Implications for Petroleum Exploration. Geological Society of London, Special Publication 196, 494 p.
- Duck, R.W., 1995. Subaqueous shrinkage cracks and early sediment fabrics preserved in Pleistocene calcareous concretions. *Journal Geological Society*, London, 152, 151-156.
- Dumont, M.A., 1849. Rapport sur la carte géologique du Royaume. *Bulletin Académie Royale de Belgique*, XVI, IIIème partie, 351-373.
- Dusar, M. & Lagrou, D., 2007. Cretaceous flooding of the Brabant Massif and the lithostratigraphic characteristics of its chalk cover in northern Belgium. *Geologica Belgica*, 10/1-2, 27-38.
- Elderfield, H., 1986. Sr isotope stratigraphy. *Paleogeography, Paleoclimatology, Paleoecology*, 57, 71-90.
- Folk, R.L., 2005. Nannobacteria and the formation of framboidal pyrite: Textural evidence. *J. Earth Syst. Sci* 114/3, 369-374.
- Glibert, M., 1955. Quelques espèces nouvelles ou mal connu de l'Oligocène Moyen et Supérieur de la Belgique. *Bulletin Institut Royal Sciences Naturelles de Belgique*, XXXI, n°86.
- Glibert, M., 1957. Pélécytopes et gastropodes du Rupélien supérieur et du Chattien de la Belgique. *Mém. Bulletin Institut Royal Sciences Naturelles de Belgique*, nr. 137, 91p, 6 Pl.
- Glibert, M. & de Heinzelin, J., 1954. L'Oligocène inférieur belge. *Institut Royal Sciences Naturelles de Belgique Volume Jubilaire Victor Van Straelen*, tome I, Bruxelles, 279-438, 7 Pl.
- Govaerts, J., Weetjens, E., Beerten, K., 2011. Numerical simulation of Permafrost Depth at the Mol site. External Report of the Belgian Nuclear Research Centre, Mol, Belgium: SCK•CEN-ER-148.
- Grimm, K.I. & Steurbaut, E., 2001. Foraminiferal Biofacies Analysis of the Boom Clay Formation in the Rupel area (Oligocene, Belgium) and Correlation with the Mainz Basin (Germany), *Aardkundige Mededelingen* 2001, 11, 9-20, Leuven University Press, Belgium.
- Gulinck, M., 1954. L'Oligocène de la Basse et de la Moyenne Belgique. In: P. Fourmarier, *Prodrome d'une description géologique de la Belgique*, Liège, 1954.
- Gulinck, M., 1965. Le passage du Bartonien au Rupélien dans la région Boom-Malines. *Bulletin de la Société belge de Géologie* 74, 115-119.
- Gullentops, F. & Vandenberghe, N., 1985. Rhythmicity in the Boom Clay (Rupelian) sedimentation, *Terra Cognita (EUG)*, 5(2-3), 245.
- Gullentops F, Bogemans F, De Moor G, Paulissen E, Pissart A. 2001. Quaternary lithostratigraphic units (Belgium). *Geologica Belgica* 4, 153-164.
- Haq B.U., Hardenbol J. & Vail P.R., 1987. Chronology of fluctuating sea levels since the Triassic (250 million years ago to present). *Science*, 235, 1156-1167.
- Haq, B.U., Hardenbol, J. & Vail, P.R., 1988. Mesozoic and Cenozoic chronostratigraphy and cycles of sea-level change. In: Wilgus, C.K., Hastings, B.S., Kendall, C.G., Posmantier, H.W., Ross, C.A., Van Wagoner, J.C. (Eds.), *Sea-level changes: an integrated approach*, Special Publication Society Economic Geology, Paleontology and Mineralogy, 42, 71-108.
- Hardenbol, J., Thierry, J., Farley, M.B., Jacquin, T., de Graciansky, P.-C. & Vail, P.R., 1998. Mesozoic and Cenozoic Sequence Chronostratigraphic Framework of European Basins. In: De Graciansky, P.-C., Hardenbol, J., Jaquin, T. & Vail, P.R. (eds.) *Mesozoic and Cenozoic Sequence Stratigraphy of European Basins*, SEPM Society of Sedimentary Geology Special Publication 60, 3-14, charts
- Henriet, J.P., Schittekat, J., Heldens, P., 1983. Borehole seismic profiling and tube wave applications in a dam site investigation, *Geophysical Prospecting* 31(1), 72-86.
- Herman, J., 1984. Additions to the Eocene (and Oligocene) fauna of Belgium. 7. Discovery of *Gymnura* teeth in Ypresian, Paniselian and Rupelian strata. *Tertiary Research*, 6(2), 47-54.
- Hoehler, T.M., Alperin, M. J., Albert, D.B., Martens, C.S., 1994. Field and laboratory studies of methane oxidation in an anoxic marine sediment - evidence for a methanogen-sulfate reducer consortium, *Global Biogeochemical Cycles*, 8, 451-463.
- Hooyberghs, H., 1983. Contribution to the study of planktonic foraminifera in the Belgian Tertiary, *Aardkundige Mededelingen*, 2, 131p.
- Hooyberghs, H., Vercauteren, T., De Meuter, F. & Symons, F., 1992. Benthonic Foraminiferal Associations of the Boom Formation (Oligocene) in the region of Boom (N. Belgium), *Belgian Geological Survey, Professional Paper*, 258.

- Houthuys, R., 2014. A reinterpretation of the Neogene emersion of central-Belgium based on the sedimentary environment of the Diest Formation and the origin of the drainage pattern. Accepted for publication in *Geologica Belgica*.
- International Marine and Dredging Consultants, 2005. *Hydraulisch randvoorwaardenboek Vlaamse kust: editie 2005*. Ministerie van de Vlaamse Gemeenschap. Afdeling Waterwegen Kust: Oostende
- Janssen, A.W., 1981. Molluskenfauna's en de stratigrafie van Oligocene afzettingen in een tweetal kleigroeven te Sint-Niklaas, provincie Oost-Vlaanderen, België. *Annalen Koninklijke Oudheidkundige Kring van het Land van Waas*, 84/2, 9-39.
- Key, A.J., 1957. Eocene and Oligocene ostracoda of Belgium. *Mémoire de l'Institut Royal des Sciences Naturelles de Belgique*, N° 136, 210p, 23Pl.
- Knox, R., Bosch, A., Skovbjerg Rasmussen, E., Heilmann-Clausen, C., Hiss, M., de Lugt, I., Kasiński, J., King, C., Köthe, A., Słodkowska, B., Standke, G., Vandenberghe, N., 2010. Cenozoic. *In: Doornenbal, H., Stevenson, A. (Eds.), Petroleum Geological Atlas of the Southern Permian Basin Area*, Chapt. 12. Houten, The Netherlands: European Association of Geoscientists and Engineers (EAGE) Publications b.v., 211-224.
- Labat, S., 2012. Sampling of Boom Clay in the clay quarry of Swenden at Rumst. SCK•CEN note 12/SLa/N-78.
- Laenen, B., 1997. Inorganic and organic geochemistry of a cyclic deposit: the Boom Clay, stratotype of the Rupelian (Belgium), doctorate Dissertation, K.U.Leuven, Belgium, 3 volumes.
- Laenen, B., 1998. The geochemical signature of relative sea-level cycles recognised in the Boom Clay. *Aardkundige Mededelingen*, 9, 61-82, University Press Leuven.
- Laenen, B. & De Craen, M., 2004. Eogenetic siderite as an indicator for fluctuations in sedimentation rate in the Oligocene Boom Clay Formation (Belgium). *Sedimentary Geology*, 163, 165-174.
- Laenen, B., Hertogen, J. & Vandenberghe, N., 1997. The variation of trace element content of fossil biogenic apatite throughout a eustatic sea-level sequence, *Palaeogeography, Palaeoclimatology, Paleoecology*, 132: 325-342.
- Laga, P., 1966. Kleidiapier in de uitgraving voor de spoorwegtunnel van de E3-weg op de rechteroever te Antwerpen. *Het ingenieursblad*, September 1966, 6-7.
- Lagrou, D., 2001. Magnetostratigrafie en gesteentemagnetisch onderzoek van de Boomse Klei (Rupeliaan) in België. Doctoral thesis, K.U. Leuven, Belgium, 210 pp.
- Lagrou, D.L., Vandenberghe, N. & Hus, J.J., 1996. Magnetostratigraphic investigation of the Rupelian in the stratotype area, Belgium, *Annales Geophysicae*, Suppl. 14, 140.
- Lagrou, D., Vandenberghe, N., Van Simaey, S. & Hus, J., 2004. Magnetostratigraphy and rock magnetism of the Boom Clay (Rupelian stratotype) in Belgium. *Netherlands Journal of Geosciences / Geologie en Mijnbouw*, 83/3, 209-225.
- Langenaeker, V., 2000. The Campine Basin. Stratigraphy, Structural Geology, Coalification and Hydrocarbon Potential for the Devonian to Jurassic. *Aardkundige Mededelingen 10*, Leuven University Press, 142p, 4 maps.
- Laskar, J., Robutel, P., Joutel, F., Gastineau, M., Correia, A.C.M. & Levrard, B., 2004. A long-term numerical solution for the insolation quantities of the Earth. *Astron. Astrophys.*, 428, 261-281. Doi: 10.1051/0004-6361:20041335.
- Leriche, M., 1910. Les poissons Oligocènes de la Belgique. *Mémoire Musée Royal d'Histoire Naturelle de Belgique*, Bruxelles, V, 230-363.
- Lozouet, P. (ed), 2013. Stratotype Stampien. Collection Patrimoine Géologique. Publications Scientifiques du Musée d'Histoire Naturelle, Paris. Ed. Biotope, Mèze, 461p.
- Matthijs, J., 1999. Toelichtingen bij de Geologische kaart van België, Vlaams Gewest, Kaartblad 25, Hasselt 1:50.000, Ministerie van de Vlaamse Gemeenschap, Afdeling Natuurlijke Rijkdommen en Energie, Brussel.
- McArthur, J.M., 1994. Recent trends in Sr isotope stratigraphy. *Terra Nova*, 6, 331-35.
- McArthur, J.M., Howarth, R.J. & Bailey, T.R., 2001. Strontium isotopic stratigraphy: LOWESS version 3: Best fit to the marine Sr-isotopic curve for 0-509 Ma and accompanying Look-up table for deriving numerical age. *Journal of Geology*, 109, 155-170.
- Merklin, R.L., 1962. Sur la stratigraphie de l'Oligocène moyen et supérieur dans le sud de l'URSS. *Mémoire Bureau Recherche Géologique Minière* nr. 28. II.
- Mertens, J., 2005a. Burial history of the two potential host formations (Boom Clay; Ypresian Clays) ONDRAF/NIRAS Technical note 2005-006.
- Mertens, J., 2005b. Comparison of interlayers in the Boom Clay throughout the Campine area. ONDRAF/NIRAS Technical note 2005-0059.
- Mertens, J. & Wouters, L., 2003. 3D Model of the Boom Clay around the HADES-URF, Construction of an AUTOCAD 3D-model of the URF, together with the internal clay layering. *NIROND* 2003-02, 31p, 4ap.

- Mertens, J., Vandenberghe, N., Wouters, L. & Sintubin, M., 2003. The origin and development of joints in the Boom Clay Formation (Rupelian) in Belgium. Geological Society, London, Special Publications, 216, 309-321.
- Miller, K.G., Wright, J.D. & Fairbanks, R.G., 1991. Unlocking the Ice House: Oligocene-Miocene Oxygen Isotopes, Eustasy, and Margin Erosion, *Journal of Geophysical Research*, 96(B4), 6829-6848.
- Moorkens, T., Hooyberghs, H., De Coninck, J., 1997. Vertical distribution of foraminifera in the Boom Formation (Rupelian unit-stratotype) and dinoflagellate cysts in the basal Oligocene of Belgium: implications on biostratigraphy, changing climates and paleoenvironments. Proceedings of the Joint meeting of the regional committees on Northern Paleogene and Neogene Stratigraphy, Geological survey of Denmark and Greenland, Denmark.
- Murray, J.W., Codispoti, L.A. and Friederich, G.E., 1995. Oxidation-reduction environments: The suboxic zone in the Black Sea. *In: Huang, C.P., O'Melia, C.R. and Morgan, J.J. (eds), Aquatic Chemistry: Interfacial and Interspecies Processes*. American Chemical Society, 157-176.
- Neal, J.E., Stein, J.A., Gamber, J.H., 1998. Nested stratigraphic cycles and depositional systems of the Paleogene Central North Sea. *In: de Graciansky, P.-C., Hardenbol, J., Jaquin, T. & Vail, P.R. (eds.), Mesozoic and Cenozoic Sequence Stratigraphy of European Basins*, SEPM Society Sedimentary Geology, Special Publication 60, 261-288.
- Neerdael, B., Vandenberghe, N., Bonne, A., Fierens, E., Laga, P. & Manfroy, P., 1981. Utilisation des diagraphies dans la détermination des caractéristiques lithologiques dans l'argile de Boom et leur intérêt pour les corrélations dans l'argile. Réunion de travail sur le choix des sites des dépôts de déchets radioactifs dans des formations géologiques: OCDE/AEN, Paris 19-22 Mai 1981, 17p.
- Nosovsky, M.F., 1962. Le Paléogène supérieur de la dépression de la région de la Mer Noire (Ukraine du Sud). Mémoire Bureau Recherche Géologique Minière, 28, t II.
- ONDRAF/NIRAS (2001) SAFIR 2: Safety Assessment and Feasibility Interim Report 2, NIROND 2001-06 E.
- Orphan, V. J., House, C. H., Hinrichs, K-U., McKeegan, K. D., DeLong, E. F., 2002. Multiple microbial groups mediate methane oxidation in anoxic marine sediments, *Proc. Nat. Acad. Sci.*, 99, 7663-7668.
- Ortlieb, J. & Dollfus, G., 1873. Compte rendu de géologie stratigraphique de l'excursion de la société malacologique de Belgique dans le Limbourg belge le 18 et 19 mai 1873. *Annales Société Royale Malacologique de Belgique*, VIII, 38-57.
- Raiswell, R., 1987. Non-steady state microbiological diagenesis and the origin of concretions and nodular limestones. *In: Marshall J.D.(ed.), Diagenesis of Sedimentary Sequences*, Geological Society Special Publications, London, 36, 41-54.
- Raiswell, R., 1988. Chemical model for the origin of minor limestone-shale cycles by anaerobic methane oxidation. *Geology*, 16, 641-644.
- Roche, E., 1978. Analyse sporopollinique de dépôts Oligocènes à Waasmunster. Belgian Geological Survey Professional paper 1978/8 N°156, 27p.
- Roche, E. & Schuler, M., 1979. Analyse palynologique de l'Argile de Boom. Belgian Geological Survey Professional Paper, 176, 1-18.
- Rögl, F., 1998. Palaeogeographic considerations for Mediterranean and Paratethys Seaways (Oligocene to Miocene). *Annalen des Natur-Historisches Museum Wien*, 99A, 297-310.
- Rögl, F., 1999. Mediterranean and Paratethys. Facts and hypotheses of an Oligocene to Miocene Paleogeography (Short overview). *Geologica Carpathica* 50,4, 339-349.
- Saeyns, R., Verheyen, A. & Vandenberghe, N. (2004): A rapid clay-mineral change in the earliest Priabonian of the North Sea Basin. *Netherlands Journal of Geosciences*, 83, 179-185.
- Sawlowicz, Z., 1993. Pyrite framboids and their development: a new conceptual mechanism. *Geologische Rundschau*, 82, 148-156.
- Schittekat, J., Henriët, J.P. & Vandenberghe, N., 1983. Geology and geotechnique of the Scheldt surge barrier characteristics of an overconsolidated clay. Proc. 8th Harbour Congress, Antwerp, 2, 121-135.
- Schwarzacher, W., 1993. Cyclostratigraphy and the Milankovitch theory. *Developments in Sedimentology*, 52, 1-225, Elsevier.
- Shaw, R., Hobbs, P.R.N., Dobbs, M.R. & Cuss, R.J., 2011. Desk based study and literature review of diapirism in plastic clays and an analysis of the critical state of Boom Clay. British Geological Survey, Minerals & Waste, Commercial Report CR/11/012.
- Shepard, F.P., 1954. Nomenclature based on sand-silt-clay ratios. *Journal of Sedimentary Petrology*, 24, 151-158.
- Sissingh, W., 2003. Tertiary paleogeographic and tectonostratigraphic evolution of the Rhenish Triple Junction. *Palaeogeography, Palaeoclimatology, Palaeoecology*, 196, 229-263.

- Sissingh, W., 2006. Syn-kinematic palaeogeographic evolution of the West European Platform: correlation with Alpine plate collision and foreland deformation. *Netherlands Journal of Geosciences/Geologie en Mijnbouw* 85,2, 131-180.
- Stainier, X., 1887. *Coeloma rupeliense*. Brachyoure nouveau de l'argile rupélienne. *Annales de la Société Géologique de Belgique*, 14, 86-96, pl. 5
- Sturbaut, E., 1992. Integrated stratigraphic analysis of Lower Rupelian deposits (Oligocene) in the Belgian Basin, *Annales Société Géologique Belgique*, 115(1), 287-306.
- Sturbaut, E. & Herman, J., 1978. Biostratigraphie et poissons fossils de la formation de l'Argile de Boom (Oligocène Moyen, du Bassin Belge). *Géobios* 11, 297-325.
- Stover, L.E. & Hardenbol, J., 1994. Dinoflagellates and depositional sequences in the Lower Oligocene (Rupelian) Boom Clay Formation, Belgium, *Bulletin van de Belgische Vereniging voor Geologie*, 102, 5-77.
- Van Baelen, H. and Sintubin, M., 2006. Evaluation of tectonic activity in the Roer valley Graben (NE Belgium). NIROND-TR 2006-01.
- Van Bakel, B.W.M., Artal, P., Fraije, R.H.B. & Jagt, J.W.M., 2009. A new early Oligocene crab (Decapoda, Brachyura, Dromiacea) from Northwest Belgium, with comments on its Palaeobiology. *Geologica Belgica*, 12 (1-2), 45-58.
- Van Beneden, P., 1872. Sur la découverte d'un homard fossile dans l'argile de Rupelmonde. *Bulletin de l'Académie Royale de la Belgique*, 33, 316-321.
- Vancampenhout, P., Welkenhuysen, K. & De Ceukelaire, M., 2008. Quasi-3D Onder-Rupeliaan-Tongerian model. Eindrapport. Koninklijk Belgisch Instituut voor Natuurwetenschappen, Belgische Geologische Dienst. Studie in opdracht van SCK•CEN.
- Vandenbergh, J., 2001. Permafrost during the Pleistocene in north west and central Europe. In: R. Paepe & V. Melnikov (eds.) *Permafrost Response on Economic Development, Environmental Security, and Natural Resources*, 185-194.
- Vandenbergh, N., 1974. Een sedimentologische studie van de Boomse klei. Doctorale verhandeling, K.U.Leuven.
- Vandenbergh, N., 1976. Phytoclasts as provenance indicators in the Belgian septaria clay of Boom (Rupelian age), *Sedimentology*, 23, 141-145.
- Vandenbergh, N., 1978. Sedimentology of the Boom Clay (Rupelian) in Belgium, *Verhandelingen van de Koninklijke Academie voor Wetenschappen, Letteren en Schone Kunsten van België, Klasse der Wetenschappen*, XL, 147, 137 p.
- Vandenbergh, N., 1983. Itinéraire 11: L'argile de Boom dans le Pays de Waas et la vallée du Rupel-Oligocène Moyen. In: Robaszynski, F. and Dupuis, C. (eds). *Belgique. Guides Géologiques Régionaux*, Masson, 161-167.
- Vandenbergh, N., 1999. Interpretatie van de boring Doel 2b. Unpubl. report SCK-CEN.
- Vandenbergh, N. & Gullentops, F., 2001. Toelichtingen bij de Geologische kaart van België. Vlaams gewest Kaartblad 32 Leuven 1:50 000, 77p ISSN 1370-3803.
- Vandenbergh, N. & Laga, P., 1986. The septaria of the Boom Clay (Rupelian) in its type area in Belgium. *Aardkundige Mededelingen, Leuven University Press*, 3, 229-238.
- Vandenbergh, N. & Mertens, J., 2013. Differentiating between tectonic and eustasy signals in the Rupelian Boom Clay cycles (Southern North Sea Basin). *Newsletters on Stratigraphy*, 46/3, 319-337.
- Vandenbergh, N. & Van Echelpoel, E., 1987. A field guide to the Rupelian stratotype, *Bulletin de la Société Belge de Géologie*, 96, 325-337.
- Vandenbergh, N. & Wouters, L., 2011. Rupel Group. National Stratigraphic Commission. <http://ncs.drupalgardens.com/paleogene-neogene/paleogene-original-lithostratigraphy>
- Vandenbergh, N., Laenen, B., Van Echelpoel, E. & Lagrou, D., 1997. Cyclostratigraphy and climatic eustasy. Example of the Rupelian stratotype. *Comptes Rendus Académie Sciences. Paris. Earth & Planetary Sciences*, 385, 305-315.
- Vandenbergh, N., Laga, P., Sturbaut, E., Hardenbol, J. & Vail, P., 1998. Tertiary Sequence stratigraphy at the southern border of the North Sea Basin in Belgium. In: De Graciansky, P.C., Hardenbol, J., Jacquin, T., Vail, P.R. & Farley, M.B. (eds), *Mesozoic-Cenozoic Sequence Stratigraphy of European Basins*, SEPM Society Sedimentary Geology Special Publication, 60, 119-154.
- Vandenbergh, N., Hager, H., van den Bosch, M., Verstraelen, A., Leroi, S., Sturbaut, E., Prüfert, J., & Laga, P., 2001. Stratigraphical Correlation by calibrated well logs in the Rupel Group between North Belgium, the Lower-Rhine area in Germany and Southern Limburg and the achterhoek, in *The Netherlands: Aardkundige Mededelingen, University Press Leuven*, 11, 69-84.
- Vandenbergh, N., Herman, J. & Sturbaut, E., 2002. Detailed Analysis of the Rupelian Ru-1 Transgressive Surface in the Type Area (Belgium). In: Gürs, K. (ed), *Northern European Cenozoic stratigraphy, Proc. 8th Bienn. Meet. RCNNS/RCNPS. Landesamt für Natur und Umwelt des Landes Schleswig-Holstein. Flintbek 2002*, 67-83.

- Vandenbergh, N., Brinkhuis, H. & Steurbaut, E., 2003. The Eocene/Oligocene Boundary in the North Sea Area: A Sequence Stratigraphic Approach. *In: Prothero, D.R., Ivany, L.C., Nesbitt, E.A. (eds), From greenhouse to icehouse: the marine Eocene-Oligocene transition.* Columbia University Press, New York, Chapter 24, 419-437.
- Vandenbergh, N., Van Simaey, S., De Man, E., Steurbaut, E., 2003. Field Guide to the Rupelian stratotype. Symposium on the Paleogene. Preparing for Modern Life and Climate, 25-30 August 2003, Leuven, Belgium. International Subcommission on Paleogene Stratigraphy. 43p.
- Vandenbergh, N., Van Simaey, S., Steurbaut, E., Jagt, J.W.M. & Felder, P.J., 2004. Stratigraphic architecture of the Upper Cretaceous and Cenozoic along the southern border of the North Sea Basin in Belgium. *Netherlands Journal of Geosciences*, 83, 155-171.
- Vandenbergh, N., Mertens, J., Wouters, L., Van Simaey, S. & Laenen, B., 2005. Relationship between Sedimentation, Stratigraphy and Vertical Tectonics: an example from the Rupelian and early Chattian at the Southern Border of the North Sea Basin in North Belgium. 24th IAS Meeting on Sedimentology, Oman, 10-13/01/2005.
- Vandenbergh, N., Hilgen, F.J., Speijer, R.P., with collaboration of Ogg, J.G., Gradstein, F.M., Hammer, O., Hollis, C.J., Hooker, J.J., 2012. The Paleogene Period. *In: Gradstein, F.M., Ogg, J.G., Schmitz, M.D. & Ogg, G.M. (eds), The Geological Time Scale 2012. Vol 2, 855-921.*
- Van Den Broeck, M.E., 1883. Carte géologique de la Belgique, Bilsen 1:20.000. Edition 1883.
- Van Den Broeck, M.E., 1884. Sur un faciès nouveau ou peu connu de l'argile supérieure rupélienne et sur les erreurs d'interprétation auxquelles il peut donner lieu. *Bulletin Société Royale Malacologique de Belgique*, XIX, troisième série, IV, LXXI-LXXV.
- Van Den Broeck, M., 1887. L'argile de Boom. *Causerie Géologique faite à l'occasion de l'Excursion à la fabrique de ciment de la Société de Niel-on-Rupel.* Société Belge des Ingénieurs et des Industriels, Bruxelles.
- Van Den Broeck, M.E., 1893. Coup d'oeil synthétique sur l'Oligocène belge et observations sur le Tongrien Supérieur du Brabant. *Bulletin Société Belge Géologie*, 7, 208-302.
- Van Den Broeck, M.E. & Rutot, A., 1883. Explication de la feuille de Bilsen. *Musée Royal d'Histoire Naturelle de Belgique, Service de la Carte Géologique du Royaume*, 1883.
- Van Echelpoel, E., 1991. Kwantitatieve Cyclostratigrafie van de Formatie van Boom (Rupeliaan, België), doctorate Dissertation, Katholieke Universiteit Leuven, Belgium, 164p.
- Van Echelpoel, E., 1994. Identification of regular sedimentary cycles using Walsh spectral analysis with results from the Boom clay. *In: De Boer, P.L. and Smith, D.G. (Eds.), Orbital Forcing and Cyclic Sequences, Special Publication International Association Sedimentology*, 19, 63-76.
- Van Echelpoel, E. & Weedon, G.P., 1990. Milankovitch cyclicity and the Boom Clay Formation: an Oligocene siliciclastic shelf sequence in Belgium, *Geological Magazine*, 127, 599-604.
- Van Geet, M., Maes, N. & Dierckx, A., 2003. Characteristics of the Boom Clay organic matter, a review. *Geological Survey of Belgium, Professional Paper 2003/1 Nr. 298*, 23p.
- Van Mechelen, J., 1982. Geomorfologie van de westelijke rand van het Kempens Plateau en micro-eolisatieverschijnselen op grind, Licentiaatsthesis, Groep Aard- en Delfstofkunde, K.U.Leuven.
- Van Riessen, E.D. & Vandenbergh, N., 1996. An Early Oligocene oil seepage at the southern rim of the North Sea Basin, near Leuven (Belgium). *Geologie en Mijnbouw*, 74, 301-312.
- Van Simaey, S., 2004a. Stratigraphic and Palaeoenvironmental Analysis of the Rupelian and Chattian in their type regions: implications for Global Oligocene Chronostratigraphy. Doctoral thesis Geology K.U. Leuven, 201 p.
- Van Simaey, S., 2004b. The Rupelian-Chattian boundary in the North Sea Basin and its calibration to the international time scale. *Netherlands Journal of Geosciences*, 83, 241-248.
- Van Simaey, S. & Vandenbergh, N., 2006. Rupelian. *Geologica Belgica* 9/1-2, 95-101.
- Van Simaey, S., De Man, E., Vandenbergh, N., Brinkhuis, H. & Steurbaut, E., 2004. Stratigraphic and palaeoenvironmental analysis of the Rupelian-Chattian transition in the type region: evidence from dinoflagellate cysts, Foraminifera and calcareous nannofossils. *Palaeogeography, Palaeoclimatology, Palaeoecology*, 208, 31-58.
- Van Simaey, S., Brinkhuis, H., Pross, J., Williams, G.L. & Zachos, J.C., 2005. Arctic dinoflagellate migrations mark the strongest Oligocene glaciations. *Geology*, 33/9, 709-712.
- Van Tassel, R., 1966. De Septaria van de Boomse Klei. *Het Ingenieursblad*, September 1966, 4-6.

- Veizer, J., Buhl, D., Diener, A., Bebneth, S., Podlaha, O.K., Bruckschen, P. & Jasper, T., 1997. Strontium isotope stratigraphy: potential resolution and event correlation. *Palaeogeography, Palaeoclimatology, Palaeoecology*, 132, 65-77.
- Verheyden, T., 2002. Decapods from the Boom Clay (Rupelian, Oligocene) in Belgium. *Bulletin de l'Institut Royal des Sciences Naturelles de Belgique, Sciences de la Terre*, 72, 171-191.
- Vervoenen, M., 1995. Taphonomy of some cenozoic seabeds from the Fleemish region, Belgium. *Belgian Geological Survey, Professional Paper 1994/5*, 272, 115p.
- Vincent, G., 1889. Nouvelle liste de la faune conchyliologique de l'Argile Rupélienne. *Annales Société Royale Malacologie de Belgique*, XXIII, XXXVIII-XL.
- Vochten, R., Geys, J., Bauten, P., 1975. Sur la présence de concrétions sidériteuses tubulaires dans l'argile de Boom (Rupélien), à Herselt (prov. Antwerpen, Belgique). *Annales Société Géologique de Belgique*, 98, 273-285.
- Wade, B.S. & Pälike, H., 2004. Oligocene climate dynamics. *Paleoceanography*, 19, PA4019, doi: 10.1029/2004PA001042.
- Wartel, S., 1980. The Tertiary and Quaternary subbottom of the Schelde estuary near Antwerpen (Belgium). *Geologie en Mijnbouw*, 59 (3), 233-240.
- Welkenhuysen, K., Vancampenhout, P., De Ceukelaire, M., 2012. Quasi-3D model van de Formatie van Maldegem, De Groep van Tongeren en de Groep van de Rupel. *Geological Survey of Belgium Professional paper 2012/1*, 311, 46p.
- Wildenborg, A.F.B., Orlic, B., Thimus, J.F., De Lange, G., De Cock, S., de Leeuw, C.S. & Veling, E.J.M., 2003. Radionuclide transport in clay during climate change. *Netherlands Journal of Geosciences/Geologie en Mijnbouw*, 82/1, 19-30.
- Williams, G.L., Brinkhuis, H., Fensome, R.A., Pearce, M.A. & Weegink, J.W., 2004. Southern ocean and global dinoflagellate cyst events compared; index events for the Late Cretaceous-Neogene. *In: Exon, N.F., Kennett, J.P. & Malone, M.J. (Eds.), Proceedings of the Ocean Drilling Program, Scientific Results ODP Leg 189, College Station, Texas*, 98 p.
- Wong, Th.E., de Lugt, I.R., Kuhlmann, G. & Overeem, I., 2007. Tertiary. *In: Wong, T., Batjes, D.A.J., de Jager, J. (eds), Geology of the Netherlands. Royal Netherlands Academy of Arts and Sciences*, 2007, 151-171.
- Wouters, L. & Vandenberghe, N., 1994. *Geologie van de Kempen. Een synthese. NIRAS-ONDRAF, Brussel*, 208p.
- Wright, L.D. & Friedrichs, C.T., 2006. Gravity-driven sediment transport on continental shelves: A status report. *Continental Shelf Research*, 26/17, 2092-2107.
- Zachos, J.C., Quinn, T.M. & Salmey, S., 1996. High-resolution (10^4 years) deep-sea foraminiferal stable isotope records of the Eocene-Oligocene climate transition. *Paleoceanography*, 11/3, 251-266.
- Zachos, J., Pagani, M., Sloan, L., Thomas, E., & Billups, K., 2001. Trends, rhythms, and aberrations in global climate 65 Ma to present. *Science*, 292, 686-693.
- Zachos, J. C., Dickens, G. R. and Zeebe, R. E. , 2008. An early Cenozoic perspective on greenhouse warming and carbon-cycle dynamics, *Nature*, 451 (7176), 279-283, doi: 10.1038/nature06588.

Manuscript received 15.11.2013, accepted in revised form 14.3.2014.

Memoirs of the Geological Survey of Belgium

The series, which started in 1955, welcomes papers dealing with all aspects of the earth sciences, with a particular emphasis on the regional geology of Belgium and adjacent areas. Submitted papers should present the results of syntheses of original studies (e.g. PhD theses, cartography). High scientific standards are required. Papers written in English are preferred.

Each paper will be reviewed by at least by two reviewers.

Editor in chief

Michiel Dusar

Royal Belgian Institute of Natural Sciences – Geological Survey of Belgium

[michiel.dusar@naturalsciences.be]

Editorial Board

Cecile Baeteman

Léon Dejonghe

Xavier Devleeschouwer

Jean-Clair Duchesne Geologica Belgica

Eric Goemaere

David Lagrou VITO

Kris Piessens

Edouard Poty ULiège

Noel Vandenberghe KU Leuven

Jacques Verniers, UGent

Instructions for authors, website information

Guide for authors : see website Geologica Belgica

<http://www.geologicabelgica.be>

Guide for authors : see website Geologica Belgica

<http://www.geologicabelgica.be>

List of publications and conditions of sale : see website Geological Survey of Belgium

<http://www.naturalsciences.be/geology/products/pp>

Publication address: Geological Survey of Belgium, 13 rue Jenner - B-1000 Brussels

ISSN 0408-9510

© Geological Survey of Belgium

Impression: Service public fédéral Economie,
P.M.E., Classes moyennes et Energie

Drukwerk: Federale Overheidsdienst Economie,
K.M.O., Middenstand en Energie

“The Geological Survey of Belgium cannot be held responsible for the accuracy of the contents, the opinions given and the statements made in the articles published in this series, the responsibility resting with the authors.”